

AD 654718

ARC DISCHARGE SOURCES

FINAL REPORT
16 OCTOBER 1964 TO 28 FEBRUARY 1967

31 MARCH 1967

CONTRACT Nonr 4647(00)
ARPA ORDER NO. 306-62
CODE 473C
REQ: NO. NR-012-511, 7 JANUARY 1966

A 26-MONTH CONTRACT
EXPIRATION DATE 28 FEBRUARY 1967
COST \$195,933

Charles H. Church, Principal Investigator (412) 256-3678
B. W. Swanson E. Geil
J. Lowke L. Armstrong
R. Liebermann G. Basi
P. Buchhave D. Sun
I. Liberman R. S. de Voto

This document has been approved
for public release and its
distribution is unclassified

D D C
RECEIVED
R JUL 17 RECEIVED
R JUL 21 1967
C
CESTI 1967

DISCLAIMER NOTICE

**THIS DOCUMENT IS THE BEST
QUALITY AVAILABLE.**

**COPY FURNISHED CONTAINED
A SIGNIFICANT NUMBER OF
PAGES WHICH DO NOT
REPRODUCE LEGIBLY.**

ARC DISARGE SOURCES

FINAL REPORT
16 OCTOBER 1964 TO 28 FEBRUARY 1967

31 MARCH 1967

CONTRACT Nonr 4647(00)
ARPA ORDER NO. 306-62
CODE 4730
REQ: NO. NR-012-511, 7 JANUARY 1966

A 28-MONTH CONTRACT
EXPIRATION DATE 28 FEBRUARY 1967
COST \$195,933

Charles H. Church, Principal Investigator (412) 256-3678
B. W. Swanson E. Geil
J. Lowke L. Armstrong
R. Liebermann G. Basi
P. Buchhave D. Sun
I. Liberman R. S. de Voto

BLANK PAGE

TABLE OF CONTENTS

	<u>Page</u>
PREFACE	iii
ABSTRACT.	iv
I. INTRODUCTION.	1
II. BASIC PRINCIPLES OF HIGHLY RADIATIVE ARCS	4
2.1 Electrical and Thermal Conductivity.	6
2.2 The Spectral Absorptivity.	6
2.3 The Arc Models	8
III. COUPLING THE PUMP INTO THE LASER ROD.	14
IV. RECENT EXPERIMENTAL MEASUREMENTS ON THE ARC	19
V. SUMMARY AND CONCLUSIONS	28
VI. ACKNOWLEDGMENTS	29
VII. REFERENCES.	30
VIII. APPENDICES.	
A. A Program for the Calculation of the Electrical and Thermal Conductivity of Xenon as a Function of Temperature and Pressure. By R. S. deVoto.	
B. Calculation of Bound-Bound Transition Probabilities. By D. Sun	
C. Calculation of the Optical Radiation Emitted by a Cylindrical Arc of Known Temperature Profile. By R. Liebermann	
D. Whittaker and Gamma Functions-Description of Two ALGOL Procedures. By G. Basi	
E. Radiative Transport in a Xenon Arc. By B. W. Swanson.	
F. Analysis of Xenon Discharges. By J. J. Lowke	

LIST OF FIGURES

	<u>Page</u>
Figure 1 - The equations relating the electrical power input to the optical radiation and the thermal conduction.	5
Figure 2 - The information flow for the calculation procedures in the appendices.	7
Figure 3 - The calculated spectral absorptivity of xenon I over a range of temperature for a pressure of 5 Atm.	9
Figure 4 - The calculated spectral radiance along a .8 cm diameter homogeneous temperature xenon plasma at 12000°K and 5 Atm pressure.	11
Figure 5 - The calculated spectral radiant emittance for .8 cm and 1.4 cm diameter homogeneous cylindrical plasmas in xenon at 12000°K and 5 Atm pressure.	12
Figure 6 - Simplified representation of laser rod-coaxial laser pump system.	15
Figure 7 - Multiple rod coaxial laser pump.	17
Figure 8 - Geometry of the spherical reflector.	18
Figure 9 - Black body temperatures corresponding to measured spectral radiances.	21
Figure 10 - Black body temperatures corresponding to same spectral radiance as 13 mm flash tube as a function of input power density.	22
Figure 11 - Spectral radiance of linear cylindrical Xe flash tubes of different diameters as a function of power density input.	23
Figure 12 - Spectral radiance of linear cylindrical Xe flash tubes of different diameters as a function of power input.	24
Figure 13 - Spectral radiance distribution for an EG & G Inc. FX-52 flash tube single & double pulsed.	25
Figure 14 - The spectral radiance at 3000 \AA viewed end on and side on for a 13 mm diameter arc tube.	27

PREFACE

This report presents the work since the previous semiannual report on Contract Nonr 4647(00). It also summarizes the previous work on the contract toward the development of quantitative models for high energy pulsed arcs of the type that are used for the optical pumping of high energy lasers. The studies in this contract have been concerned primarily with xenon as this gas has been used most successfully for high energy laser pumping; the principles contained in the models for the arcs are applicable to other highly radiative arcs, though in many cases the necessary quantitative descriptions of the physical properties of the arc plasma are not available at the present time.

Recent developments in pumping geometries and in additive lamps, arising, in part, from this work and from work in a closely related area, the optical pumping of continuous lasers, under Contracts DA-28-043-AMC-00292(E) and DA-28-043-AMC-02097(E), indicate new promise for efficient optically pumped lasers. The principles discussed in this report provide a basis for an understanding of the optical pumps for lasers.

ABSTRACT

This report summarizes the studies made on Contract Nonr 4647(00) towards the development of models for the highly radiative arcs used for the high energy pumping of lasers. The report also presents the experimental and theoretical studies since the last semi-annual report. The experimental investigations were primarily concerned with more extensive measurements of the spectral radiance of the plasma to provide verification for the models. The theoretical work has resulted in computer methods, described in the appendices, to calculate the transport properties, the spectral absorptivities for the lines and the continuum of xenon, and the spectral radiance and temperature profiles in cylindrical arcs. Also included as an appendix is a theoretical analysis of the xenon arc using radiative transport techniques developed in other studies.

May 29, 1967

ARC DISCHARGE SOURCES

Charles H. Church, Principal Investigator (412) 256-3678
B. W. Swanson E. Geil
J. Lowke L. Armstrong
R. Liebermann G. Basi
P. Buchhave D. Sun
I. Liberman R. S. de Voto

I. INTRODUCTION

The optically pumped solid state laser provides the highest peak power and highest peak energy available from coherent sources. This report summarizes the work on Contract Nonr 4647(00) toward the development of quantitative models for the highly radiative arcs used to excite these lasers. Contained in the appendices to this report are computer programs developed in this work for the calculation of many features of these arcs. The calculation procedures are for xenon, though in principle, they are applicable to other atomic systems.

The theoretical and the experimental research on this contract has been directed towards the creation of quantitative models for the flash lamps that in turn would be useful in the improvement of high energy lasers. The development of the models required basic studies of the many aspects of highly radiative arcs, and lead to considerable expansion of the experimental techniques available for the study of these dense plasmas. These plasmas may be encountered in many situations other than the flash tubes for pumping high energy lasers, including re-entry shock waves and high voltage switch gear.

The effort in this contract can be divided into three areas: (1) the development of theoretical techniques to calculate the necessary physical properties of arc plasmas, (2) the applications of these techniques to create models for the high radiative arcs, and (3) the experimental measurements required to formulate and then to verify the models.

The earlier reports (references 1, 2, 3 & 4) described many aspects of the problem more fully. The computer programs resulting from this work are all in the ALGOL language for a Burroughs B5500 DISK computer.

The development of the models required techniques for calculating the transport properties (electrical and thermal conductivity), and the spectral absorptivity (the broadened spectral lines plus the continuum) as a function of temperature and pressure. In addition, methods for handling energy transport within highly radiative inhomogeneous temperature arc plasmas were required.

For the transport properties of xenon, we were fortunate in obtaining the assistance of Dr. R. S. de Voto of Stanford University, who has developed computer programs for calculating the properties of partially ionized monatomic gases. His program for the calculation of the electrical and thermal conductivities of xenon as a function of temperature and pressure is in Appendix A.

The calculation of the spectral absorptivity of xenon required consideration of the broadened lines and the continuum. The final program given in Appendix B is due to the efforts of many people, particularly D. Sun of California Institute of Technology, E. Corinaldesi, now at Boston University, and R. G. Schlecht, now at Aeroneutronics Division of Ford Motor Company. Appendix C uses the bound-bound transition probabilities and other information on xenon to calculate the optical radiation emitted by a cylindrical arc of a given temperature profile and pressure. Appendix D presents calculations for Whittaker functions of real and imaginary argument for use in calculations of the matrix elements for bound-free and free-free transitions. We will discuss details of these calculations in a later section.

Two approaches were followed in the creation of the models for the arc. In one approach, we assumed the arc to be homogeneous in temperature and neglected thermal conduction to the walls. Experimental measurements had indicated that this was a reasonable assumption for the central core. Such model would explain a number of the observed characteristics, such as the arc radiant emission saturation in the infrared and in the visible, and account for a major portion of the input power.

The pressure to be used for this homogeneous temperature model is open to question due to the actual temperature gradient which exists near the walls. In the other approach, the electric field across the arc, the inside diameter of the arc tube, and the pressure of heavy particle number density are to be specified and the radial absolute temperature distribution is to be sought. With the temperature distribution, we could calculate all of the observed properties of the arc including the spectral radiance at the walls (Appendix C). This calculation required the solution to the energy balance equation for a non-grav, nonhomogeneous temperature plasma. An approximate analysis described in Appendix E was applied to this problem to obtain a better initial temperature distribution. The final program developed in this work is given in Appendix F.

The experimental measurements were intended to aid in the formulation and verification of the models. In the course of the work, the flash lamp or more completely, the confined wall-stabilized pulsed arc discharge, was found to be a useful vehicle to study high power density, high pressure, highly radiative plasmas. Plasmas with these characteristics in gases other than xenon are of interest to workers in many fields of research and applications. In the course of this work and in the closely associated company sponsored research, techniques have been and are being developed to study these plasmas. These techniques have included two rapid scanning spectrometers, one of high resolution scanning over a limited range⁽⁶⁾, the other of decreased resolution but with a much wider spectral range⁽⁷⁾.

A problem still exists in the accurate measurement of the instantaneous pressure. The pressure is crucial to an accurate description of the arc as the pressure varies widely with the temperature gradient near the wall. Currently a laser interferometer similar to that of Gerardo et al.⁽⁸⁾ is being set up to allow electron density measurements. These electron density measurements will serve to check the values we have assumed in the calculations.

II. BASIC PRINCIPLES OF HIGHLY RADIATIVE ARCS

The arcs used for pumping high energy lasers have many features in common with arcs used for continuous laser pumping. The primary difference between these arcs lies in the size of the arc column and the power density in the arc. In both cases, the arcs are near or above atmospheric pressure. As the efficiency of the laser systems increase, the differences between the two arc applications are becoming less marked.

The usual form of the arc used in high energy laser pumping is a cylindrical arc surrounded by a wall. We have only investigated this wall stabilized arc. In the arc, current flow carries power into the arc; radiation external to the arc and thermal conduction to the arc surroundings (i.e.: the wall) carry power away from the arc. Convective power transport can be neglected in this type of wall stabilized confined arc unless there is gas flow--which we have not considered in this work. A wall stabilized highly radiative arc such as those used for high energy laser pumping has a central plasma core at the temperature of the fully ionized plasma (the actual temperature varying with the composition of the plasma) with the temperature at the wall dependent upon the rate at which power is carried away from the walls. (A fully ionized plasma may be only .01% ionized. It is characterized by the dominance of the electron-electron and electron-ion interaction over the other particle interaction).

The relation between the input power and that carried away from the arc by radiation and conduction can be put into equation form. Figure 1 presents the family of equations that relate the power input per unit volume to the power carried away by radiation and conduction. We consider the arc to be in local thermal equilibrium (LTE) and thus describable by Boltzmann's equation, Saha's equation and a simple radiation law. The electrical and thermal conductivities as well as the spectral absorptivities are functions of the local temperature and pressure for each constituent. The various constituents of the plasma interact with each other through the ionization law

The Energy Balance

$$\tau \cdot (\bar{F}_{RAD} + \bar{F}_{TC}) = \sigma (p,T) E^2$$

where E is the electric field in Volts cm^{-1} , σ is the electrical conductivity in $(\text{ohm cm})^{-1}$ and is dependent upon the pressure (p) and the temperature (T). \bar{F}_{TC} is the thermally conducted power flux in Watts cm^{-2} and is given by

$$\bar{F}_{TC} = -K(p,T) \text{ grad } T$$

K is the thermal conductivity in Watts $\text{cm}^{-2} \cdot \text{K}^{-1}$. \bar{F}_{RAD} is the radiant emittance (i.e. radiative flux) in Watts cm^{-2} and is expressed in terms of $F_{v,RAD}$, or $F_{\lambda,RAD}$. The spectral radiant emittance

$$\bar{F}_{RAD} = \int_0^\infty \bar{F}_{v,RAD} dv = \int_0^\infty \bar{F}_{\lambda,RAD} d\lambda$$

where v is the frequency and λ the wavelength in consistent units. Consider the x component of $\bar{F}_{v,RAD}$; it is expressed in terms of $I_{v,RAD}$:

$$F_x = \int_{-\pi/2}^{\pi/2} I_v(\bar{s}) \cos(x, \bar{s}) d\omega$$

I_v is the spectral radiance (i.e. specific intensity) in Watts cm^{-2} Steradian frequency unit $^{-1}$ along the \bar{s} direction. ω is the solid angle over which the integral is to be taken. I_v is the solution to the equation of transfer for the geometry being considered:

$$\frac{dI_v(\bar{s})}{ds} = \kappa'_v(p,T) [B_v(T) - I_v(\bar{s})]$$

in which s is the magnitude of the direction vector \bar{s} and κ'_v is the spectral absorptivity including stimulated emission in cm^{-1} and is given by

$$\kappa'_v = \kappa_v(p,T)(1 - e^{-hv/kT})$$

$B_v(T)$ is the Planck distribution function. h is Planck's constant, k is Boltzmann's constant and are to be in units consistent with T and v . κ_v is the spectral absorptivity in cm^{-1} which in turn is the sum of the spectral absorptivities for bound-bound transitions, κ_v^{bb} , the spectral absorptivity for bound-free transitions, κ_v^{bf} , and the spectral absorptivity for free-free transitions, κ_v^{ff} :

$$\kappa_v = \kappa_v^{bb} + \kappa_v^{bf} + \kappa_v^{ff}$$

The relations between the spectral absorptivities and the transition probabilities for these processes will be presented in Appendix C.

FIGURE 1

The equations relating the electrical power input to the optical radiation and thermal conduction.

(Saha's equation) and thus the electron density, and in broadening the lines through electron, ion, and Van der Waals mechanisms.

2.1 Electrical and Thermal Conductivity

The transport properties (i.e., the electrical and thermal conductivities) of partially ionized gases are currently under extensive investigation in many laboratories. We have used de Voto's calculations^(9, 10) as applied to xenon using the momentum transfer cross section of Frost and Phelps.⁽¹¹⁾ The program for the electrical and thermal conductivities of xenon is given in Appendix A.

2.2 The Spectral Absorptivity

The spectral absorptivity of atomic species can now be calculated (in theory) to a relatively high precision without exorbitant computer time using "quantum defect" methods to obtain the transition probabilities for bound-bound transitions and the cross sections of the bound-free and free-free transitions. The electron broadening was calculated using the line broadening theory outlined by Griem⁽¹²⁾ as applied by Corinaldesi.⁽¹³⁾ Figure 2 shows schematically the calculation⁽³⁾ of the spectral absorptivities which are carried out in appendices C and D and how they relate to the other programs.

The population of the initial level is one of the most important determinants of the strength of an absorption as the population in the initial level can vary in orders of magnitude as the temperature changes a few thousand degrees. If the line in bound-bound transition arises from a ground or very low lying state, the population in the level is very high in the cooler gas near the walls, thereby leading to a high spectral absorptivity. Examples for these ground state transition are the resonances lines of xenon lying in the vacuum ultraviolet and the yellow doublet of sodium. The high spectral absorptivity will be manifested in the arc discharge by very broadened and self reversed emission bands.

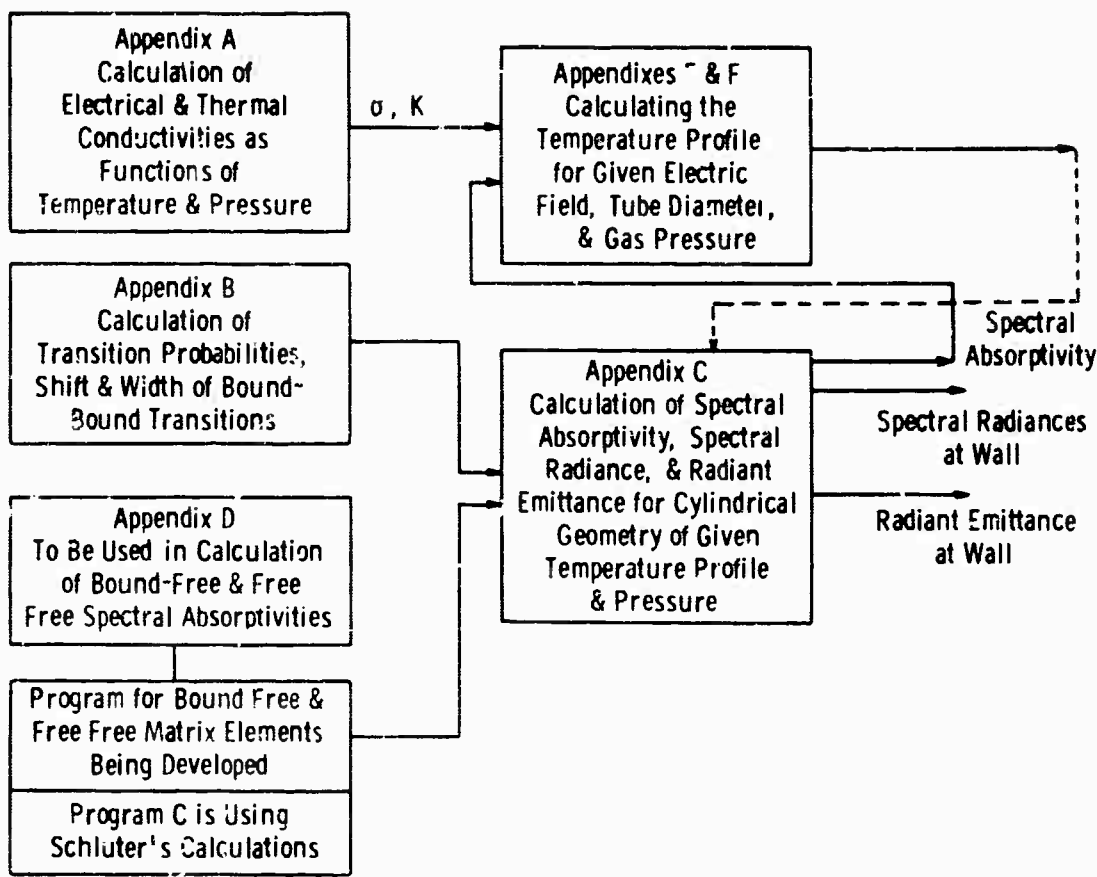


Fig. 2-The information flow for the calculation procedures in the appendixes

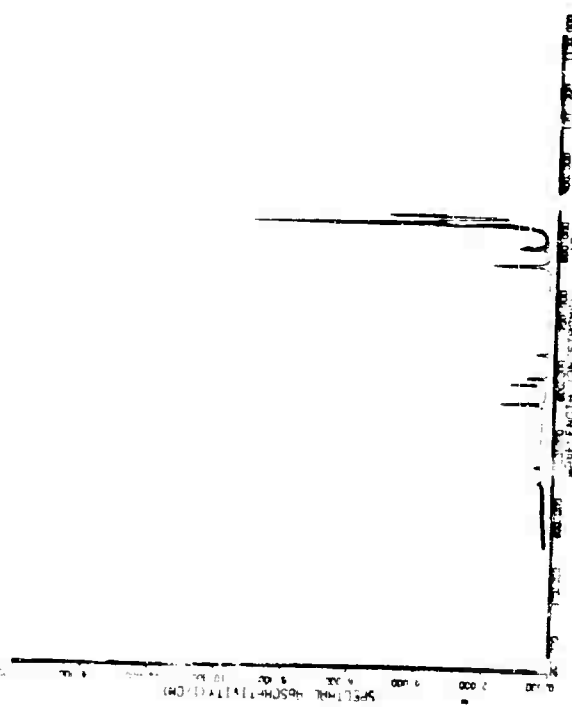
The shape of the line determines how the absorption varies with wavelength. We have considered the lines in the dense highly radiative plasmas treated herein to have a Lorentzian shape. The line width, w , and the shift, d , arises in the cases being considered from electron broadening in the center of the arc (Stark broadening theory), and neutral particle broadening near the edge (Van de Waals or resonance broadening).

The various broadening mechanisms are calculatable (in theory at least) for atomic systems such as xenon. Figure 3 shows the spectral absorptivities for xenon for a range of temperatures at the same pressure; 5 atm. The program for this is in Appendix C. The spectral absorptivities shown in Figure 3 include the broadened lines and the continuum. The lines were calculated using an intermediate coupling program described in the last report⁽⁴⁾ and in Appendix B which was the extension to xenon of the calculation of Garstang and Van Blerkom.⁽¹⁴⁾ The continuum was that calculated by Schluter⁽¹⁵⁾ and is described in an earlier report and in Appendix C. The upper limit on the spectral absorptivities that may be calculated by this program is limited to below those temperatures for which Xenon II becomes appreciable ($\sim < 14,000^{\circ}\text{K}$) (We are modifying the programs to include XeII, but this work was not available for this report.) The effect of the XeII will be to increase the continuum and the emission in the blue and ultraviolet as XeII does not have the strong infrared lines that XeI exhibits.

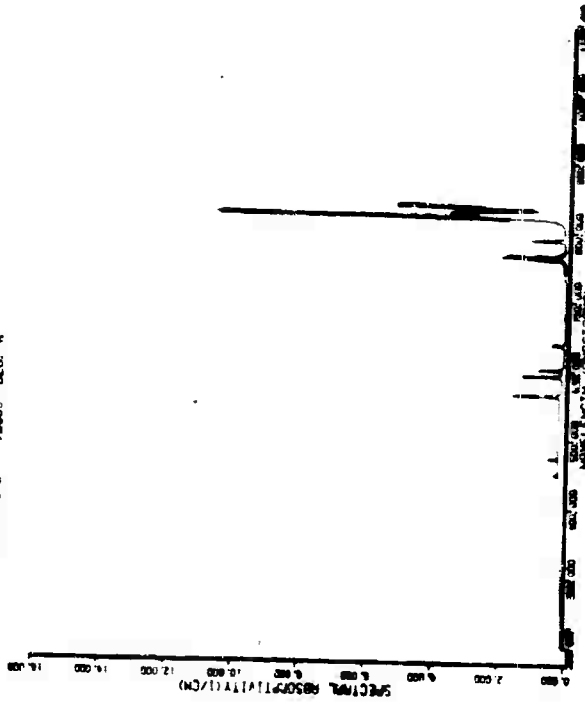
2.3 The Arc Models

Two approaches were used in the creation of models for the arc. In the simplest, the arc was assumed to be homogeneous in temperature and thermal conduction to the walls was neglected. In the more complete approach, the absolute temperature profile is calculated for a given electric field and tube diameter. From the temperature profile, the spectral radiance through the arc, the radiation external to the arc, and the thermal conduction to the walls can be calculated.

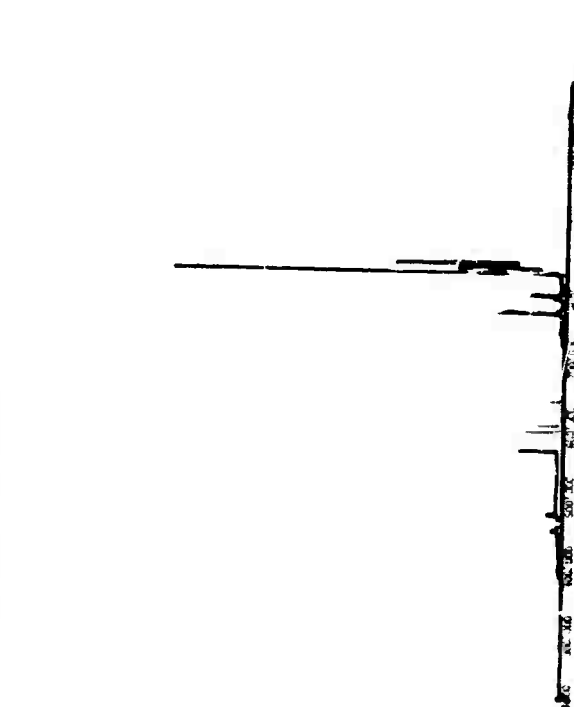
TEMPERATURE = 1100 K



TEMPERATURE = 1200 K DEG. K



TEMPERATURE = 1000 K



TEMPERATURE = 1000 K DEG. K

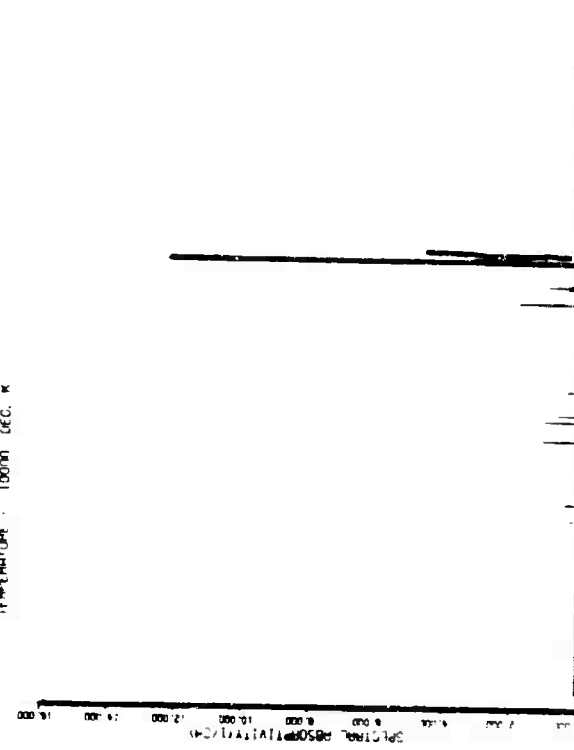


Fig. 3-The calculated spectral emissivity of Xenon I over a range of temperatures for a pressure of 5 atm

The inclusion of the free-free transitions and the more complete calculations of the bound-free transitions required more extended application of the quantum defect methods of Seaton⁽¹⁶⁾, and Burgess and Seaton⁽¹⁷⁾. Peach^(18,19), Schlüter⁽¹⁵⁾, and a series of papers by Biberman and Norman and their collaborators⁽²⁰⁾ have indicated improvements using the Coulomb field; Stewart and Rotenberg⁽²¹⁾ and McGuire⁽²²⁾ have extended the theory to the non-Coulomb potential found in the inner part of the atom. The rise of these methods required programs for calculating Whittaker functions⁽²³⁾ of real and imaginary argument. Appendix D presents ALGOL translation of and corrections to the FORTRAN programs of McGuire⁽²⁴⁾. These programs are to be used as entry points for the numerical integrations of the radial matrix elements for bound-free and free-free transitions.

The homogeneous temperature models considered the arc to be a cylinder of uniform temperature with the arc diameter to be an input parameter. The homogeneous temperature models for the pulsed arcs were found to give reasonable agreement with experiment if the arc diameter were properly chosen. In the previous report, the electrical conductivity determined from a .41 cm bore tube was used to calculate the arc core diameters for the larger tubes at the same temperatures using temperatures measured from a region of the spectrum that was assumed to be radiating like a black body. The radiant emittances (neglecting lines) calculated for the respective core diameters at the temperatures studied were found to account for the major portion of energy delivered to the flash tube.

The spectral radiance along a .8 cm diameter for a homogeneous temperature discharge of 12,000°A and 5 atm. is shown in Figure 4.

The spectral radiant emittances for two homogeneous temperature cylindrical arcs of .8 and 1.4 cm diameter are shown in Figure 5. The radiant emittance (i.e. radiative flux) is shown in the figure. The radiated power per unit length is simply the product of the radiant emittance and the surface area of the arc. The program for the calculation of the radiant emittance is part of Appendix C.

SPECTRAL RADIANCE AT SURFACE OF CYLINDRICAL HRC COLUMN
 FROM ALONG LINE OF SIGHT OF DIAMETER HAVING A SPATIAL
 TEMPERATURE GRADIENT.
 PRESSURE = 5.000 ATM

SPECTRAL RADIANCE (WATTS/CM²/STER, CM)
 $\times 10^3$

100,000 200,000 300,000 400,000 500,000 1000,000 1500,000 2000,000 2500,000 3000,000 3500,000 4000,000

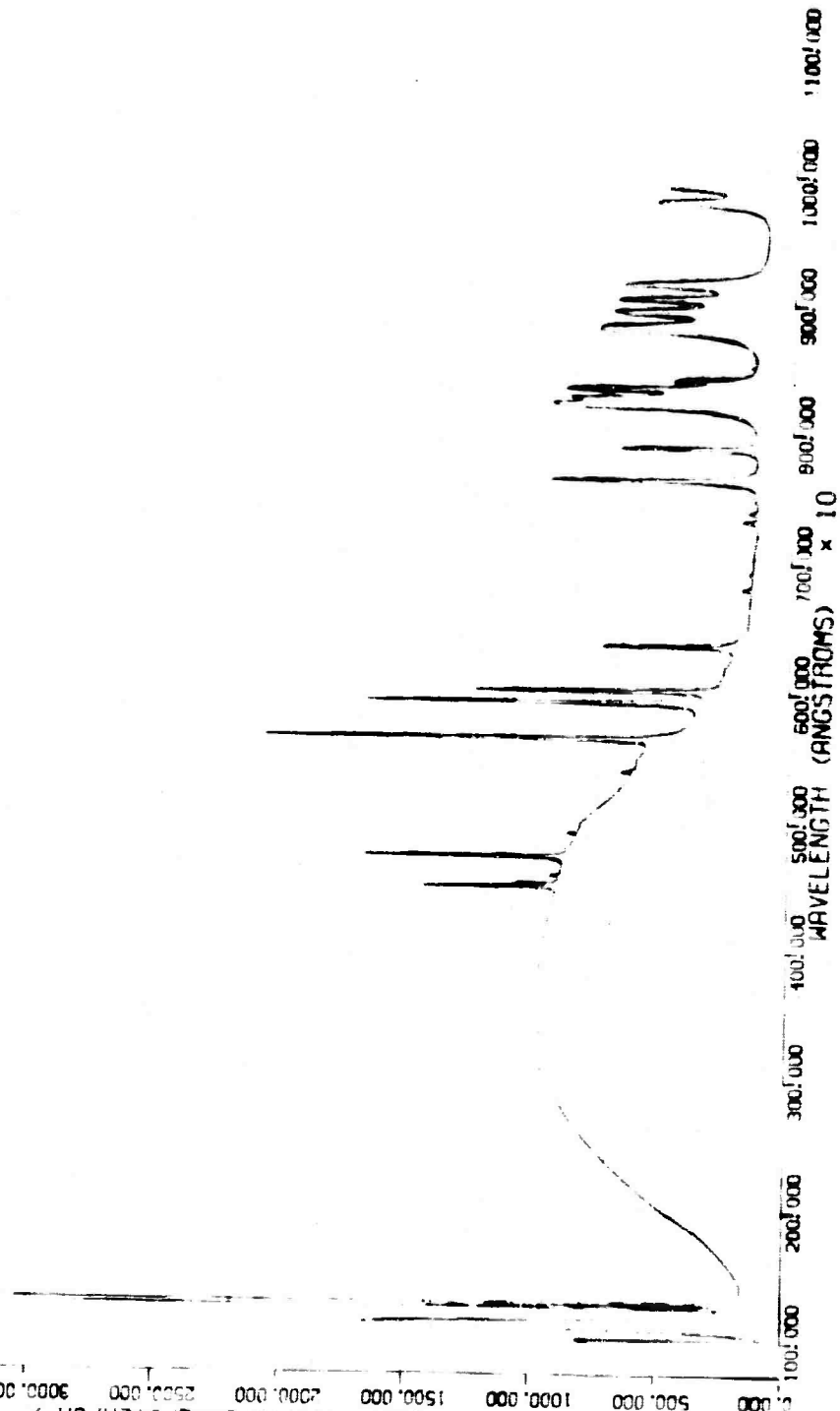
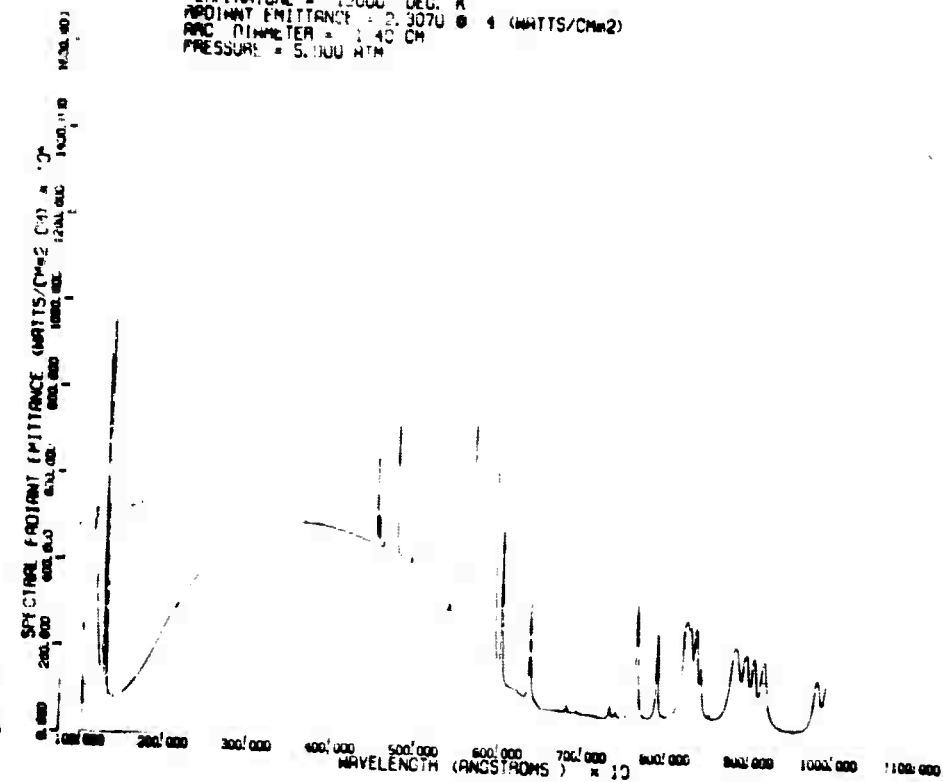


Fig. 4-The calculated spectral radiance along a .3 cm diameter homogeneous temperature Xenon plasma at 12000°K and 5 atm pressure

TEMPERATURE = 12000 DEG. K
 RADIANT EMITTANCE = 2.3070 \times 1 (WATTS/CM²)
 ARC DIAMETER = 1.40 CM
 PRESSURE = 5.000 ATM



TEMPERATURE = 12000 DEG. K
 RADIANT EMITTANCE = 7.4709 \times 1 (WATTS/CM²)
 ARC DIAMETER = 0.80 CM
 PRESSURE = 5.000 ATM

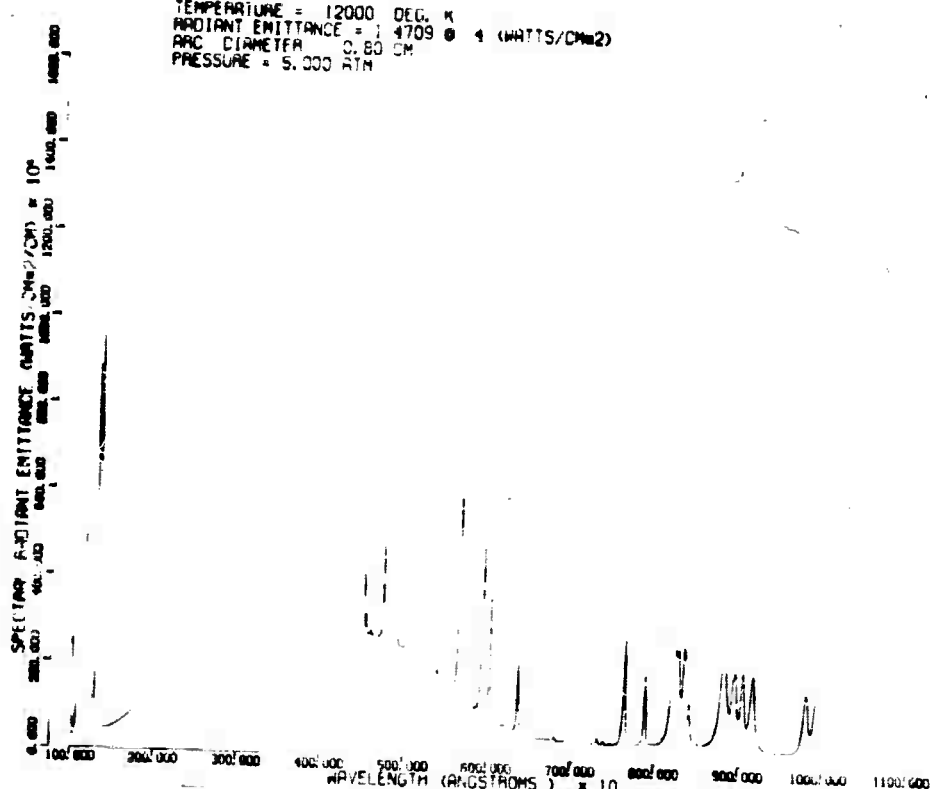


Fig. 3-The calculated spectral radiant emittances for .8 cm and 1.4 cm diameter homogeneous temperature cylindrical plasmas in Xenon at 12000°K & 5 atm pressure

The ideal model for the arc is one in which the characteristics of the arc discharge are determined by the input parameters: the electric field across the arc, the geometry of the a.c. container (i.e., the inside diameter of the cylinder), and the pressure and composition of the fill gas. But this model requires the solution to an integral-differential equation, called the energy balance equation, shown in part in Figure 1. The result of the application of the equation is simply the temperature distribution within the arc column.

We have explored a few methods for solving the energy balance equation for non-gray, nonhomogeneous plasma. The problem may be divided into two phases: determining the radiative flux (i.e., radiant emittance) throughout the arc column, and using the radiative flux together with the transport properties to find the temperature profile that satisfies the integral differential equation.

In this work, on Contract Nonr 4647(00), the radiative flux was calculated using an exact integration (described in Reference 2 and 25) and an approximate integration based upon a technique of Sampson⁽²⁶⁾. The latter method was approximately ten times faster to compute than the former, and has given good agreement for the cases tested though it does not as yet include lines nor very steep ionization edges.

The temperature profile is calculated by using a relaxation method applied to the energy balance equation. In this, the radiative flux for an assumed (best guess) temperature profile is calculated. Using this radiative flux in a time dependent energy balance equation, the contributions of the other components of the energy balance equation are then calculated. By iterating the process over and over, a temperature profile that satisfies the equation could be calculated (i.e., where the time dependent part equals zero). This is described in Appendix E.

A program has been developed which combines the exact and approximate calculations to obtain a profile. The results of a sample calculation together with the program are given in Appendix E also.

To provide further insight into this calculation, an analysis procedure devised in other work⁽⁵⁾ was applied to the xenon arc. The complete analysis together with calculated fluxes and temperature profiles is in Appendix F.

In all of these calculations, the pressure throughout the discharge is considered to be constant; that is, radiation and magnetic effects upon the pressure were neglected^(1,2). The gas pressure before the initiation of the discharge is known (typically, it is 150 to 300 torr for the xenon-filled flash tubes). Recent calculations have indicated that the final pressure in the fully developed arc is strongly dependent upon the temperature profile. A simple example will illustrate this dependence. Consider a simple two temperature confined arc in which the arc core is at 10,000°K, the volume near the walls is at 1000°K, and neglect the electron contribution to the pressure. It is simply shown that a cool arc volume of only 10% of the central core volume will reduce the arc pressure by a factor of two from the pressure that would occur if the central core occupied the whole volume as we had assumed in the earlier homogeneous temperature models^(1,2,3). This consideration in the pressure becomes very important for the larger diameters with larger cool portions⁽⁴⁾.

III. COUPLING THE PUMP INTO THE LASER ROD

The ideal pump for optical lasers is one in which a major fraction of the energy radiated can be coupled or at least incident upon the laser rod. There are two general methods to do this: the diffusely reflecting cavity and the focussing cavity. We have investigated a particular diffusely reflecting cavity, the coaxial laser pump, which is well suited for use with large high energy pulsed laser, and a high image quality focussing system, the spherical cavity, which has demonstrated high efficiency in continuously operating laser systems⁽²⁸⁾.

Figure 6 shows a cross sectional drawing transverse to the rod of a current design coaxial lamp. The radiation from the plasma surrounds the laser rod. The MgO layer diffusely reflects the radiation back toward the laser rod. As Whittle and Skinner⁽²⁹⁾ point out, in a recent paper, the efficiency of the system may be obtained roughly by comparing the product of the area and energy absorbed by the rod with the sum of the products of areas and absorptions for the whole system. In this analysis

Dwg. 746A824

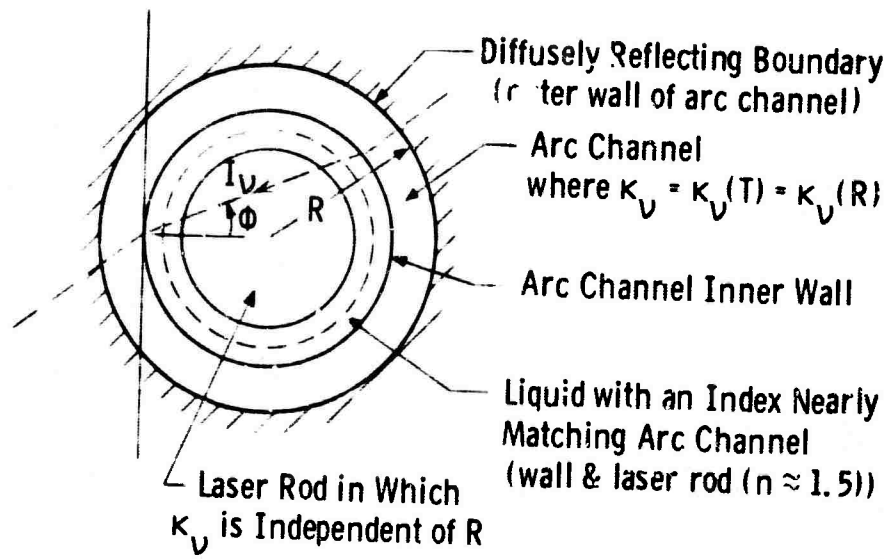


Fig. 6—Simplified representation of laser rod-coaxial laser pump system

an open area is considered to be complete absorption. Good laser pump design would seek to minimize openings (as for electrodes) and minimize non-laser rod area. This line of reasoning is counter balanced partially by the need to minimize thermal conduction which varies with the gradient and may vary with plasma thickness. An unknown quantity in the analysis of an MgO reflector coaxial lamp is the reflectivity of the MgO layer under the conditions in the flash tube. This important parameter would need to be determined for a quantitative analysis of this pumping geometry.

Figure 7 is of a possible evolution of the coaxial laser pump which minimizes thermal losses, and allows very high energy outputs from energy limited laser rods. The minimizing of the thermal losses arises from the reduction per unit laser rod area of absorbing diffusely reflecting surfaces and of thermally conducting walls

To date our efforts in the use of the spherical cavity have been with small rods though the geometry need not be limited to them. Figure 8 from Ref. 28 shows the geometry of the spherical cavity with the laser rod and laser pump symmetrically disposed about the radius of curvature. If the laser rod length is small enough relative to the diameter of this sphere (and the spherical mirrors are of optical quality), the image of the lamp can be placed upon the rod for a very large fraction of the total solid angle. The data we have at present were obtained on 3 x 30 mm laser rods in which were obtained an efficiency of 1.15% and a total power of 3.6 watts for a Nd:YAG rod with external resonators. The application of this high efficiency system to larger laser rods is underway.

The spherical cavity has many advantages for laser pumping and a major disadvantage, this being the size sphere required for a rod of a given length (the diameter of the sphere should be considerably larger than the rod length). Some of the advantages include a high transfer efficiency (that can be calculated and ray traced readily), and a relatively remote reflecting surface (less subject to radiation damage).

Dwg. 852A867

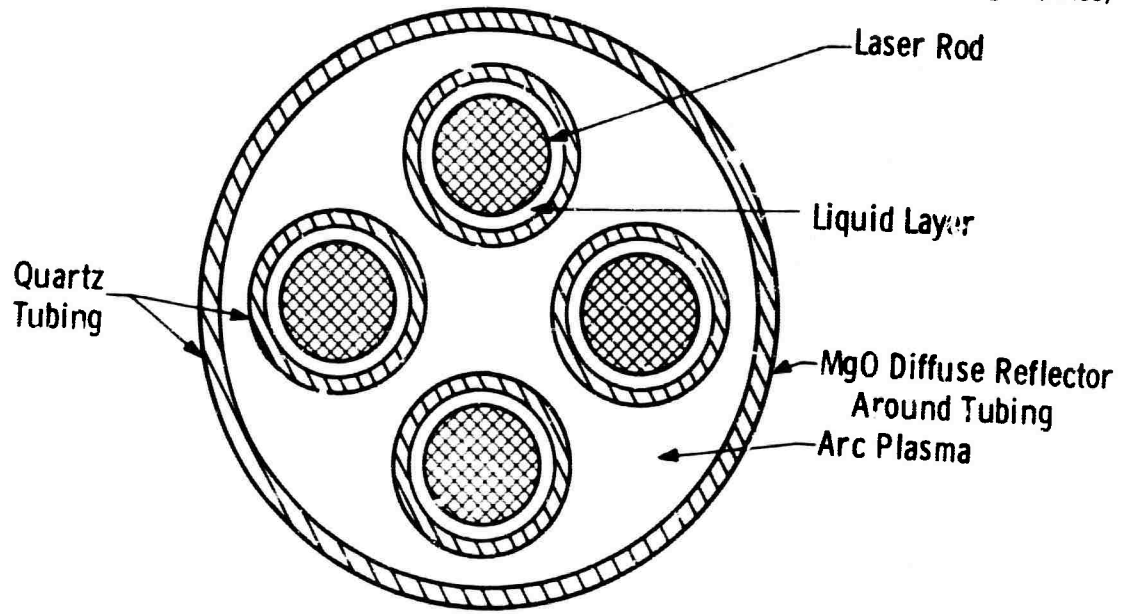


Fig. 7—Multiple rod coaxial laser pump

Dwg. 852A390

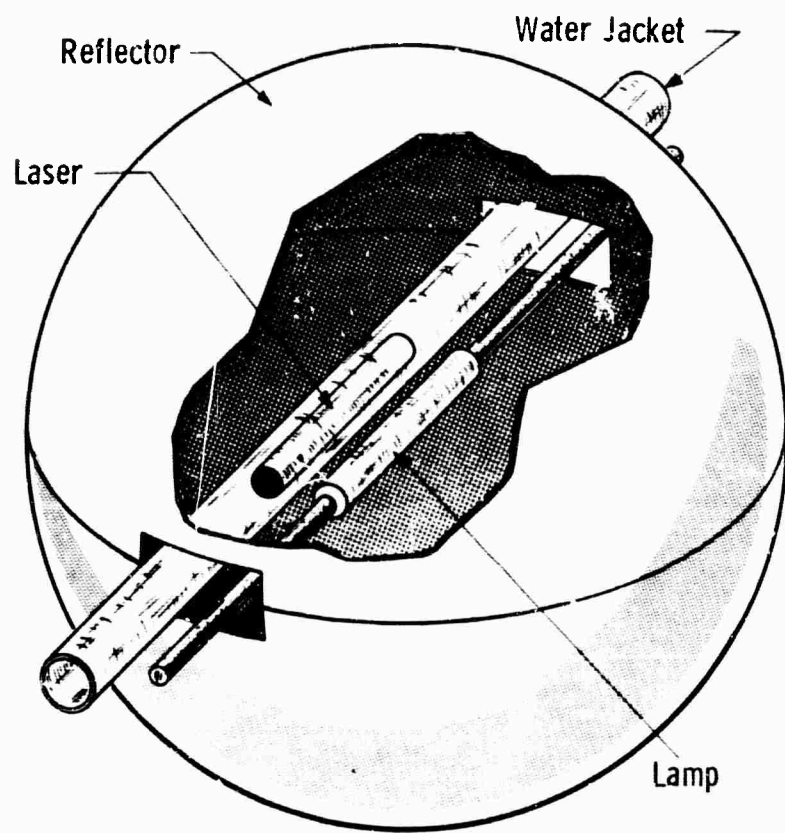


Fig. 3-Geometry of the spherical reflector

The sphere may be fabricated in large sizes readily to optical tolerances. The results obtained with the spherical cavity indicate promise for use in high energy laser pumping.

IV. RECENT EXPERIMENTAL MEASUREMENTS ON THE ARC

The experimental measurements taken throughout this work have been directed towards improving and verifying the information used in the models. Early in the work, we developed a technique to measure the temperature of the plasma (More correctly we developed a technique to measure the lower bound of the temperature - we will treat this more thoroughly in the discussion in double pulsed arcs). To calculate the spectral properties, we needed to know the pressure in the discharge. As we had the initial pressure of the gas (typically 150 torr) and the arc filled the tube to a first approximation, we initially assumed a homogeneous temperature. The arc was measured from the radial distribution of the spectral radiance in the ultraviolet to be relatively homogeneous for a large fraction of the radius - though subsequent estimates from the electrical conductivity discussed in the last semi-annual report⁽⁴⁾ indicated this fraction varied with flash tube inside diameter. Recent analysis of the effect upon the pressure of the temperature profile within the tube indicated that measurements of the pressure or the electron density were required.

The experimental work in the past few months has been concerned with measurements of the pressure using a piezoelectric transducer, a Kistler Instrument Co. 603A, and of the spectral radiance in the vicinity of some lines and in various continuum regions for the arc under power densities over 1.5 MW/cm^3 (using pulse preionization⁽⁷⁾). Measurements were also made of the spectral radiance in the ultraviolet (at 3000 Å) for the arc viewed side in and viewed end on. These measurements from the side and end would give a path length difference of ten or more depending upon the tube.

The pressure measurements for the 12.7 and 19 mm inside diameter tubes had shown a pressure considerably lower than that calculated for a homogeneous temperature distribution. The transducer output was very oscillatory reducing the accuracy. These measurements indicated that there was a cool volume near the walls which could change considerably during the arc cycle. A laser interferometer is being set up to measure the electron density in the center of the arc, but no final results are available for this report. The interferometer is similar to that of Gerardo et. al.⁽⁸⁾ in which the flash tube is inside a reference cavity which is in series with the laser cavity. Measurements of the electron density with the interferometer together with those of temperatures will characterize more fully the arc plasma.

The measurements of the temperature in the double pulsed arc required finding spectral regions in which the emission from the arc was not self-reversed but still optically thick. The 8231.6^oA line of XeI was suspected to be self-reversed at power densities above about .1 MW/cm³. This was confirmed using the high resolution rapid scanning spectrometer⁽⁶⁾. Calculations of the spectral radiance (using the program in Appendix C) for a temperature profile similar to that expected in the arc showed self reversal in the immediate vicinity of the 8231.6^oA lines.

The spectral radiances measured for the lines and the continuum are shown in Figures 9 through 12 for power densities over 1.5 MW/cm³. In Figures 9 and 10, the spectral radiance is plotted in terms of the equivalent black body temperature. The power is the input power dissipated in the lamp per unit volume. The flash tube diameters ranged from .41 cm to 1.94 cm. The tubes were preionized with a .5 ms pulse (100-600 μ F in series with 100 μ H). The main pulse was about 50 μ s long (50-100 μ F and the residual inductance \sim 3 μ H). The main pulse was switched in by means of an ignitron using the circuit shown in Reference 6. The self reversal of the 8231.6^oA line of XeI was considered to be the primary reason for the reduction in the spectral radiances for the larger diameter flash tubes. Figure 13 gives the spectral radiance distribution for an EG & G Inc. FX-52 flash tube under single and double pulsed conditions. The data was taken with a spectral width of about 1^oA at the wavelengths indicated.

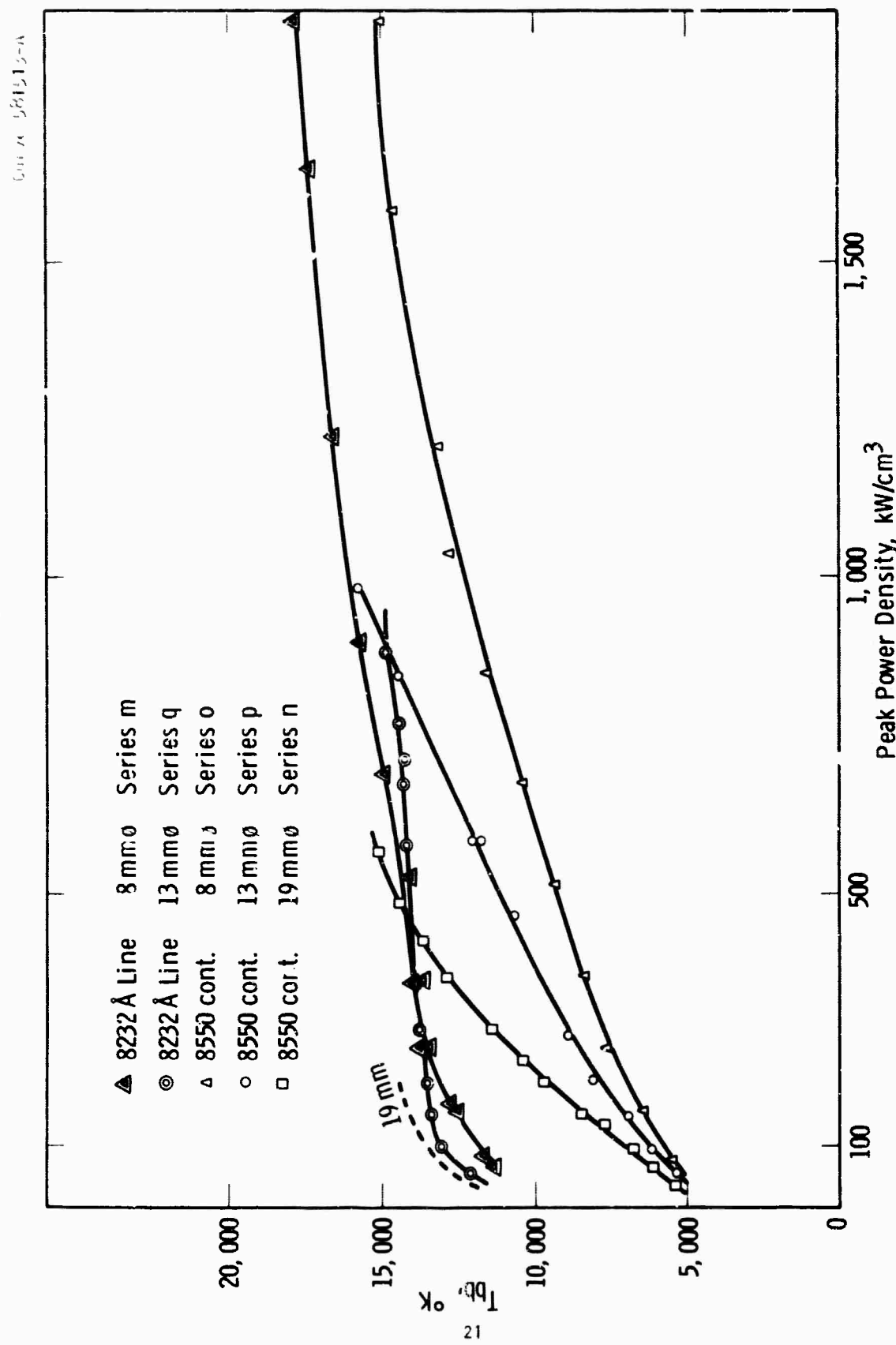


Fig. 9—Black body temperature corresponding to measured spectral radiance
as a function of input power density

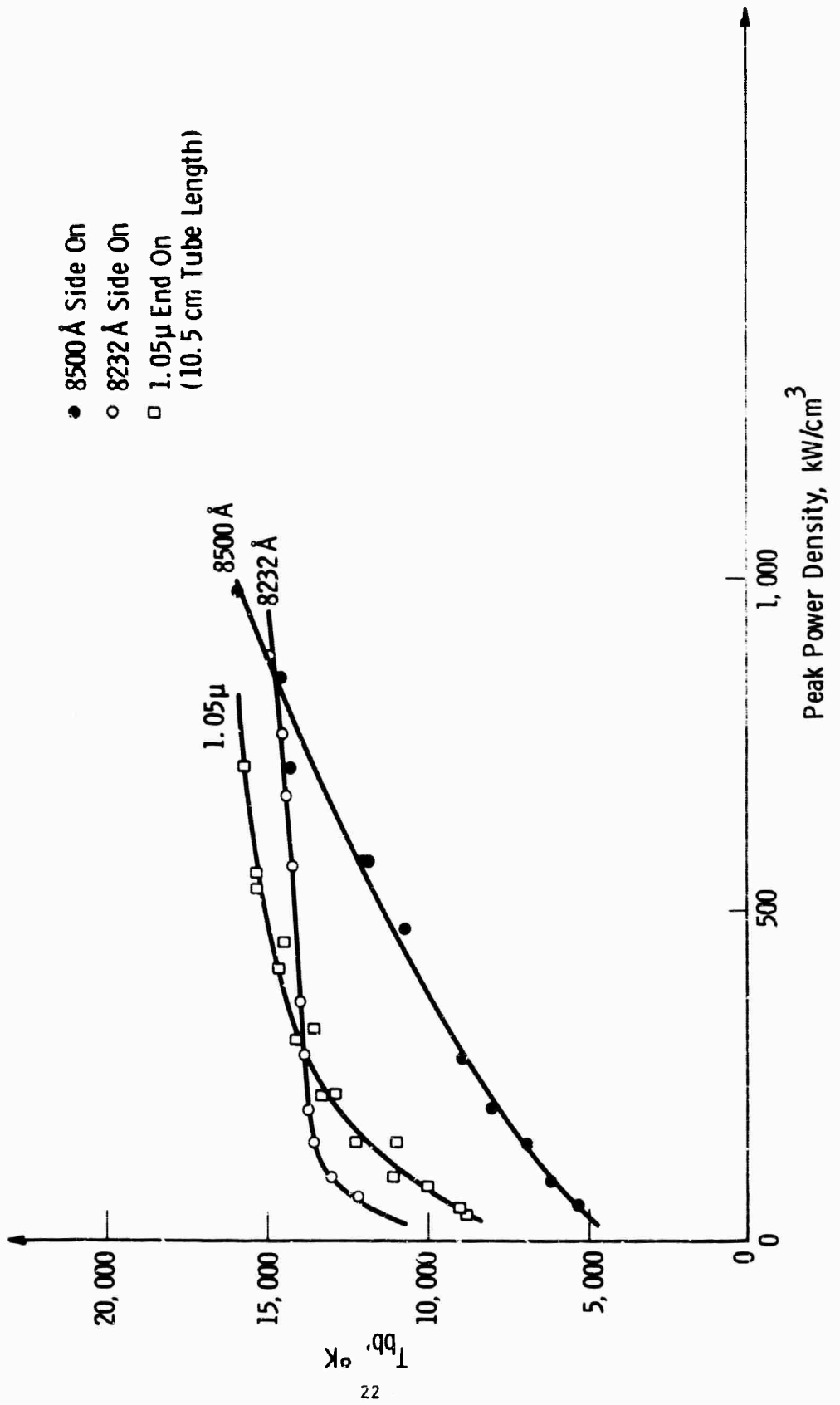


Fig. 10—Black body temperature corresponding to same spectral radiance as 13 mm flash tube as a function of input power density

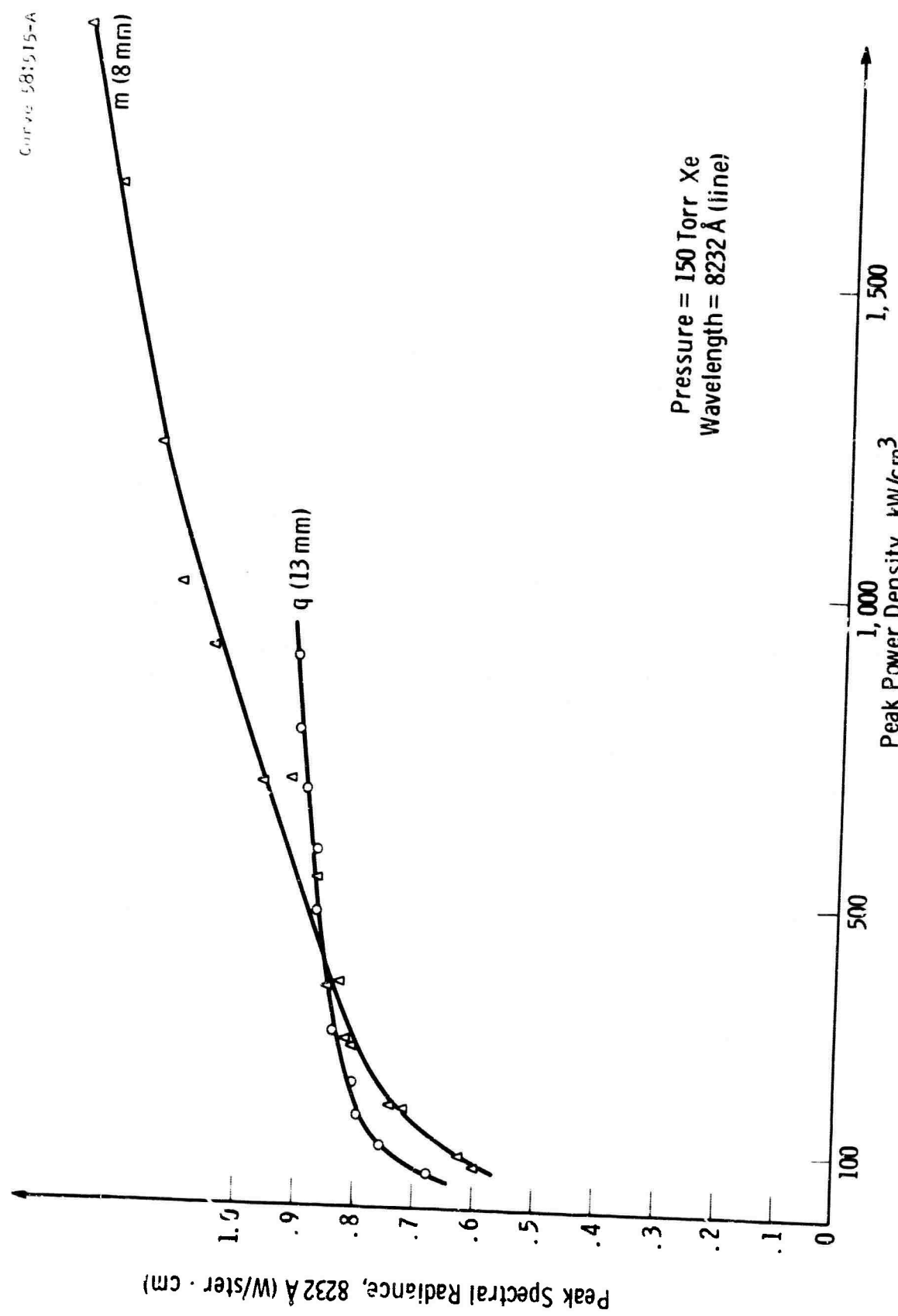


Fig. 11—Spectral radiance of linear cylindrical Xe flash tubes of different diameters as a function of power density input

Curve 58151t-A

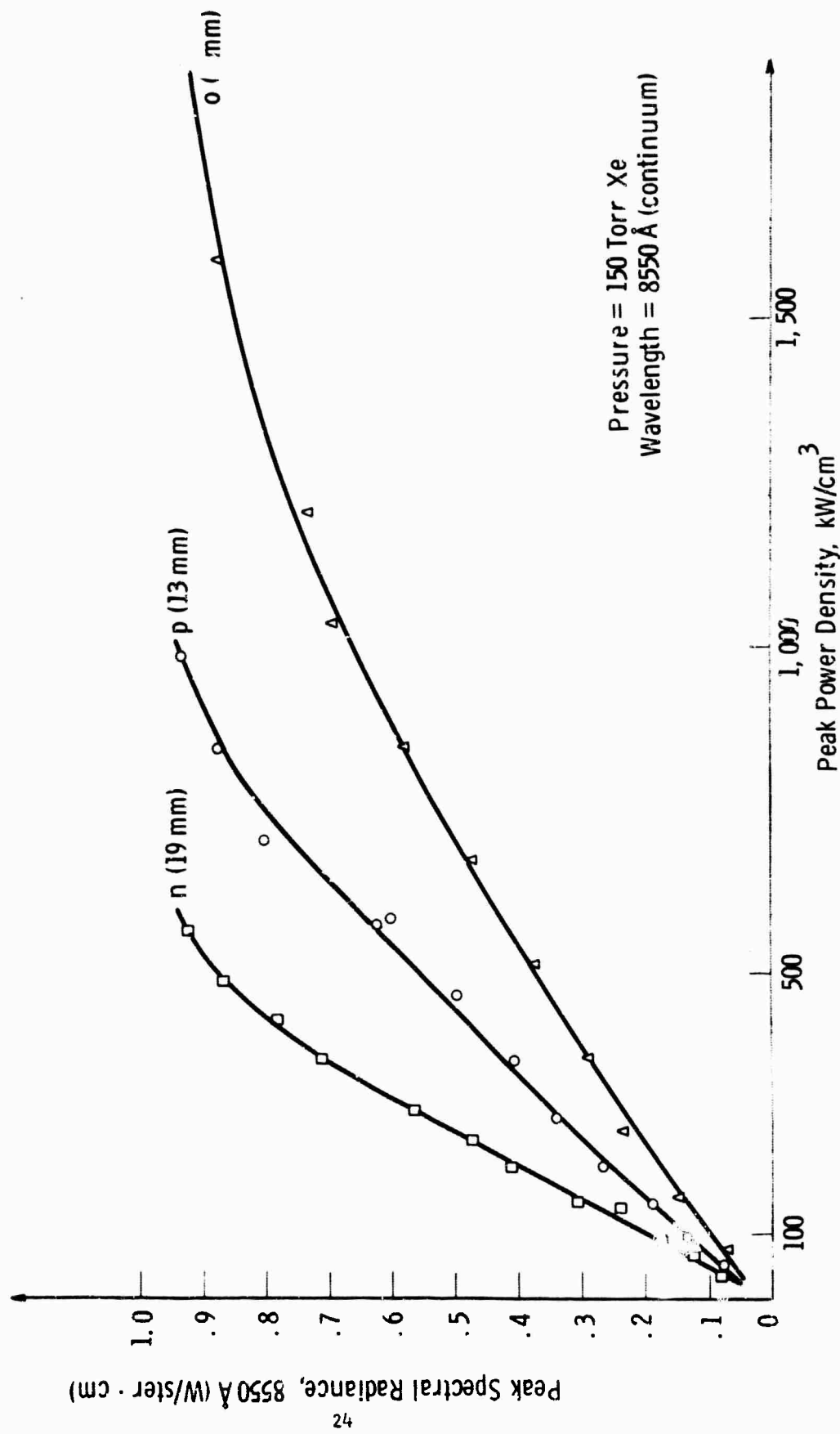


Fig. 12—Spectral radiance of linear cylindrical Xe flash tubes of different diameters as a function of power input

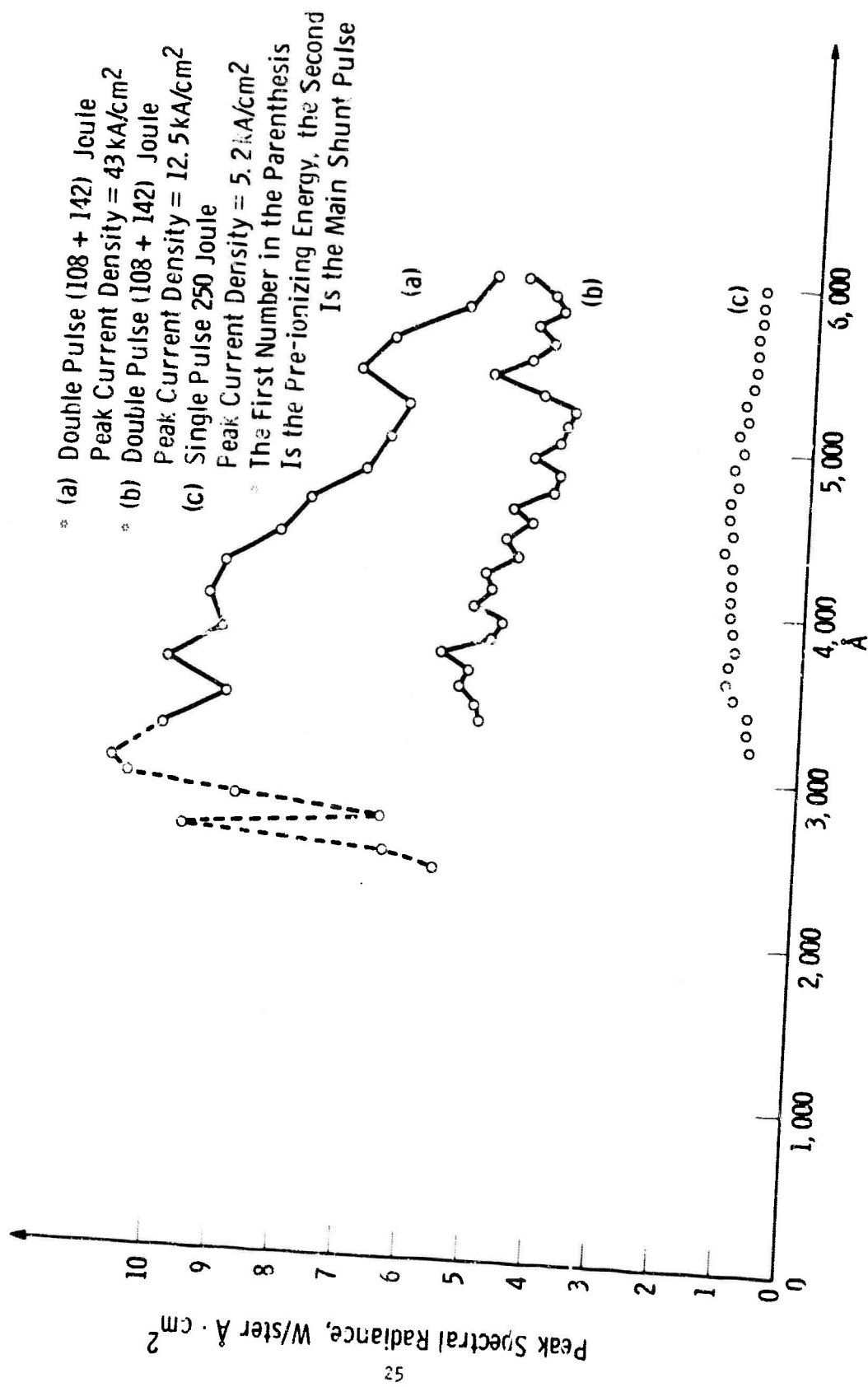


Fig. 13—Spectral radiance distribution for an EG & G Inc. FX-52 flash tube single & double pulsed

The measurements of the spectral radiance at 3000 Å on flash tubes viewed side on and viewed end on yielded the theoretical ratio of the length of the tube to diameter of the tube for lower energies only when the tungsten electrodes were moved back out of the arc. The ratio again deviated at the higher currents as shown in Figure 14. This may arise in part from further tungsten injection, but also may be due to the plasma becoming thick for the flash tube length being viewed.

We have not yet made a detailed comparison of the calculated radiances with those measured experimentally. This requires a more accurate knowledge of the pressure and/or the electron density than we currently have. We shall be making these comparisons after the laser interferometer is completed. To compare the spectral radiances observed in Figure 13 with the calculated values in Figure 4, multiply the values in Figure 13 by 10^8 to obtain the values in Figure 4 ($\text{W}/\text{cm}^2 \text{ Ster cm}$). The single pulsed values correspond with those for the plot in Figure 4; the exact agreement requiring better values of pressure than we currently have.

Curve 561518-A

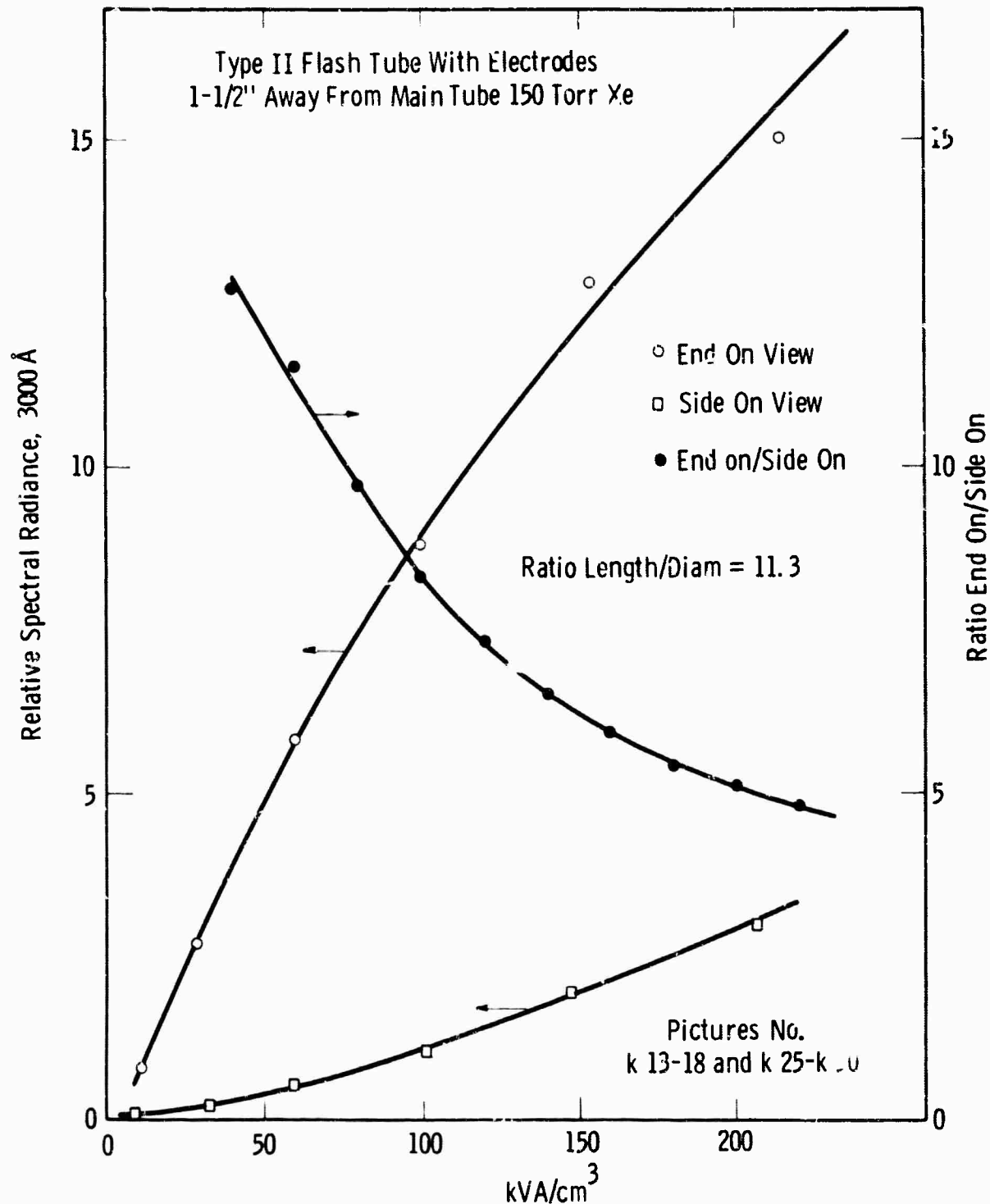


Fig. 14-The spectral radiance viewed at 3000 Å end on and side on
for a 13 mm diameter arc tube

V. SUMMARY AND CONCLUSIONS

This report presents a description of the work carried out on Contract No. 4647(00) towards the creation of quantitative models for the pulsed arc discharge that is used for the optical pumping of high energy solid state lasers. The primary results of these studies are computer programs for the calculations of the physical properties of the arc plasma, using xenon as the working gas, and for determining the balance within the arc between radiation external to the arc and thermal losses to the walls. The experimental results obtained since the last semiannual reports are also described. The experimental studies have been concerned with measurements of the pressure within the arc, and the characterization of the arcs at very high power densities.

The models for the arc developed in this work are at present only semi-quantitative. They possess the main features of the arc, exhibiting the saturation of the radiation in the infrared, the strong dependence upon power density of the radiation emitted in the ultraviolet; and the nearly homogeneous temperature distribution that have been observed in these arcs. To improve the accuracy of the models, more complete and accurate measurements of the physical properties need to be made. Through the use of the model calculations, quantitative comparisons can be made between the power input, the average electrical conductivity, the spectral absorptivities in various regions of the continuum and in the vicinity of selected lines, and of the pressure and electron density to make a consistent picture.

The full implications of these models are still being explored. The models are allowing a new insight into the behavior of the high density arc. The arc models help to remove the high density plasma - the light emitting plasmas - from the "art" area of technology.

We hope that the work described in this series of reports will assist the designer of optically pumped lasers in the development and improvement of this area of laser technology.

Through this work, we hope that we are bringing to bear on an old problem-- light sources--some of the new techniques in both theory and experiment that were developed by a wide variety of people working in areas far removed from the optical pumping of lasers.

VI. ACKNOWLEDGMENTS

We wish to acknowledge the assistance and real contribution of many people to this series of research programs. R. D. Haun, Jr., of Westinghouse Research Laboratories, J. McNall of the Lamp Division of Westinghouse Electric Corp., and Elliot Weinberg of ONR-San Francisco, contributed encouragement of both the moral and physical varieties. Contributors to this work other than the listed include E. F. G. Arrott, A. V. Phelps, L. S. Frost, R. G. Schlecht (now at Aeroneutronics), and L. Gampel (now at Electro Optical Systems, Inc.). We would also like to thank E. Corinaldesi of Boston University, D. Sun of California Institute of Technology, R. A. Day of Harvard College Observatory, and R. S. de Voto of Stanford University for their share of the developing of the computer programs used on this work. The technicians involved in the measurements included R. L. Grassell, J. Humphreys, J. Russell, J. Nee, and R. Webb.

The reproduction of the man reports for this work was carried under the directions of Miss E. Marko, with the assistance of Mrs. M. Howard, Mrs. J. Connors, and many others. The drafting was supervised by Mr. J. Getsko and Mr. M. Bowman; the reproductions were under Messers. K. Moelk, H. Payne, and J. MacKenzie.

To all of the above, we wish to give a sincere thank you.

REFERENCES

1. C. H. Church and R. G. Schlecht, "Arc Discharge Sources, Semiannual Report on Contract Nonr 4647(00)", 15 May 1965, AD 462 792.
2. C. H. Church, R. G. Schlecht, I. Liberman, B. W. Swanson, E. G. F. Arnott and E. Geil, "Arc Discharge Sources, Final (Actually Semiannual) Report on Contract Nonr 4647(00)", 15 November 1965, AD 473 996.
3. C. H. Church, R. G. Schlecht, I. Liberman, B. W. Swanson and E. Geil, "Arc Discharge Sources, Semiannual Report on Contract Nonr 4647(00)", 15 May 1966, AD 632 892.
4. C. H. Church, B. W. Swanson, P. Buchhave, G. Basi, R. Liebermann, E. Geil and L. A. C. Weaver, "Arc Discharge Sources, Semiannual Report on Contract Nonr 4647(00)", 15 November 1966, AD 803 542.
5. J. J. Lowke and E. R. Capriotti, Westinghouse Research Labs, Scientific Report 66-1E2-GASES-R1 (1966).
6. I. Liberman, C. H. Church and J. Asars, Appl. Optics 6, 279 (1967).
7. C. H. Church and L. Gampel, Appl. Optics 5, 241 (1966).
8. J. B. Gerardo and J. T. Verdeyen, Proc. IEEE 52, 690 (1964).
J. B. Gerardo, J. T. Verdeyen and M. A. Gusinow, J. Appl. Phys. 36, 2 146 (1965).
J. B. Gerardo and R. A. Hill, Phys. Rev. Letters 17, 623 (1966).
9. R. S. de Voto, Physics of Fluids 9, 1230 (1966).
10. R. S. de Voto, "Simplified Expressions for the Transport Properties of Ionized Monatomic bases", Stanford University, Report No. SUDAAR No. 283 (July 1966).
11. L. Frost and A. Phelps, Phys. Rev. 136, 1538 (1964).
12. H. Griem, Plasma Spectroscopy, McGraw Hill Book Co., New York (1964). See also J. Cooper "Plasma Spectroscopy" in Reports of Progress in Physics 29, pt. 1, 35 (1966).
13. E. Corinaldesi, private communication.
14. R. Garstang and J. Van Blerkom, J. Opt. Soc. Am. 55, 1054 (1965).
15. D. Schiüter, Z. Astrophys. 61, 67 (1965) and private communication.

16. M. Seaton, Mon. Not. Roy. Astron. Soc. 118, 504 (1958).
17. A. Burgess and M. Seaton, Mon. Not. Roy. Astron. Soc. 120, 121 (1960).
18. G. Peach, Mon. Not. Roy. Astron. Soc. 130, 361 (1965).
19. G. Peach, to be published in Memoirs Roy. Astron. Soc.
20. See for example L. M. Biberman and G. Norman, J. Quant. Spect. Rad. Transfer 3, 221 (1963). Translated in General Atomics - San Diego Translation GA tr 4943, there are many other papers by this group, primarily published in Optics and Spectroscopy.
21. J. C. Stewart and M. Rotenberg, Phys. Rev. 140, A 1508 (1965).
22. E. McGuire, Thesis, Cornell University, (1965).
23. M. Abramowitz and I. Stegun, Editors, "Handbook of Mathematical Functions with Formula, Graphs and Mathematical Tables", National Bureau of Standards, Applied Mathematical Series 55, U.S. Government Printing Office, Washington D.C., 20402 (1964).
24. E. McGuire, private communication.
25. C. H. Church, R. G. Schlecht, I. Liberman, and B. W. Swanson, A.I.A.A. Journal 4, 1947 (1966).
26. D. Sampson, J. Quant. Spect. Rad. Transfer 5, 211 (1965).
27. J. L. Emmett and A. L. Schawlow, Appl. Phys. Letters 2, 204 (1963).
28. C. H. Church and I. Liberman, "The Spherical Reflector for Use in the Optical Pumping of Lasers", Westinghouse Scientific Paper 66-9C1-LHICW-P1 (1966).
29. J. Whittle and D. R. Skinner, Appl. Optics 5, 1179 (1966).

BLANK PAGE

APPENDIX A

A PROGRAM FOR THE CALCULATION OF THE ELECTRICAL AND THERMAL CONDUCTIVITY OF XENON AS A FUNCTION OF TEMPERATURE AND PRESSURE

by

R. S. deVoto
Stanford University

This program, ELEC/THERM, calculates the various components of the electrical and the thermal conductivities of xenon as a function of pressure and temperature under local thermal equilibrium conditions.

The program will calculate these quantities for argon also.

The input data for argon is:

1. "ARGON", number of species - 1 (we used 2)
2. initial temperature, temperature step size, maximum temperature desired
3. number of pressures; the pressures in atmospheres
4. PHIOA (3.23 @ 4), RHOA (.224), PHIOI (5.38 @ 6), RHOI (.1965), AC (25.615), BC (1.1960), HIER (must be 0).
5. electron mass (9.1091 at -28), molec. wt. of atom (39.944), molec. wt. of first ion (39.944), molec. wt. of any other ions used.

For xenon the data required is similar to the ARGON program.

1. "XENON", 2,
2. initial temperature, step size, maximum temperature desired
3. number of pressures, the pressures (in atmospheres)
4. 3.11 @ 6, .208,0,0, 25.639, .99752,0, 9.109 @ -28, 131.3,131.3.

20122807 FRIDAY, NOVEMBER 4, 1966

ML ALGOL VERSION OF 10/20/66

PROCEDURE DETERMINE(NC,NR,N,I,DET,POR)COMMENT VERSION 10/19/65 EVALUATE NR
 ,NC,N INTEGER NC,NR,N IS DOUBLE REAL GETREAL ARRAY P(0,0)IS BEGIN COMMENT NC AN
 I, NR ARE INDICES OF FIRST ROW AND FIRST COLUMN IN ARRAY OF WHICH THE DET
 ERMINANT IS TO BE EVALUATED, N+I IS RANK INTEGER J,K,P,0,1NOREAL ARRAY

0025	IS DOAB LONG, NEXT SEG 0002
0010	SC 21 1912
0020	SC 21 1912
0030	SC 21 1912
0040	SC 21 1912
START OF SEGMENT *****	0026
0050	SC 21 010
0060	SC 21 010
0070	SC 21 1A11
0080	SC 21 2712
0090	SC 21 3211
0100	SC 21 3A19
0110	SC 21 6712
0120	SC 21 5A13
0130	SC 21 A113
0140	SC 21 7312
0150	SC 21 8A12
0160	SC 21 9A12
ENDNEND DTERM ;	

PROCEDURE TRANS(T,P,MAX, SIGMA,LNBDIA) ;
 COMMENT T IN DEGREES K, P IN TORR, N IS ARRAY OF NUMBER DENSITIES; 0 =
 ELECTRON, 1 = ATOM, 2 AND HIGHER = IONS, MAX IS INTEGER NUMBER OF SPECI
 ES - 1, SIGMA AND LNBDIA ARE ELECT AND THERMAL CONDUCTIVITIES ;
 VALUE T,P,MAX ;
 REAL T,P,MAX ;
 REAL T,P,SIGMA,LNBDIA ;
 BEGIN
 REAL ARRAY A(0:15,0:15,1:DIF(015)) ;
 INTEGER I,J,L,M,K2,EXND,EXDNH ;
 LABEL L1 ;
 REAL ION J ;
 REAL TROD1,T50,NTOT,RHO,LNDAE,ML2,NUM,DPNOM,NMAX, TH1,M12,
 ML4, LMDAEL,MLM1 ;
 OWN REAL AC,RCR,PHIO1,PHIO2,PHIO3,PHIO4,PHIO5,PHIO6,PHIO7,PHIO8,PHIO9,PHIO10 ;
 OWN REAL ARRAY M1015,ML1015,ML1015,ML1015 ;
 OWN DOUBLE PRECISION M1015,ML1015,ML1015,ML1015 ;
 OFFLINE F1M = FOR I = 1 STEP 1 UNTIL MAX DO ;
 F1JIM = FOR J = 1 STEP 1 UNTIL MAX DO ;
 F1LM = FOR L = 1 STEP 1 UNTIL MAX DO ;
 F1JM = FOR J = 1 STEP 1 UNTIL MAX DO ;
 F1OM = FOR I = 0 STEP 1 UNTIL MAX DO ;
 F1JM = FOR J = 0 STEP 1 UNTIL MAX DO ;
 LTST Y1C RHIO1,RHOA,PHIO1,PHIO2,BC, MIER, FROM M111 ;
 FORMAT FCROSS (*"CROSS SECTIONS.,,*"/ (9(F11.6,X13))) ;

0026	IS 0105 LONG, NEXT SEG 0002
WEST0002	SC 21 1912
WEST0003	SC 21 1912
WEST0004	SC 21 1912
WEST0005	SC 21 1912
WEST0006	SC 21 1912
WEST0007	SC 21 1912
WEST0008	SC 21 1912
WEST0009	SC 21 1912
START OF SEGMENT *****	0027
WEST0010	SC 21 113
WEST0011	SC 21 113
WEST0012	SC 21 113
WEST0013	SC 21 113
WEST0014	SC 21 113
WEST0015	SC 21 517
WEST0016	SC 21 517
WEST0017	SC 21 517
WEST0018	SC 21 517
WEST0019	SC 21 517
WEST0020	SC 21 517
WEST0021	SC 21 517
WEST0022	SC 21 517
WEST0023	SC 21 517
WEST0024	SC 21 2A12
START OF SEGMENT *****	0028
WEST0025	SC 21 2A12

ETHERM/C "THERMAL CONDUCTIVITY CONTRIBUTIONS AT T = "F7.0," ARE1".

0028	IS 00A1 LONG, NEXT SEG 0027
WEST0026	SC 271 2A12
SC	271 2013
WE	10030 SC 271 1311
WEST0031	SC 271 1311
WEST0032	SC 271 1311
WEST0033	SC 271 6111
WEST0034	SC 271 6111
WEST0035	SC 271 6111
WEST0036	SC 271 6111
WEST0037	SC 271 6111
WEST0038	SC 271 6111
WEST0039	SC 271 6111
WEST0040	SC 271 6111
WEST0041	SC 271 6111
WEST0042	SC 271 7110
WEST0043	SC 271 7210
WEST0044	SC 271 7210
WEST0045	SC 271 7210
WEST0046	SC 271 7210
WEST0047	SC 271 8110
WEST0048	SC 271 8110
WEST0049	SC 271 8110
WEST0050	SC 271 9A11
WEST0051	SC 271 10011
WEST0052	SC 271 10011
WEST0053	SC 271 11011
WEST0054	SC 271 11A11
WEST0055	SC 271 11A11
WEST0056	SC 271 11910
WEST0057	SC 271 12111
WEST0058	SC 271 12111
WEST0059	SC 271 13110
WEST0060	SC 271 13110
WEST0061	SC 271 14A12
WEST0062	SC 271 14A12
WEST0063	SC 271 14A12
WEST0064	SC 271 14B12
WEST0065	SC 271 14B12
WEST0066	SC 271 15112
WEST0067	SC 271 15112
WEST0068	SC 271 15112
L + 3 W (MAX + 1) ;	

```

FOR I = 0 STEP 1 UNTIL L DO
  FOR J = 1 STEP 1 UNTIL L DO
    A(I,J) = A(I,J) + 0.1
  NMAX = N(0,1)
  FLIN
  IF NETT > NMAX THEN NMAX = NETT
  FJIN
  NETT = NETT / NMAX
  FJIN
  COMMENT Q001(J)
  REGTN
  FLIN
  A(I,J) = A(I,J) + NETT * Q(1,1,I,J,1)
  A(I,J) = R * NETT * MRT(J,I,J) = A(I,J) / MRT(J,I,J)
  ENO
  FJIN
  COMMENT Q001(J)
  BEGIN
  FLIN
  IF L = J THEN A(I,J) = A(I,J) + NETT * (MRT(L,L) / MRT(J,I,J))
  A(I,J) = A(I,J)
  A(I,J) = R * NETT * (NETT * Q(1,1,I,J,1) + A(I,J) + MRT(I,J,1))
  ENO
  FJIN
  COMMENT Q001(J)
  FJIN
  IF I = J THEN BEGIN
    FLIN
    IF L = I THEN A(I,J) = A(I,J) + NETT * MRT(L,I) / MRT(I,I)
    A(I,J) = R * NETT * (Q(1,1,I,I,1) / MRT(I,I)) + MRT(I,I)
    A(I,J) = R * NETT * (A(I,J) + NETT * MRT(1,I,I) + Q(1,1,I,I))
    / MRT(I,I)
    END
  FJIN
  COMMENT Q0111
  A(0,K) = A(0,K) + NETT * (2.5 * Q(1,1,0,1) - 3 * Q(1,2,0,1))
  A(0,K) = R * NETT * A(0,K)
  FJIN
  BEGIN COMMENT Q0111
  FLIN
  IF L = I THEN A(I,K) = A(I,K) + NETT * MRT(L,I) / MRT(I,I)
  3 * (2.5 * Q(1,1,I,I,1) - 3 * Q(1,2,2,I,I))
  A(I,K) = R * NETT * A(I,K)
  END
  FJIN
  BEGIN COMMENT Q011J,Q011J
  A(I,K) = R * NETT * NETT * (2.5 * Q(1,1,0,J) - 3 * Q(1,2,0,J))
  A(0,J) = A(J,J) * MRT(0,0,1) / MRT(J,J)
  END
  FJIN
  COMMENT Q011J
  FJIN
  BEGIN
  REGTN
  A(I,J) = R * NETT * NETT * (Q(1,1,I,J,1) / MRT(I,J,1) + (2.5 * Q(1,1,I,J,1) - 3 * Q(1,2,2,I,J,1))
  + A(I,J) / MRT(I,J,1) + (MRT(I,J,1) * MRT(I,I,J,1)) / 3)
  END
  FJIN
  COMMENT Q011J
  FJIN
  A(I,J) = (NETT / M(1)) * A(I,J)
  FJIN
  COMMENT Q1111
  A(K,K) = A(K,K) + NETT * (0.25 * Q(1,1,0,1) - 15 * Q(1,2,0,1))
  A(K,K) = R * NETT * (A(K,K) + 1.5 * A(1,1,0,1) - 0.25 * Q(1,2,0,1))
  FJIN
  BEGIN COMMENT Q111J,Q111J
  A(K,J) = R * NETT * NETT * (Q(1,1,K,J,1) / MRT(K,J,1) + (13.75 * Q(1,1,K,J,1) - 15 * Q(1,2,2,K,J,1) + 12 * Q(1,3,0,K,J,1) - A * Q(1,2,2,K,J,1))
  + A(K,J) / MRT(K,J,1) / MRT(K,K,J,1))
  END
  FJIN
  COMMENT Q1111
  BEGIN
  FLIN
  NL2 = M(L) * 2
  A(I,I,NETT) = A(I,I,NETT) + NETT * MRT(L,I,I) * (1.25 * R * A(MT(I,I)))
  + 5 * M(2) * M(1) * M(2) * M(1) + 15 * M(2) * M(2) * M(1) * M(1) + 12 * M(2) * M(2) * M(2) * M(1)
  + 2 * M(2) * M(2) * M(2) * M(2) / MRT(I,I,I,I)
  END
  A(K,I,NETT) = R * NETT * (A(K,I,NETT) + 1.5 * A(K,I,NETT) * M(1) * M(1))
  END
  FJIN
  COMMENT Q111J
  FJIN
  REGTN
  A(I,I,K,J,1) = R * NETT * NETT * (Q(1,1,I,J,1) / MRT(I,J,1) + (13.75 * Q(1,1,I,J,1) - 15 * Q(1,2,2,I,J,1) + 12 * Q(1,3,0,I,J,1) - A * Q(1,2,2,I,J,1))
  + A(K,I,NETT) / MRT(I,J,1) * A(K,I,K,J,1) / MRT(I,I,I,I))
  END
  FJIN
  COMMENT COMPUTE HEAVY CONTRIBUTION TO THERMAL CONDUCTIVITY
  K2 = 0.1
  K = 2 * K1
  THT = 3.47118E-7 * TROOT / MNSOR
  FJIN
  A(K,K,NETT) = NETT / MRT(I,I,I,I)
  FJIN

```

```

      AT&K2+I&K1 + N(1) ;
      PETERNC( K2+1,K2+1,K2+2,A,DEFN04,EXN ) ;
      LMDAA + TH1 + NUM + 104(EXN=EX01 / DEFN04
      L + 3 * EXN + 12 ) ;
      A(L,M2+1,1) ;
      P114
      BEGIN
      AT&K2+I&L1 + A(K2+I,&K1) ;
      AT&K2+I,&K1 + 0 ) ;
      END ;
      P114
      AT&K2+I+11 + 0 ) ;
      BEGIN
      INTEGER NEMBLOCK ;

```

COMMENT 01211 ;

$$AT&K2+K1 + AT&K2,K1 + N(1,1 + (10,0375*Q(1,1)*Q,L1 - 39,3775*Q(1,1)*Q,L1
 + 57*Q(1,1,3,0,L1) - 37*Q(1,1,4,0,L1)) ;
 A(K2+K1 + N(0) * (1,1,2)1&K(N(0)(1,1)*Q(2,2)*Q,0,0,1 + 14*Q(2,3)*Q,0,0,1)
 + A * A(K2+K1)) ;
 P114
 COMMENT 01211 ;
 BEGIN
 J + K + I + J - H + K2 + 1 ;
 M2 + MEL1 + MEL1 ;
 P114
 BEGIN
 M2 + MEL1 + MEL1 ;
 IF L < E THEN
 A(M,EJ1 + A(EH1) + MEL1 * MRT(L,L1+2,0,L1+2) + (2,187Kx
 (12MEL2 + 5MEL2*Q(1,1)*Q,L1 - 31,4K*Q(2,1,2)*Q,0,0,1
 + Q(1,2)*Q(L1 + 37*Q(1,2,3,0,L1) + 37*Q(1,2,4,0,L1) +
 14*Q(1,3)*Q(2,2)*Q,0,0,1) - (A(EH1)*M(L1+2,0,0,L1+2))) ;
 END ;
 AT&H1J + N(0) * (1,1,4,214,HE1) + (4*Q(2,2)*Q,1,L1 + 14*Q(2,3)*Q,1,L1
 + A * A(H1J)) ;
 END ;
 P114
 COMMENT 0121J,012J1 ;
 BEGIN
 AT&K2+J,&J1 + N(E1)N(2,1)J1*Q(4*Q(2,0,0,J1) + Q(2,1,2)*Q(2,0,0,J1)
 + 70,875 * (1,2,0,J1) + 57*Q(1,1,3,0,J1) + 30*Q(1,1,4,0,J1)
 + 14*Q(2,2,0,0,J1) + 14*Q(2,3,0,0,J1)) ;
 A(K2+J,&J1 + (MRT(J,J1)/MRT(1,1,1,1,1) + A(K2+K1)) ;
 END ;
 P114
 COMMENT 0121J ;$$

START OF SEGMENT	00020
WEST01010	SC 291 54910
WEST01011	SC 291 57410
WEST01012	SC 291 58711
WEST01013	SC 291 58712
WEST01014	SC 291 58711
WEST01015	SC 291 58710
WEST01016	SC 291 58710
WEST01017	SC 291 58712
WEST01018	SC 291 58712
WEST01019	SC 291 58712
WEST0101A	SC 291 58712
WEST0101B	SC 291 58712
WEST0101C	SC 291 58712
WEST0101D	SC 291 58712
WEST0101E	SC 291 58712
WEST0101F	SC 291 58712
WEST0101G	SC 291 58712
WEST0101H	SC 291 58712
WEST0101I	SC 291 58712
WEST0101J	SC 291 58712
WEST0101K	SC 291 58712
WEST0101L	SC 291 58712
WEST0101M	SC 291 58712
WEST0101N	SC 291 58712
WEST0101O	SC 291 58712
WEST0101P	SC 291 58712
WEST0101Q	SC 291 58712
WEST0101R	SC 291 58712
WEST0101S	SC 291 58712
WEST0101T	SC 291 58712
WEST0101U	SC 291 58712
WEST0101V	SC 291 58712
WEST0101W	SC 291 58712
WEST0101X	SC 291 58712
WEST0101Y	SC 291 58712
WEST0101Z	SC 291 58712
WEST01020	SC 291 58712
WEST01021	SC 291 58712
WEST01022	SC 291 58712
WEST01023	SC 291 58712
WEST01024	SC 291 58712
WEST01025	SC 291 58712
WEST01026	SC 291 58712
WEST01027	SC 291 58712
WEST01028	SC 291 58712
WEST01029	SC 291 58712
WEST0102A	SC 291 58712
WEST0102B	SC 291 58712
WEST0102C	SC 291 58712
WEST0102D	SC 291 58712
WEST0102E	SC 291 58712
WEST0102F	SC 291 58712
WEST0102G	SC 291 58712
WEST0102H	SC 291 58712
WEST0102I	SC 291 58712
WEST0102J	SC 291 58712
WEST0102K	SC 291 58712
WEST0102L	SC 291 58712
WEST0102M	SC 291 58712
WEST0102N	SC 291 58712
WEST0102O	SC 291 58712
WEST0102P	SC 291 58712
WEST0102Q	SC 291 58712
WEST0102R	SC 291 58712
WEST0102S	SC 291 58712
WEST0102T	SC 291 58712
WEST0102U	SC 291 58712
WEST0102V	SC 291 58712
WEST0102W	SC 291 58712
WEST0102X	SC 291 58712
WEST0102Y	SC 291 58712
WEST0102Z	SC 291 58712

COMMENT 02211 ;

$$AT&K2+I&K1 + 48 * N(1) + N(0) * (MRT(1,1,1,1,1) / MRT(1,1,1,1,1) *
 (37,1875*Q(1,1)*Q,1,L1 + 70,875*Q(1,1)*Q,2,L1) + 57*Q(1,1,1,2,0,L1) +
 30*Q(1,1,1,3,0,L1) + 14*Q(1,1,2,0,L1) + 14*Q(1,1,3,0,L1)) +
 AT&K2+K1 + N(0) * (MRT(1,1,1,1,1) / MRT(1,1,1,1,1) +
 48*Q(2,2,0,0,J1) + A * R(EH1)) ;
 P114
 COMMENT 02211 ;
 BEGIN
 M2 + MEL1 + MEL1 ;
 J + K + I + J - H + K2 + 1 ;
 P114
 BEGIN
 M2 + MEL1 + MEL1 ;
 M2 + MEL1 + MEL1 ;
 IF L < E THEN
 A(EH1) + R(EH1) + MEL1 * MRT(L,L1+2,0,L1+2) + (2,187Kx
 (12MEL2 + 5MEL2*Q(1,1)*Q,L1 - 31,4K*Q(2,1,2)*Q,0,0,1
 + Q(1,2)*Q(L1 + 37*Q(1,2,3,0,L1) + 37*Q(1,2,4,0,L1) +
 14*Q(1,3)*Q(2,2)*Q,0,0,1) - (A(EH1)*M(L1+2,0,0,L1+2))) ;
 END ;
 AT&H1J + N(0) * (1,1,702107*4*Q(2,0,0,J1) * (77*Q(2,2)*Q,1,L1 + 112*Q(2,3)*Q,1,L1
 + R(EH1) * (2,1,2)*Q,0,0,1) + A * A(H1J)) ;
 END ;
 P114
 COMMENT 0221J,022J1 ;
 BEGIN
 AT&K2+J,&J1 + N(E1)N(2,1)J1*Q(4*Q(2,0,0,J1) + Q(2,1,2)*Q(2,0,0,J1)
 + 712,375*Q(1,1,2,0,J1) + 341,5*Q(1,1,3,0,J1) + 21*Q(1,1,4,0,J1) +
 20*Q(1,1,5,0,J1) + 73*Q(2,2,0,0,J1) + 112*Q(2,3,0,0,J1) + 50*Q(2,4,0,0,J1)
 + 28*Q(1,3,0,0,J1) + N(0)1 * R(EH1)) ;
 A(EH1),R(EH1) + (MRT(1,1,1,1,1) / MRT(1,1,1,1,1) * A(EH1),R(EH1)) ;
 END ;
 P114
 COMMENT 0221J ;
 P114$$

WEST02004	SC 291 19010
WEST02005	SC 291 19011
WEST02006	SC 291 19311
WEST02007	SC 291 19412
WEST02008	SC 291 19412
WEST02009	SC 291 19412
WEST02010	SC 291 19412
WEST02011	SC 291 19511
WEST02012	SC 291 20011
WEST02013	SC 291 20112
WEST02014	SC 291 20212
WEST02015	SC 291 20313
WEST02016	SC 291 20313
WEST02017	SC 291 20313
WEST02018	SC 291 20412
WEST02019	SC 291 20412
WEST02020	SC 291 20412
WEST02021	SC 291 20412
WEST02022	SC 291 20412
WEST02023	SC 291 20412
WEST02024	SC 291 20412
WEST02025	SC 291 20412
WEST02026	SC 291 20412
WEST02027	SC 291 20412
WEST02028	SC 291 20412
WEST02029	SC 291 20412
WEST02030	SC 291 20412
WEST02031	SC 291 20412
WEST02032	SC 291 20412
WEST02033	SC 291 20412
WEST02034	SC 291 20412
WEST02035	SC 291 20412
WEST02036	SC 291 20412
WEST02037	SC 291 20412
WEST02038	SC 291 20412
WEST02039	SC 291 20412
WEST02040	SC 291 20412
WEST02041	SC 291 20412
WEST02042	SC 291 20412
WEST02043	SC 291 20412
WEST02044	SC 291 20412
WEST02045	SC 291 20412
WEST02046	SC 291 20412
WEST02047	SC 291 20412
WEST02048	SC 291 20412
WEST02049	SC 291 20412

```

      BEGIN
        A(K+K,J) = PRAXX(T)*H(X(J))*(MRT(T,I,J)+5*XH(X(J))+5)/MRT(T,L,J)+50 * 
          (112.490625*Q(I,L,I,J,J) + 312.175*Q(I,I,J,I,J,J) + 381.5* 
          Q(I,I,J,I,J,J) + 210*Q(I,I,J,J,J) + 60*Q(I,I,J,J,J,J) + 77*Q(I,I,J,J,J,J) 
          + 112*Q(I,I,J,J,J,J,J) + 40*Q(I,I,J,J,J,J,J,J) + 24*Q(I,I,J,J,J,J,J,J,J) + 11) +
        A(K+L,K+J) + MRT(T,J,J)*A(K+L,K+J)/MRT(T,L,J) +
      END I

      COMMENT COMPUTE ELECTRON THERM. COND. I
      DETERM(X2=X2,K=1,I=1,DENOM=FXD1) I
      DETERM(X2=X2,K=2,I=1,DENOM=FXD2) I
      LNDIF = TMT_K_X2_M_X10*(FXN - FXD1) * NFD1 / (DENOM * MRTD0,011) I
      K = 1 X (MAX + 1) I
      A(K+K,J) = 0 I
    FROM
      A(K+K,J) = 0 I
      K = 2 X (MAX + 1) I
    FL1M      COMMENT 00211 I
      A(D,K) = A(D,K) + N(L,J) * (4.375*Q(I,I,J,O,L,I) + 10.5*Q(I,I,J,O,L,I) 
        + A(K,I,I,J,O,L,I)) I
      A(D,K) = A = N(O,I) * A(D,K) I
    FL1M      COMMENT 00211 I
      BEGIN
        J = K+I I
    FL1M
        IF L = I THEN A(I,J) + A(I,J,I) * N(L,J)*(MRT(T,L,I,L))/MRT(T,L,I,I) +
          (4.375*Q(I,I,I,I,I,I,L) + 10.5*Q(I,I,I,I,I,I,L) + A(K,I,I,I,I,I,L)) I
        A(I,J) = B * N(I,I) * A(I,J) I
      END I

    FL1M      COMMENT 00211,00212 I
      BEGIN
        A(I,J,I) = B * N(I,I) * N(I,I,J) * (4.375*Q(I,I,I,I,I,I,J) + 10.5*Q(I,I,I,I,I,I,J) 
          + A(K,I,I,I,I,I,J)) I
        A(I,J,I,I) = MRTD0,01/MRT(T,I,I,I,I,I,I,J) * A(I,J,I) I
      END I

    FL1M      COMMENT 00212 I
      BEGIN
        A(I,J,I,I) = B * N(I,I,I,I) * N(I,I,I,J) * N(I,I,I,J,I) * (MRT(T,I,I,I,I,I,I,J) + 5*XH(X(J)) * 
          Q(I,I,I,I,I,I,J) + 10.5*Q(I,I,I,I,I,I,J) + A(K,I,I,I,I,I,J)) I
        A(I,J,I,I,I) = (MRT(T,I,I,I,I,I,I,J)/MRT(T,I,I,I,I,I,I,J) + 5 * A(I,J,I,I)) I
      END I

    FL1M      COMMENT 00212 I
      BEGIN
        A(I,J,I,I,I) = B * N(I,I,I,I,I,I) * N(I,I,I,I,I,J) * N(I,I,I,I,J,I) * (MRT(T,I,I,I,I,I,I,J) + 5*XH(X(J)) * 
          Q(I,I,I,I,I,I,J) + 10.5*Q(I,I,I,I,I,I,J) + A(K,I,I,I,I,I,J)) I
        A(I,J,I,I,I,I) = (MRT(T,I,I,I,I,I,I,J)/MRT(T,I,I,I,I,I,I,J) + 5 * A(I,J,I,I,I)) I
      END I

```

```

      NTOT = 9.657301A + P / T ;
      NCG1 = NC21 * ALF + NTOT /(1 + ALF) ;
      NCG1 = NTOT * (1 - ALF) / (1 + ALF) ;
      TRANS( TAP,4, MAX, SIGMA(11),LMRDA ) ;
      WRITE( GETL,FL,T, FOR I = 0 STEP 1 UNTIL 2 DO ET,NET))NTOT/NET0+
      N(I),DERYF,FLT(1,LMRDA,SIGMA(11),LMRDA ) ;
      ET=ET+1;
      ENDO;
      WRITE( GETL);
      WRITE( GETL,CLOCK,TTIME(2)/60,TTIME(3)/60);
      ET=ET+1;
      ENDO;
      CL/SEOFCK(PUNCH,GETL);
      ENDO.

```

0002 IS 0177 LONG. NEXT SEG 0001

PRP	IS SEGMENT NUMBER 0030. PRT ADDRESS IS 011A
LN	0031 0117
RO4T	0032 0121
OUTPUT#1	0033 0032
BLOCK CONTROL	0034 (.005
INPUT#1	0035 0100
X TO TMF 1	0036 0120
ALGOL WRITE	0037 001A
ALGOL READ	0038 0015
ALGOL SELECT	0039 001A

NUMBER OF ERRORS DETECTED = 000 LAST CARD WITH ERROR HAS SEQ #
 PRP STEP=0141 TOTAL SEGMENT SIZE=02A12 WORDS OTSK STORAGE REG.=0101A WORDS NO. SEGS.=00020.
 ESTIMATED CORE STORAGE REQUIREMENT = 0407A WORDS.
 2012310A FRIDAY 12 NOON PROCESSOR TIME = 37.47 SECONDS I/O TIME = 51.02 SECONDS

— LABEL 000000000LINE 0016A3092 COMPILE FLEC/THERM LIBRARY

160428CC ALGOL

APPENDIX B

CALCULATION OF BOUND-BOUND TRANSITION PROBABILITIES by D. Sun

The overall purpose of the system of programs being developed is to represent the spectrum of an atomic species in a plasma, including all lines and portions of the continuum which carry a significant portion of the energy. Hence it will be necessary to calculate large numbers of transition probabilities for bound-bound, bound-free, and free-free transitions.

Calculation of the bound-bound case to be discussed here is fairly complete; the other two types of transitions have not been ad'ded yet. The program to be described. presently called GIANT/FIASCO, consists of four sub-programs, (following the format of E. Corinaldesi) between which information is transferred by three disc files, READF1, RE.DF2, and READF3. Programs 1 and 2 are run together, and accepting as their input the quantum numbers and energies of the various energy levels of a species as they are given in Moore's tables.¹ Program 2 prints out transition probabilities for all transitions allowed by the selecti : rules within the range considered. These are also placed on the disc READF2 where they may be tapped by Program 3 or by an auxillary program FIASCO/RESULTS, which merely prints out the results in a number of convenient forms. Program 3 calculates the Stark shift and broadening of each level, while Program 4 combines these into the shift and broadening of each spectral line. However, this paper is concerned primarily with Programs1 and 2, the calculation of bound-bound transition probabilities.

The heart of the matter is the calculation of $|\langle \psi_n | z | \psi_m \rangle|^2$ where ψ_n , and ψ_m are the two states between which a transition may occur

¹C. Moore, Atomic Energy Levels, National Bureau of Standards, Circular 467, U.S. Government Printing Office, Washington, D.C.

²E. Corinaldesi, to be published.

and $z=r \cos \theta$ is the electric dipole operator. (Quadrupole and magnetic dipole transitions are ignored.) Although ψ_n , ψ_m , and z actually involve all the electrons in the atom, in practice, it is possible to use the one-electron wave functions of the outer electron which makes the transition (Condon and Shortley, Section 6').³ Now each energy level consists of $2J+1$ states with different z -components of angular momentum. For transitions from n to m , it is necessary to sum the square of the matrix element for all of the m -states, and average it over all of the initial n -states. The oscillator strength f_{nm} is $\frac{4\pi m c v}{f_n}$ times this quantity, and the following relations hold:

$$(2 J_n + 1)f_{nm} = gf = (2 J_m + 1)f_{mn}$$

$$A_{nm} = 0.667 \times \bar{v}^2 \quad \text{where } \bar{v} \text{ is in cm}^{-1}$$

$$(2 J_n + 1)A_{nm} = (2 J_m + 1)A_{mn}$$

The solutions to Schroedinger's equation separate into two parts, giving the form $\frac{R(r)}{r} Y(\theta, \phi)$. $R(r)$ is known as the radial wave function while $Y(\theta, \phi)$ is the angular part. Hence the problem separates into a radial integral $\int_0^\infty R_n R_m r dr$, and an averaging and summing process which is carried out using Racah coefficients of the quantum numbers of the initial and final states.

THE ANGULAR PART (COUPLING SCHEMES)

When an atom with more than one electron is being considered, there are several ways to add the multiple orbital and spin angular momentums. For example, one might add all the orbital angular momentum

³E. Condon and G. Shortley, Theory of Atomic Spectra, Cambridge University Press, London (1935) hereafter referred to as Condon and Shortley and the Section.

operators to get a total orbital angular momentum operator, and do the same with the spin operators. Then the total orbital angular momentum operator and the total spin angular momentum operator might be added to give a total angular momentum. If the actual states of the atom closely approximate the eigenstates of the total orbital and spin angular momentum operators, then the atom is said to be LS coupled, the L and S representing good quantum numbers of the operators. One way to express the states is to put the quantum numbers of two operators in brackets to the left of the quantum number for the sum of the two operators. An LS state is written $[(S, (L_{\text{core}}, \ell)L)J]$, where L_{core} is the total L of the inner electrons, ℓ is the orbital quantum number of the outer electron, and J is the total angular momentum. A form of coupling commonly found in the rare gases is $j\ell$ coupling, given by $[(J_{\text{core}}, \ell)K, S]J$, where J_{core} is the total angular momentum of the core, s is the spin of the outer electron, and K is the intermediate quantum number.

The average and sum over the initial and final states for $|\langle \psi_n | z | \psi_m \rangle|^2$ is easily seen to be equal to one third of the same average and sum for $|\langle \psi_n | \vec{r} | \psi_m \rangle|^2$. \vec{r} turns out to be a class T operator with respect to J (See Condon and Shortley, 8³). Here it is convenient to introduce a quantity $\langle j; T; j' \rangle$ which can be related to the components of the matrix element $\langle jm | \vec{r} | j'm' \rangle$ but is itself independent of m and m', the z-components. (See Condon and Shortley, 9³). Now if $[P, J_1] = 0$ and P is class T with to $J = J_1 + J_2$, then the ratio

$$\frac{|\langle j_1 j_2 j; P; j_1 j_2' j' \rangle|^2}{|\langle j_1 j_2; P; j_1 j_2' \rangle|^2}$$

is given by Equation 11³8 of Condon and Shortley, or by
 $(2j' + 1)j_2(2j_2 + 1)(2j_2' + L)W^2(j_2; j, j_2', j'; j_1)/\Xi(j, j')$ where
 $j_2 > = \max(j_2, j_2')$, $W(j_2; j, j_2', j'; j_1)$ is the Racah coefficient, and
 $\Xi(j, j')$ is defined by:

$$\Xi(j, j+1) = (j+1)(2j+3)$$

$$\Xi(j, j) = j(j+1)$$

$$\Xi(j, j-1) = j(2j-1) \quad \text{See Condon and Shortley, 7}^4 5$$

In the program there are two procedures, XI and W2MOD, with $XI(j, j') = \Xi(j, j')$ and with $W2MOD(j_2, j, j_2', j', j_1)/XI(j, j')$ equal to the above ratio.

Returning to LS and $j\ell$ coupling, we have:

$$|\langle [S, (L_{core}, \ell)L]J; r; [S, (L_{core}, \ell')L']J' \rangle|^2 =$$

$$\frac{W2MOD(L, J, L', J', S)}{XI(J, J')} |\langle (L_{core}, \ell)L; r; (L_{core}, \ell')L' \rangle|^2 =$$

$$\frac{W2MOD(L, J, L', J', S) W2MOD(\ell, l, \ell', L', L_{core})}{XI(J, J') XI(L, L')} |\langle \ell; r; \ell' \rangle|^2$$

for LS coupling, and

$$|\langle [(J_{core}, \ell)K, s]J; r; [J_{core}, \ell')K', s]J' \rangle|^2 =$$

$$\frac{W2MOD(K, J, K', J', s)}{XI(J, J')} |\langle (J_{core}, \ell)K; r; (J_{core}, \ell')K' \rangle|^2 =$$

$$\frac{W2MOD(\ell, J, K', J', s) W2MOD(\ell, K, \ell', K', J_{core})}{XI(J, J') XI(K, K')} |\langle \ell; r; \ell' \rangle|^2$$

for $j\ell$ coupling.

Summing over all z-components of \vec{J} for both initial states and final states and dividing by $(2J+1)$ is equivalent to multiplying by $XI(J, J')$. (See Condon and Shortley, Equations 7⁴5 and 9³11)

$$|\ell |r \ell'>|^2 = \frac{1}{4\ell^2 - 1} [\int_0^\infty R R' r dr]^2$$

(R and R' are radial functions although the quantum numbers pertaining to the radial part have not been written in the above equations.) The final result for $3|\langle n|z|m\rangle|^2$ summed over final states and averaged over initial states is:

$$\frac{W2MOD(L,J,L',J',S) W2MOD(\ell,L,\ell',L',J_{core})}{\chi I(L,L')} \frac{[\int_0^\infty R R' r dr]^2}{(2\ell+1)(2\ell'+1)}$$

for LS coupling, and

$$\frac{W2MOD(L,J,K',J',s) W2MOD(\ell,K,\ell',K',J_{core})}{\chi I(K,K')} \frac{[\int_0^\infty R R' r dr]^2}{(2\ell+1)(2\ell'+1)}$$

When these quantities are multiplied by $(2J+1)$ and summed over all possible J and J' in the initial and final multiplets, the result is $G(m)$ in the notation used by Rohrlich⁴ and Griem,⁵ the m standing for "multiplet". $G(L)$ is then $(2J+1)$ times the above quantities, the L standing for "line". $G(L)$ obviously was defined to satisfy the rule $\sum_J G(J) = 1$.

A sum rule derived from first principles states that $\bar{v} |\langle n|z|m\rangle|^2$ summed over all discrete final states and integrated over continuum final states should equal the Rydberg constant in the same units as \bar{v} . In the program print out the quantity S3 or SUM3 is the sum over discrete states of $3 \bar{v} |\langle n|z|m\rangle|^2$ with \bar{v} in cm^{-1} . It should approach 329,212.

⁴F. Rohrlich, Ap. J. 129, 441,449 (1959).

⁵H. Griem, Plasma Spectroscopy, McGraw Hill Book Company, New York (1964).

Intermediate Coupling

Most elements do not fit a well-defined coupling scheme as nicely as might be desired. In other words, their states are mixtures of pure states. No matter what basis is chosen--LS, j_1 , jj , etc.--the actual states are linear combinations of the basis states, and a transformation matrix between the actual states and the pure states exists.

For the intermediate coupling (IC) program, an LS basis was used, and the elements of the transformation matrix between states of different configurations were assumed to be zero. For each type of configuration involved, a theoretical matrix expression for the electrostatic and spin-orbit perturbations to the Hamiltonian was generated in terms of F_0 , G_0 , F_2 , G_2 , ζ , and ζ' . The electrostatic parameters, F_0 , G_0 , F_2 , and G_2 , appeared only on the diagonal for the LS basis (See Condon and Shortley, ¹³), while the two spin-orbit parameters ζ and ζ' appeared in many off-diagonal positions (Condon and Shortley, ¹¹). However, no cross terms exist between states of different J , implying that J is a good quantum number in all coupling schemes.

If the theoretical expression is correct and if it is valid to ignore configuration interaction, then it should be possible to choose values for the parameters such that the diagonalized matrix corresponds closely to the observed energies, in spite of the fact that the number of energies in a configuration (the number of conditions that can be imposed on the parameters) is larger than the number of parameters. In practice, the parameters are adjusted to give a least squares fit between the energies calculated by diagonalization and the observed energies. This is done by using trace conditions from the blocks of different J within a configuration (There are no interaction terms between states of different J .) to set several of the parameters initially. As a first guess, the less significant parameters are set equal to zero. The matrix is then diagonalized and partial derivatives of the eigenvalues with respect to the parameters are calculated. A multiple-dimensional Newton's method is applied to readjust the parameters. The process is repeated until the sum of the squares of the energy differences changes by less than 0.1% from its previous value.

The matrix elements for z between various LS states are easy to calculate, although phases are somewhat of a problem. (See Condon and Shortley,⁴¹¹). Using the transformation matrices, calculation of oscillator strengths is straightforward.

THE RADIAL INTEGRAL

Schroedinger's equation for the radial wave function is:

$$R = R_{nl}/r = P_{nl}/r \frac{\partial^2 R}{\partial r^2} + [-2V(r) - \frac{l(l+1)}{r^2} + \epsilon]R = 0$$

where r is in Bohr radii

and ϵ is in Rydbergs

Both of the methods used in these programs for solving this equation, the Bates-Damgaard approximation⁶ and the scaled Thomas-Fermi method,⁷ are semi-empirical--that is, ϵ is set equal to the observed energy of a known level. The difference between the two approaches lies in the potential $V(r)$ that is chosen.

The Bates-Damgaard or Coulomb Approximation

As a first approximation one guesses that the potential in which the outer electron moves is simply a Coulomb field due to a nucleus of charge $+Z$ shielded by $NEL-1$ electrons very close to the nucleus.

Thus $V(r) = -\frac{C}{r}$ where $C = Z-NEL+1$ is the effective core charge. ($C = 1$ for neutral atoms.) Letting $\epsilon = \frac{C^2}{n^2}$ the differential equation is now:

$$\frac{\partial^2 R}{\partial r^2} + [\frac{2C}{r} - \frac{l(l+1)}{r^2} - \frac{C^2}{n^2}] R = 0$$

⁶C. Bates and A. Damgaard, Phil. Trans. Roy. Soc. (London) 242A, 101 (1949).

⁷J. Stewart and M. Rotenburg, Phys. Rev. 140, A1508 (1965).

There are two boundary conditions, that $R \rightarrow 0$ at the origin and infinity. They can both be met only when n is an integer. In complex atoms n is generally non-integral, and one condition must be dropped. Since the major contribution to $\int_0^\infty R R_m r dr$ comes from large r for most transitions, it is reasonable to forget the condition at the origin. The wave function then blows up at zero and is not normalizable.

A mathematical trick is applied at this point. An asymptotic expansion for large r is generated by making the substitution $R = ue^{-\frac{cr}{n}}$ and finding a recursion relation for u .

$$R = e^{-\frac{cr}{n}} \left(\frac{2cr}{n} \right)^n \left[1 + \sum_{t=1}^{\infty} \frac{a_t}{r^t} \right]$$

a_t is given by a recursion relation in reference 6.

As long as the \sum contains a finite number of terms, the condition at infinity holds and the one at zero does not. But, a quick check shows that the differential equation has an irregular singularity at infinity. Therefore, a power series expansion in $(1/r)$ does not necessarily converge to a solution. In fact, the sum diverges here. In spite of this, if the series is terminated at the proper term, it gives very good fit to the actual solution for $r > 2$ or 3 (depending upon n and 1, of course).

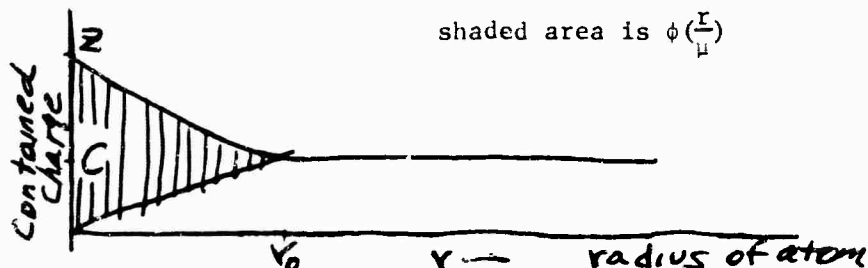
$\int_0^\infty R R_m r dr$ is now an integral of an exponential term times a power series in r , and may be expressed as a sum of gamma functions. Because the function does not have to be evaluated numerically at a number of points, very rapid computer calculations are possible. (The normalization is also given analytically.⁶) To overcome the problems of the singularity of the origin and of the diverging series, all powers of r less than 2 in the quantity $R R_m r$ are removed. These terms do not exist physically since the actual potential is not a Coulomb field near the origin. For the details of the theory and calculation, see References 6 and 8.

⁸E. Corinaldesi and E. Geil, Computer Program for Bates-Damgaard Integrals, Westinghouse Research Laboratories Scientific Paper 66-1C1-EPLAS-P4 (1966).

The Thomas-Fermi Method

The Thomas-Fermi approach utilizes a somewhat more realistic potential. Instead of assuming that the N_{e1} -1 shielding electrons are clustered within an infinitesimal distance of the nucleus, it predicts a distribution of the shielding electrons based on Fermi-Dirac statistics. The fact that the potentials formed in the above manner bring the wave functions much closer to fitting the boundary condition at the origin justifies the use of the method. Moreover, the fit can be made perfect by linearly expanding or contracting the potential in space by a scaling factor close to one. The latter is the scaled Thomas-Fermi method.

The easiest way to understand the method is to look at the net charge contained within a sphere of radius r as a function of r .



The contained charge must obviously go to Z as $r \rightarrow 0$, while for $r > r_0$ -- that is, for r outside of the core -- the contained charge is exactly C , as in the Bates-Damgaard method.

$$\text{containing charge} = \begin{cases} Z[\phi(\frac{r}{\mu}) + \frac{Cr}{r_0}] & ; \\ C & \end{cases} \quad V(r) = \begin{cases} \frac{-Z[\phi(\frac{r}{\mu}) + \frac{Cr}{r_0}]}{r} & r < r_0 \\ -C/r & r > r_0 \end{cases}$$

$$\text{where } \phi(0) = 1, \phi(x_0) = 0, \phi'(x_0) = -\frac{C}{x_0 Z}$$

$$\text{with } x = \frac{r}{\mu}, x_0 = \frac{r_0}{\mu}$$

According to Fermi-Dirac theory:

$$\mu = 0.8853 Z^{-1/3}$$

$$\frac{d^2\phi}{dx^2} = \phi^{3/2} x^{-1/2}$$

At first glance there appears to be one extra boundary condition on the differential equation for ϕ . However, x_0 has not been specified, and all three conditions are needed to uniquely determine ϕ . The equation must be solved numerically, but without x_0 the calculations are quite extensive. Luckily, the work has already been done, and a polynominal fit for the value of x_0 as a function of (C/Z) has been made.⁵ The present jl and IC programs merely solve for x_0 using the polynomial and then generate ϕ by starting at x_0 with $\phi(x_0) = 0$ and $\phi'(x_0) = -\frac{C}{x_0 Z} \cdot \phi$ automatically becomes one at zero. This calculation need only be performed once for each atomic species, for ϕ is completely determined by C and Z.

The solution to Schrödinger's equation must also be done numeric. No analytical solution is possible because $V(r)$, which depends on ϕ , is only known numerically. Two transformations are made:⁵

$$R(r) = p(y^2), \quad r = y^2, \quad R(r) = R(y^2)$$

$$\text{and } p(y) = y^{1/2} q(y), \quad dr = 2ydy$$

giving:

$$\frac{\partial^2 q}{\partial y^2} = \left\{ \frac{16 \ell(\ell+1) + 3}{4y^2} + 4y^2[2V(y^2) - \epsilon] \right\} q$$

This is solved by Numerov's method which has an error in each step on the order of h^6 (h = step size). In the program h was $y_0/32$ where $y_0 = r_0^{1/2}$.

The integration was started at a y quite a bit larger than y_0 by evaluating the asymptotic expansion of the Bates and Damgaard (BD) function at two points separated by h . Care must be taken that y is large enough for the asymptotic expansion to be sufficiently accurate and for the tail of the wave function to be negligible beyond y . Still, the starting point must not be so far out that Numerov's method drifts from the actual solution. The first term of the asymptotic expansion is of the form e^{-y^2} , and such functions do exhibit considerable drift when Numerov's method is started too far out. (The higher derivatives of

e^{-y^2} are very large compared to the function itself when y is large.) In this program the integration was started at the point where the first term of the Bates and Damgaard expansion has dropped to about 1/3000 of its maximum value.

If the scaled Thomas-Fermi method is being done, the integration is stopped at one step from the origin and the number of nodes in the wave function is checked to see if it is equal to $n_{int} - l - 1$. n_{int} is the given principal quantum number, not the effective n calculated from $\epsilon = \frac{C^2}{n^2}$. n_{int} is always an integer. If the number of nodes is not correct, then the direction in which the scaling factor must be changed is immediately determined. On the other hand, if it is correct, then the ratio of the two points closest to the origin is checked against the ratio predicted by a special asymptotic expansion for small y , obtained from a recursion relation for the approximate equation:

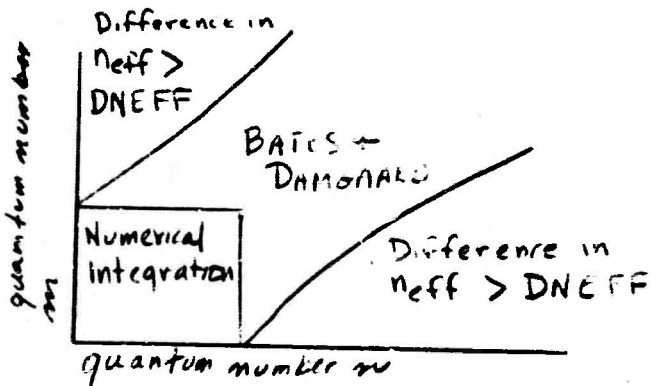
$$\frac{\partial^2 q}{\partial y^2} = \frac{16 l(l+1) + 3}{4y^2} - 8Z^2 q$$

From this the direction of the next change is found. The scaling factor steps in the proper direction by 0.05, to either 1.05 or 0.95, and the diff. eqn. is resolved with the appropriately changed potential. The scaling factor continues to move in one direction until the value which gives a boundary fit is overstepped. Then the step size is cut in half each time a new step is made. In this manner, the interval in which the correct value falls is bisected with each step. The iteration goes on until the step size is less than 1/2000 or until the ratio of the two points next to the origin is within one percent of its predicted value.

In the rare gases the ground state has too small an n_{eff} to be put into the Bates and Damgaard (BD) method. Instead the wave function of the ground state is calculated numerically by the scaled Thomas-Fermi method. Therefore, when the ground state is involved the $\int_0^\infty R_n R_m r dr$ is done numerically, implying that the wave functions of all upper states that make transitions to the ground state must be known numerically. One way of getting the upper state wave function would be to sum BD

asymtotic expansion at each point desired. However, it is quicker to simply solve Schroedinger's equation numerically since Numerov's method requires only a small number of operations at each point, whereas summing the asymtotic expansion is somewhat involved. As long as the differential equation is being solved numerically, it is just as easy--and certainly more accurate--to use the Thomas-Fermi potential in place of a pure Coulomb potential. This constitutes the unscaled Thomas-Fermi method and has roughly a factor of ten advantage in computer time over the scaled TF method. In general, wave functions generated this way will blow up at the origin and must be chopped off near $r = 0$. The program imposes the form $r^{\frac{l+1}{2}}$, the first term of the expansion of the wave function for small r , when the centrifugal potential term $\frac{16 l(l+1)}{4y^2} - 13$ begins to dominate.

GIANT/FIASCO first solves for ϕ and then generates a scaled Thomas-Fermi wave function for the ground state and unscaled Thomas-Fermi wave functions for all other states up to the point where n_{eff} is greater than the n_{eff} of the ground state by more than DNEFF an arbitrary limit fed into the program. (Transitions with a difference in n_{eff} greater than DNEFF are not considered. This is true of non-ground state transitions as well.) All generation of any kind of TF wave functions is performed by an internal procedure called THOMASFERMI. The integration of $\int_0^R R n_m r dr$ is carried out numerically when both wave functions are known numerically and is done by the Bates and Damgaard method in other cases. Of course, it is not done at all if the difference in the n_{eff} 's is larger than DNEFF.



There are several arbitrary conditions dealing with the Thomas-Fermi method specifically that are built into the program and may require modification in the future. They are:

- 1) the step size h for solving differential equations--it is $x x_0 / 4096$ for ϕ , and $y_0 / 32$ for the wave functions
- 2) the conditions for stopping the iteration in the scaled TF method
- 3) the method of chopping off the singularity at the origin in the unscaled TF process
- 4) choosing the y outside of y_0 at which to start solving Schroedinger's equation
- 5) deciding which transitions should be done by the BD method and which should be done numerically
- 6) deciding which levels should be scaled TF and which should be unscaled TF.

SYMBOL TABLE

Program I

Z: the atomic number

NEL: the number of electrons

C: the core charge seen by the outer electron $C=Z-NEL+1$

R: the Rydberg constant in reciprocal centimeters $R=109737.31$

N: an index running over the energy levels

L: orbital angular momentum of the outer electron

J: total angular momentum of the atom

T: energy of the level in cm^{-1}

TINF: energy limit of the level in cm^{-1}

In the LS program only

MULT: multiplicity = $2S+1$ where S is the total spin of the atom

LT: total orbital angular momentum of the atom

P: parity of the state

In the j1 and IC programs only

CORE: total angular momentum of the core

K: intermediate quantum number

TINFO: the value of TINF if CORE=1.5 or 0.5

TINF1: the value of TINF if CORE=1.5

TINF2: the value of TINF if CORE=0.5

NEFF: the effective principal quantum number of the outer electron

Program II

L, J, T, MULT, LT, P, CORE, K, and NEFF have the same meaning as in

Program I but are now arrays. Z, NEL, and C also have the same meaning.

N: an index running over the states. In particular, it is the index of the initial state when dealing with a transition. In PROCEDURE THOMASIERMI, however, it has the value of NEFF.

M: an index running over the final states.

K: in the LS program only, means the same thing as M does in the j1 and IC programs

DNEFF: the largest difference in NEFF for which the program will consider a transition between two levels. Also, in the j1 and IC programs, Thomas-Fermi wave functions are calculated for all levels whose NEFF is less than DNEFF & greater than NEFF of the ground state.

NMAX: the highest energy level index to be considered.

NNMAX: the highest energy level index to be considered for the initial state.

OS: the square of the matrix element of \vec{r} summed over the M_j in the final level and averaged over the M_j in the initial level.

LAMBDA: the wavelength in angstroms

TT: the energy of a transition in cm^{-1}

C1: a constant = 0.587234

YY: $C1 \times TT$

SUM1: the sum of the OS's for all transitions to a given level

SUM2: the sum of the quantity OS/TT for all transitions to a given level

SUM3: the sum of the quantity OSxTT : r all transitions to a given level

S1, S2, and S3 have the same meaning in the LS program.

A: the transition rate in sec^{-1}

I1, I2, and I3 are indices used in the Thomas-Fermi and intermediate coupling sections of the j1 and IC programs.

Variables Associated with the Thomas-Fermi Method

QQ: the independent variable in the polynomials used to initialize the ionic radius. See Stewart and Rotenberg, Appendix A.

QQSUM: the sum of the QQ polynomial

X0: the ionic radius times $Z^{1/3} / 0.8853$

AA, BB, and CC: the coefficients in the initialization polynomials

PHIM1, PHIO, and PHIPI1 are ϕ_{i+1} , ϕ_i , and ϕ_{i-1} respectively. The ϕ -function is found by solving the differential equation $\phi''(x) = [\phi(x)/x]^{1/2}$ from x_0 inward.

H: the step size used in this iteration. It is = to $X0/4096$.

H32: a variable = to $H^{3/2}$

HSTAN: the step size used in solving for the actual wave functions. It is = to $\sqrt{r_0}/32$. The independent variable in the wave function is $y\sqrt{r}$

VMOD: $8y^2$ times the Thomas-Fermi potential in Rydbergs. It is given as a function of y , at points separated by HSTAN/2.

WF: a 2-dimensional array giving $R(y^2)/\sqrt{y}$ as a function of the index of the energy level and y , at points separated by HSTAN.

NORM: the normalization factor by which WF for a given level must be multiplied.

NTF: the index of the highest energy level for which a Thomas-Fermi wave function is calculated

NPOINTS: for each level, the number of points at which WF is given. It is = to the maximum y considered divided by HSTAN.

NINT: the principal quantum number of the outer electron for a given state. (NINT stands for N integral, as opposed to N effective.) The number of nodes expected in the wave function is NJNT-L-1.

The following variables are declared inside PROCEDURE THOMASFERMI.

WFT1, WFO, and WFM1: values of WF around a given y

KSP1, KSO, and KSM1: values of K_s where the differential equation is

$$\frac{d^2}{dy^2} WF(y) = K_s(y).$$

FACTORP1, FACTORO, and FACTORM1: values of the quantity $(1 - H^2 K_s^2 / 12)$

Note: P1 and M1 stand for +1 and -1. P1 means that the value is given for a y one step closer to the origin, while M1 corresponds to a y one step farther from the origin. (The integration proceeds inward)

EPSILON: the energy eigenvalue in Rydbergs.

H (already declared outside the procedure): the step size used in solving for WF. It is readjusted as the scale factor α is varied.

H2: a variable set equal to H^2

H2T4: $4H^2$

H2012: $H^2/12$

H2T506: $5H^2/6$

Y2T4: $4y^2$

RMAX: the largest value of r considered. Outside of RMAX the wave function is assumed to be too small to make any significant contribution.

INVR: $1/RMAX$

SCALE: the scale factor α in the scaled Thomas-Fermi method

JUMP: the amount by which SCALE is varied between successive trials.

DIRECTION: the direction in which SCALE is varied. It is +1 for an increase and -1 for a decrease.

OLDDIRECTION: the previous value of DIRECTION

BEFORE: a Boolean variable which is true as long as SCALE continues to jump in one direction by steps of 0.05. When the proper value of SCALE has been overstepped, BEFORE becomes false, SCALE converges by a bisection procedure.

LASTTIME: a Boolean variable which becomes true when SCALE has converged sufficiently. It activates the normalization and cut-off procedures.

VARYSCALE: a Boolean variable which determines whether a scaled or unscaled Thomas-Fermi method is to be used. In the present program VARYSCALE is true only for the ground state.

NEWI2: the number of points at which WF is known after it has been interpolated so that the spacing between points is HSTAN

LPOLY: a function of L which is used a large number of times. It is = to $16L(L+1)+3$.

NODES: the number of times that the wave function crosses the axis each time the differential equation is solved.

RATIO: the ratio of the values of the wave function between the two points closest to the origin.

DRATIO: the change in RATIO between two successive iterations.

INSIDE: a variable which--on the last iteration--goes to true as soon as y moves from the exponential region into the oscillatory region.

NORMOD: a non-array quantity which is summed to form the array NORM, the normalization factor.

Variables Associated with Intermediate Coupling

(Not all of the variables declared are described here, but most of the important ones are mentioned.)

SPORBMATRIX (4D or 3D): the coefficients of the first spin-orbit parameter in the theoretical Hamiltonian matrix. In the 4D case, the first index is the l of the configuration, the second index is the J , and the last two are the row and the column within a J -block.

The 3D (i.e. 3-dimensional) array is missing the first index.

SPORBMATRIXP (4D or 3D): the coefficients of the second spin-orbit parameter in the Hamiltonian.

ELECMATRIX (4D or 3D): the theoretical Hamiltonian for the electrostatic parameters. In the 4D array, the first three indices are the same as in SPORBMATRIX4D while the last index identifies the electrostatic parameter under consideration. No column index is necessary since the electrostatic interaction is diagonal in the LS basis.

IELEC and NELEC: the index and total number of the electrostatic parameters.

IPARAM and NPARAM: the index and total number of parameters.

ELECPARAM: an array containing the values of the electrostatic parameters as they are adjusted by PROCEDURE DIAG.

SPORBPARAM and SPURBPARAM: the values of the two spin-orbit parameters.

IGREATER: the greater of the two l 's of two states under consideration.

STLS3D: the matrix elements of $\cos\theta$ between pairs of LS states. The first index is LGREATER and the other two are the rows and columns.

J2, J3, S2, S3, L2, and L3: the variables used to represent quantum numbers in generating the Hamiltonian matrices and the LS strengths.

HOLD: the variable that holds on to the value of L as the energy levels are read in. When the end of a configuration is reached, the next L is no longer = to HOLD and PROCEDURE DIAG is called.

T2D and N2D: arrays holding the values of T and N for the levels of a given configuration. The first index is the J of the level and the second puts the states of a given J -block in order of increasing energy.

IJ, IJMIN, and IJMAX: the index and limits for the J-blocks of a given configuration.

INDEX and BLOCK: arrays over N giving the J-block and the position in that block of every level fed into the program. The number BLOCK is distinct from one configuration to the next.

LOWERBLOCK: the lowest BLOCK in a given configuration.

SIZE2 and SIZE3: the sizes of the J-blocks as predicted by the sections which generate the theoretical Hamiltonian matrices and the LS strengths.

SIZE: the size of the J-blocks in the observed levels which are read by the program.

I2LOWER and I3LOWER: integer arrays which indicate what position in the STLS3D matrix to look for a given pair of L's and J's.

TRACE and TRACES: the traces of the J-blocks. Since the traces of the undiagonalized theoretical Hamiltonian and the traces of the observed energy matrix should be the same, enough information is present to initialize the values of the parameters for a given configuration.

H: a matrix for the Hamiltonian formed from the theoretical expressions for the Hamiltonian and the values which the parameters happen to have at the moment.

TCALC: an array containing the energies calculated by diagonalizing the H-matrix.

V3D, V2D, and VTEMP: various forms of the matrix which diagonalizes the Hamiltonian.

DERIV: a matrix of the derivatives of the calculated energy eigenvalues with respect to the parameters.

ALPHS: the coefficients of the set of simultaneous equations which are solved for the corrections to the parameters. They are calculated from the DERIV's and the differences between the observed and calculated T's.

IT: the number of times that the parameters for a configuration have been readjusted for a better least-squares fit to the observed energies.

SUMSQUARES: the sum of the squares of the differences of the observed and calculated energies.

HOLDSUM: the value of SUMSQUARES from the previous iteration. If SUMSQUARES has changed by less than 0.1%, the iteration is terminated.

REAL PROCEDURE XI is the same as -(J, J')

$$\begin{array}{ll} (J + 1)(2J + 3) & \text{if } J' = J + 1 \\ = J(J + 1) & J' = J \\ J(2J - 1) & J' = J - 1 \end{array}$$

REAL PROCEDURE W2MOD is a modified Racah coefficient squared.

$$W2MOD(L, J, L', J', S) = (2J' + 1) \cdot (2L + 1)(2L' + 1) W^2 (L, J, L', J'; S)$$

Moreover,

$$\frac{W2MOD(l, J, L', J', S)}{XI(J, J')} = \frac{| \langle SLJ \cdot P \cdot SL'J' \rangle |^2}{| \langle L \cdot P \cdot L' \rangle |^2}$$

where \vec{P} is class \vec{T} with respect to \vec{J} and $[\vec{S}, \vec{P}] = 0$

REAL PROCEDURE I calculates the radial integral $\int R_n(r)R_m(r) r dr$ by numerical integration if both N and M are less than the index of the highest state for which a Thomas-Fermi wave function has been calculated. For all other pairs the Bates-Damgaard method of integration is called through REAL PROCEDURE BD.

PROCEDURE THOMASFERMI takes NEFF, NINT, and L for the Kth level and produces a wave function.

PHI/GENERATOR produces the Thomas-Fermi potential by numerically solving a differential equation derived from the theory. All quantities calculated in this section pertain to all levels for which PROCEDURE THOMASFERMI is applied.

Section in the program which sets NINT[N] for all the energy levels for which Thomas-Fermi wave functions are calculated must be changed for every different atomic or ionic species.

The IC Program

MATRIX/GENERATOR - the part of program which generates the theoretical expressions for electrostatic and spin-orbit perturbations to the Hamiltonian. The LS basis is used and matrices similar to those on pages 268-269 of Condon and Shortley¹¹ are produced for each parameter. Section 1¹³ page 296 gives the actual coefficients generated, since the program is at present designed to do the rare gases.

LS/STRENGTHS - produces a matrix for the angular part of the dipole operator. All possible pairs of LS states are considered. When PROCEDURE DIAG has expressed each energy level as a linear combination of LS states, it is then easy to calculate the angular matrix element between any two of the actual states.

A section in the program takes the energy levels in each configuration as a group, places them in blocks of different J, and then re-orders each J-block in order of increasing energy, which are then fed into PROCEDURE DIAG, one configuration at a time.

PROCEDURE DIAG takes each configuration fed into it and compares the actual observed energies with the theoretical expressions for the Hamiltonian which have been generated by MATRIX/GENERATOR. DIAG then adjusts the theoretical parameters so that the diagonalization of the theoretical Hamiltonian gives a least-squares fit to the observed energy eigenvalues. Once this is done, the matrix which diagonalizes the Hamiltonian is merely an expansion of the observed levels in terms of LS basis states. This matrix saved for the final computation of the oscillator strengths.

INPUTS TO PROGRAMS 1 AND 2 OF GIANT/FIASCO (LS PROGRAM)

under "FIASCO" (input to Program 1):

a card with Z, the atomic number and N_{el} , the number of electrons

a card with the value of T_{inf}

for each level of Moore's tables a card giving:

L (orbital angular momentum of the outer electron)

MULT (multiplicity = $2S + 1$)

LT (total orbital angular momentum)

P (parity + +1 even, = -1 odd)

J (total angular momentum)

T (energy of the level in cm^{-1})

under "READER2" (input to Program 2):

a card with NMAX (the maximum N to be read) and NNMAX (max on the index of the initial state)

a card with DNEFF (the limitation on interacting levels)

INPUTS TO PROGRAMS 1 AND 2 OF GIANT/FIASCO (j1 and IC PROGRAM)

under "FIASCO" (input to Program 1):

a card with Z, the atomic num.: and N_{el} , the number of electrons

a card with the value of T_{inf} for CORE = 0, the value of

T_{inf} for CORE = 1.5, the value of T_{inf} for CORE = 0.5

for each level of Moore's tables a card giving:

CORE (total angular momentum of the core)

L (orbital angular momentum of the outer electron)

K (intermediate quantum number)

J (total angular momentum)

T (energy of the level in cm^{-1})

under "READER2" (input to Program 2):

a card with NMAX (the maximum N to be read)

a card with DNEFF (the limitation on interacting levels)

15 cards giving the coefficients of the three initialization polynomials for the Thomas-Fermi function. Each card has four numbers:

the index of the coefficient,

A(index),

B(index),

C(index),

(See Stewart and Rotenberg⁵, Appendix A)

and, for the IC program only, for each possible L ($L = 0, 1, 2, 3$) a card with:

LM1 (coeff of F_2 if $L_{total} = L - 1$),

LSAME (coeff of F_2 if $L_{total} = L$),

LP1 (coeff of F_2 if $L_{total} = L + 1$),

LM1SC (coeff of G_0 if $L_{total} = L - 1$ and $S = 0$),

LP1SO (coeff of G_2 if $L_{total} = L + 1$ and $S = 0$),

(See Condon and Shortley, pp 281-299).

ON EXTENDING PROGRAMS 1 AND 2

LS Program: For elements in which the L of the parent term is non-zero, the expression for OS must be changed from $W2MOD (l, J, L', J', S) \sigma^2$ to

$$W2MOD (l, J, L', J', S) \frac{W2MOD (l, L, l', L', L_{parent})}{\chi(l, L')} \sigma^2$$

In more complex elements, coefficients of fractional parentage must also be added.

J1 and IC Programs: To do other rare gases, the only change necessary is the setting of NINT (the principal quantum number) for all of the levels to be done by Thomas-Fermi method.

To do other elements the cards which define the ground state as a $'S_0$ state and multiply the strengths of ground state transitions by six, must be altered.

7

IC Program: NMAX must be set low enough that no configuration with fewer than the predicted number of levels gets read by Program 2. NMAX should be one greater than the last level in the highest configuration to be done. Although this greatly limits the IC Program, it would be possible to do many more transitions if PROCEDURE DIAG expanded the actual states in terms of j1 basis states instead of LS states. Higher states in incomplete configurations could then be approximated as pure j1 states. Therefore, a matrix which transforms the LS basis to the j1 basis would be a useful addition. For elements with more complex configurations, the variables which identify the states and the J-blocks must be changed, along with the generator of the theoretical Hamiltonian and the LS strengths. This involves rewriting most of the procedures.

OUTPUT FROM PROGRAM 2 OF GIANT/FIASCO

Following the listing of the energy levels from Program 1, Program 2 will print out varying quantities of fairly self-explanatory information, depending upon the coupling scheme--that is, LS, jl, or IC.

The jl and IC programs will first list all the Thomas-Fermi wave functions as a function of the number of steps from the origin in y . (The function printed is actually $q(y)$; see the section describing GIANT/FIASCO.) Note that the first ten steps are given, and then jumps of five steps are taken to save space. Immediately below each wave function is printed the expected number of nodes, which is simply n_{int}^{-1-1} , and the actual number of nodes in the wave function shown. The two numbers are always the same for levels done by the scaled TF method, but in the unscaled cases (These can be identified by the fact that SCALE = 1.000.) there is no guarantee that this is so. When the two are the same, it is an indication that the Thomas-Fermi method is valid.

The IC program will now print out the transformation matrices from LS states to the observed states. Double lines separate different configurations, while single lines separate the iterations approaching a leastsquares fit for a given configuration. For each block of a different J , the observed energies and the energies calculated by diagonalizing the theoretical Hamiltonian appear next to the corresponding rows of the transformation matrix. (Note that some of the matrices are rectangular although all of them should be square. Extra columns on the right should be ignored.) Directly below, and within the same J block, are the derivatives of the calculated energy eigenvalues with respect to the various adjustable parameters. The rows are in order of increasing energy eigenvalues, and the columns are in the same order as the list of parameters, which appears once for each iteration. (Derivatives for parameters which are not involved--that is, parameters which are zero after the first iteration--should be ignored.)

Finally, the LS, jl, and IC programs all print out the transition probabilities in the form $3|\langle n|z|m\rangle|^2$, which had already been summed

over final states for m and averaged over initial states for n. At the far right is Einstein's spontaneous emission coefficient in the form $A_{nm} \times 10^{-8}$. However, at present the j1 and IC programs have a card near the end of Program 2 which reads:

```
A+Ax(2xJ(N)+1/(2xJ(M)+1);
```

This reverses the indexes n and m so that $A_{mn} \times 10^{-8}$ is printed out instead of $A_{nm} \times 10^{-8}$ as the comment cards in Program 2 claim.

AUXILIARY PROGRAM FIASCO/RESULTS

This program merely reads the stored output of Program 2 from the disc READF2 and prints out the transition probabilities in several forms. GF is gf, FNM is f_{nm} , ANM is A_{nm} , and AMN is A_{mn} . Input is just the levels of Moore's tables with the same cards that go into Program 1.

ISRAIAS BECOME BOAT, MAY 10, 1967
BEGIN

NAL ALGOL VERSION OF 3/93/87

```

      WRITE (READOF1,PA,2,NEL,C)
      WRITE (PRINTERIOBL1,F2))
      NO1:
      READ(READER1,1,TINFO1,TINF1,TINF2))
      2START: READ(READER1,1,CONE,L,PLA,J,T)(ERRIT))
      IF CONE=1,8 THEN TINFO=TINF1 ELSE
      IF CONE=0,9 THEN TINFO=TINF2 ELSE
      TINFO=TINFO1
      NEFF=COBERT(R/(TINF-T)))
      NO1:
      WRITE (PRINTER1,F3,N,NEFF,ACUM,PLA,K,J,TINF1)
      WRITE (READOF1,F3,N,NEFF,COE=LINK,R,T))
      GO TO START1
      EXIT:
      RETURN
      END

```

20 31 301
30 31 431
30 31 461
30 31 471
30 31 501
30 31 721

COMMENT IMPACT BROADENING AND SHIFT OF SPECTRAL LINES BY ELECTRONS
---PROGRAM S100---FOR HEAVY ELEMENTS (TENTATIVE)---
INPUT1 CARO WITH NMAX (N MAXIMUM N TO BE MEAO), AND NNMAX
 IN MAXIMUM N TO BE CONSIDERED FOR THE INITIAL STATE),
 CARO WITH ONEFF (LIMITATION ON INTERACTING LEVELS)
 AND, 1A CAROS GIVING THE COEFFICIENTS OF THE 3
 INITIALIZATION POLYNOMIALS OF THE THOMAS-FERMI FUNCTION
 EACH CARO HAS A NUMBERS;
 THE INDEX OF THE COEFFS. A(INDEA), B(INDEXB), C(INDEA
 AND, FOR EACH POSSIBLE L (L=0,1,2,3) A CARD WITH
 LM1LSAME(LPI1,LPI2,LPI3).
 THESE ARE THE COEFFICIENTS IN THE ELECTROSTATIC MATRIX
 LM1=COEFF OF F2 IF LTOL=1,
 LM2=COEFF OF F2 IF LTOL=2,
 LSAME=COEFF OF F2 IF LTOL,
 LM150=COEFF OF G0 IF LTOL=1 AND SPO,
 LM180=COEFF OF G2 IF LTOL=1 AND SPO,
 FROM PROGRAM II.
CARO WITH Z,NEL,C
 A CARO FOR EACH LEVEL WITH N,NEFF, CORE, L, N, J, T,
 (CAROS WITH NNMAX WILL NOT BE READ)
OUTPUT1 TABLES GIVING Z,NEL,C,NMAX,ONEFF,
 AND, FOR EACH NUMERICALLY GENERATED WAVE FUNCTION
 A TABLE OF R(Y02)/SQR(T1) VERSUS THE NUMBER OF STEPS OF
 SIZE H THAT Y HAS TAKEN FROM TWO
 WHERE H IS THE RADIAL WAVE FUNCTION AND Y(SQRT(RADIUS)),
 AND, FOR THE GENERATION OF THE IC COUPLING MATRICES.


```

PPR 11=1 STEP 1 UNTIL NODES=00
  A(11)=0/(2*11)*(N+L-11)*H*(N+L-11)*(N+L-1)
PPR=10*LN(PI)
RHAT=H*H/(N*(N+L*LN(H*MAX(L,N*H*PPR)))/C)
SCALE=11
JUMP=0.043
REVERSE=TRUE
DIRECT=TRUE
LASTTIME=0
INSIDE=FALSE
VARYSCALE=1
DIRECTION=DIRECTIONS
NODESP=0
REPEAT
  IF JUMP>0.005 OR ABS(LASTTIME)>0.005 THEN LASTTIME=TRUE
  SCALE=SCALE*DIRECTION*NODESP
  NODES=0
  H=HSTONES(SORT(SCALE))
  I2=SORTR(PDAT)/N
  INVP=(I2+1)*H/(I-2)
  RPP1=0
  FOR I1=ENTIER(N+L+1) STEP -1 UNTIL 0 DO
    #P1=6*11/(16*INVPP*RPP1)
    RPP1=EXP(-C/(INVP*INVR))+INVH*(-N+0.25)*RPP1
    INVR=((I2+2)*H)/(I-2)
    RFD=0
    FOR I2=ENTIER(N+L+1) STEP -1 UNTIL 0 DO
      #P0=6*11/(16*INVRR*RFD)
      RFD=EXP(-C/(INVR*INVR))+INVH*(-N+0.25)*RFD
      R2T=0.894621
      H2T=12*H/12
      H2T*H0=9*H*H*9/61
      K3P1=LPOLY((H2T*H=(I2+1)+2)*VM0012*H2+2)+P2T*((I2+1)+2)*EPSILON
      K30 =LPOLY/(H2T*H=(I2+1)+2)*VP0012*H2+2+A1+P2T*((I2+1)+2)*EPSILON
      FACTORH1=1-PP012*K3P1
      FACTORH0=1-PP012*K30
      FOR I1=12 STEP -1 UNTIL 1 DO BEGIN
        #P1=0
        #P0=0
        RFD=0
        H2T=0
        H30=0
        FACTORP1=FACTORM1
        FACTORP0=FACTORM0
        Y2T=0+2*Tan(I-2)
        K3P1=LPOLY/Y2T+4*VP0012*K3P1+Y2T*EPSILON
        FACTORP1=1-PP012*K3P1
        #P1=12+2*275064*SD0=RFD=FACTORM1*#P1/FACTORM0
      END
    END
  END
  IF SIGN(#P1)>SIGN(#P0) THEN NODESP=1
  IF LASTTIME THEN BEGIN
    NODESP=NODESP*(11+PP012)/P((11*#P1)+2)
    IF VARYSCALE THEN SS=FF1111*#P1 ELSE BEGIN
      FF1111=#P1
      IF SIGN(#P1)->0 THEN INSIDE=TRUE
      IF INSIDE THEN IF #P1>0 THEN BEGIN
        FOR I1=11+1 STEP -1 UNTIL 1 DO BEGIN
          #P1=FF1111*(11/[11+1.5])
          NODESP=NODESP*(16/[11+2])*(13*#P1+FF1111)+2
        END
      END
    END
    GO TO QUIT1
  END
  END
END
IF LASTTIME THEN GO TO QUIT1
OLD=DIRECTION*DIRECTIONS
DIRECTION=1 IF NODESP<INT(L-1) THEN 1 ELSE -1
IF NODESP=INT(L-1) THEN BEGIN
  RATIO=2*(N+L-1)*H*(L-1+2)*H*2*TAN/L
  DIRECTION=RATIO=RFD/#P1
  DIRECTION=SIGN(DIRECTION)
END
IF REPODE THEN
  IF ABS(DIRECTION-OLD*DIRECTION)<1E-5 THEN GO TO REPEAT
  ELSE BEFORE=FALSE
IF NOT BEFORE THEN JUMP=JUMP/2
GO TO REPEAT
QUIT1
IF VARYSCALE THEN NODES=1
NEW=2*ENTIER((2*H*H*TAN))
FOR I1=1 STEP 1 UNTIL NODES DO #P1=FF1111*LAG(SINH*TAN,0,D,0.5*H,12)
  I2=NEW+1
END
NORM(C)=SORT(0.73/(N+3)*NP0001)
NPOINTSCN=12
PRITE(PRINTER(OBL),FTF+R/4,SCALE,PSTAN)
FOR TIME STEP 1 UNTIL 10/15 STEP 5 UNTIL 12 DO
  PRITE(PRINTER,FHTF+R/4,INVR,I1)
  PRITE(PRINTER,FHTH,NORMH,I1-1,NODES)
  TYPE1=PRINTER1
  ARITE(PRINTER,FL1)
END OF PROCEDURE THOPASPERP1

```



```

IF SIZE=1 THEN BEGIN
  TCALC1:=0;E1=1;
  V20[1,1]:=1;
  GO TO SKIP1;
END1;
FOR I2=1 STEP 1 UNTIL SIZE DO
FOR I4=1 STEP 1 UNTIL SIZE DO
  VTEMP1[2,I4]:=(I2*I4+1);
JACOBIK(SIZE,VTEMP1,P00,R00,WCT);
FOR I4=1 STEP 1 UNTIL SIZE DO BEGIN
  FOR I3=1 STEP 1 WHILE MILA[1,I3]>TCALC1 DO BEGIN
    TCALC1+=TCALC1+1;
    FOR I2=1 STEP 1 UNTIL SIZE DO
      V20[12,I3]:=V20[12,I3]+1;
  END1;
  TCALC1+=P(I4,I4);
  FOR I2=1 STEP 1 UNTIL SIZE DO
    V20[12,I3]:=V20[12,I3];
END1;
SKIP1:
WRITE (PRINTER,F15,LOMERRBLOCK+1);
FOR I1=1 STEP 1 UNTIL SIZE DO BEGIN
  WRITE (PRINTER,FV,T20F15,I1,TCALC1),FOR I2=1,2,3,8 ON V20[12,I1];
  FOR I2=1 STEP 1 UNTIL SIZE DO
    V20[12,I1]:=V20[12,I1];
END1;
FOR I1=1 STEP 1 UNTIL IMAX1 DO BEGIN
  FOR IEC1=1 STEP 1 UNTIL NELEC DO BEGIN
    DERIV00=0;
    FOR I2=1 STEP 1 UNTIL SIZE DO
      DEPI100=DERIV00+V20[12,I1]*PLECHATR1X3U(I2,IELEC)*
        V20[12,I1];
    DERIVE11=IELEC*DERIV00;
    END1;
    DERIV00=0;
    FOR I2=1 STEP 1 UNTIL SIZE DO
      DERIV00=DERIV00+V20[12,I1]*SPORMATRIX1X30(I1,I2+13)=V20[13,I1];
    DERIVE11=NELEC*DERIV00;
    IF MOLDO THEN BEGIN
      DERIV00=0;
      FOR I2=1 STEP 1 UNTIL SIZE DO
        FOR I3=1 STEP 1 UNTIL SIZE DO
          DERIV00=DERIV00+V20[12,I1]*SPORMATRIX30(I1,I2+13)*
            V20[13,I1];
    END1;
    DERIVC11=NELEC*2)+DERIV00;
  END1;
END1;
OR I1=1 STEP 1 UNTIL SIZE DO
  WRITE (PRINTER,DERIV1,FOR IPARAP=1 STEP 1 UNTIL 6 DO OPR1V(I1,IPARAM));
  IF MOLDO THEN WRITE (PRINTER,FBL1),FCHECK,0,0,0) ELSE
    PITE (PRINTER(OR1),FCHECK,BD,Tp,CT);
FOR I1=1 STEP 1 UNTIL IMAX1 DO BEGIN
  SUMSQUARES=SUMSQUARES+(TCALC1+1)-T20(I1,I1))+2;
  FOR IPARAPV1=1 STEP 1 UNTIL IPARAP DO BEGIN
    ALPHS1=IPARAVV,IPARAM+1)+ALPHS1(IPARAVV,IPARAM+1)
    -(TCALC1+1)-T20(I1,I1));DERIVE111=IPARAVV;
    FOR IPARAH01=1 STEP 1 UNTIL IPARAH DO
      ALPHS1(IPARAVV,IPARAM)+ALPHS1(IPARAVV,IPARAM)
      +DERIV111,IPARAVV);DERIVE111,IPARAH);
  END1;
END1;
NOT1:
  BREALBMS,NRAHAW,JUMB,NPARAH+1);
  IF JUMB>0 THEN WRITE (PRINTER,F10E3),FERROR;
  OR IELEC=1 STEP 1 UNTIL NELEC DO
    ELECPARAM1(IELEC)=ELECPARAM1(IELEC)+ALPHS1(IELEC,NPARAH+1)
    *PORMPARAM+SPORMPARAM+ALPHS1(IELEC+1,NPARAH+1);
    IF MOLDO THEN
      PORMPARAM+SPORMPARAM+ALPHR1(YELC+2,NPARAH+1));
  TOT11:
    WRITE (PRINTER(FBL1),FSUM,SUMSQUARES,IT1);
    WRITE (PRINTER,F15);
    IF ABS(NOMLOSS-SUMSQUARES)>SUMSQUARES*3 THEN GO TO LTTYPE2;
  END1;
  NO OF PROCEDURE DIAG1
LTTYPE1(PRINTER);
END (READER //NNMAX,NNMAX);
END (READER //,ONEFF);
END (READER //Z,NCNLAC);
RITE (RRI1,TEPDR1,F1,Z,NCNLAC,CNPAY,ONEFF);
RITE (READF2,F2,Z,NCNLAC,NNMAX,ONEFF);
10,589234;
OR N=1 STEP 1 UNTIL NMAX DO
  READ (READF1,NNMAX,NNMAX,ONEFF);
  ENINIDREADF1;
  DERIREADF1;
  OR N=1 STEP 1 UNTIL 31 DO NINTEN();
  IF N>31 THEN ALEN();
  END1;

```

```

    ELSE P-L(4)
    FOR II=0 STEP 1 UNTIL 15 DO
    READ (READER, //, I2, AII(2), BII(2), CII(2))
    IF C/50,1 THEN BEGIN
        00=L4(C/2)
        00SUM=0
        FOR II=10 STEP +1 UNTIL 0 00
            00SUM=CII(1)+00SUM+00
        XD=FP*(200000)
    END ELSE L1 //, I2, 0,5 THEN BEGIN
        00=L4(C/2)
        00SUM=0
        FOR II=12 STEP -1 UNTIL 0 00
            00SUM=0BII(1)+00SUM+00
        XD=00SUM
    END ELSE BEGIN
        00=(I-C/2)*(2/3)
        00SUM=0
        FOR II=15 STEP -1 UNTIL 0 00
            00SUM=AII(1)+00SUM+00
        XD=00SUM
    END
    RM01
    M=X0/40000
    M32=0M1,93
    I2=0M1
    PMP1=0
    PM10=C-(40000Z)
    FOR II=4000 STEP -1 UNTIL 1 DO BEGIN
        PM11=PM10
        PM10=PM11
        PM11=PM1C*(2+M32*NSRT/(PM10/I1))+PM11
        IF I1<2+2 THEN BEGIN
            V=00(I2)=I1=C/512-B*2*PM10
            I2=I2+1
        END
    END
    ENO1
    FOR I2=0M1 STEP 1 UNTIL 500 00 V=M0D(I2)=AII(C)
    M32=M0C(I2,0,0053*Z*(=1/3)*X0)/32
    TIMEIT(PRINTER,1)
    WRITE (PRINTER,FL)
    FOR N=1 STEP 1 WHILE NEFF(N)=NEFF(1)&ONEFF 00
        TH0MASPERMIN(N,NEFF(N),LEN),NINTEN,1)
    NTF=N+1
    FOR MOLO=0 STEP 1 UNTIL 3 00 BEGIN
    RE=0 (READER, //, LNI, LSAME, LP1, LM150, LP150)

```

```

FOR J2=MOLO+2 STEP 1 UNTIL MOLO+3 00 IF J2>0 THEN BEGIN
    I2=0
    FOR S2=0,1 00
    FOR L2=ABS(J2+52) STEP 1 UNTIL J2+52 DO
    IF L2>485(MOLO+1) AND L2<MOLO+1 THEN BEGIN
        I2=I2+1
        ELECHATRIXAD(MOLO,J2,I2,1)+1
        IF MOLO=0 THEN ELECHATRIXAD(0,J2,I2+2)+1 IF S2=0 THEN 1 ELSE +1
        ELSE BEGIN
            L2=MOLO+1 THEN BEGIN
                ELECHATRIXAD(MOLO,J2,I2+2)+LM13
                ELECHATRIXAD(MOLO,J2,I2+3)+1 IF S2=C THEN LM150 ELSE 01
                ELECHATRIXAD(MOLO,J2,I2+4)+0
            END ELSE IF L2>MOLO THEN BEGIN
                ELECHATRIXAD(MOLO,J2,I2+2)+LM14EJ
                ELECHATRIXAD(MOLO,J2,I2+3)+0
                ELECHATRIXAD(MOLO,J2,I2+4)+ J
            END ELSE BEGIN
                ELECHATRIXAD(MOLO,J2,I2+2)+LP11
                ELECHATRIXAD(MOLO,J2,I2+3)+0
                ELECHATRIXAD(MOLO,J2,I2+4)+1 IF S2=0 THEN LP150 ELSE 01
            END
        END END
        I2=0
        OR S3=0,1 00
    FOR L3=0M1(J2+53) STEP 1 UNTIL J2+53 DO
    IF L3>485(MOLO+1) AND L3<MOLO+1 THEN BEGIN
        I3=I3+1
        IF ABS(L3-L2)<1 AND L2>L3P0 THEN BEGIN
            S0=2M0D(1,L2+1+L3,MOLO)
            SPP0=M2H0D(1,L2,MOLO,L3,1)
            G=2M0D(S2,L2+33,L3,I2)/2*(L2+33)
            IF L3=L2+2 THEN G=G*GL3H(2*L2+1) ELSE
            IF L3>L2+2 THEN G=G*GL2*(L2+1) ELSE
            G=G*GL2*(2*L2+1)
            SP=S0M1((3*NG)/2)
            S=SP*SRT(S0P0)
            IF SP>S340 THEN SP=SP
            IF L2>L3P0 THEN SP=SP
            IF S2>S3 AND S2+S3>L3-L2 THEN BEGIN SP+=SP1 SPP+=SPP1 ENO1
            IF L2>L3 AND L2<(L2+1)-2*M0D=(MOLO+1) THEN SP=SP1
            IF L2>L3 AND L2<(L2+1)+MOLO=(MOLO+1)+2 THEN SPP+=SPP1
            IF L2>L3 AND S2>S3 AND S2-S3>1 THEN S2=2*(L2+1)+S2-(S2+1) THEN
            BEGIN SP+=SP1 SPP+=SPP1 ENO1
            END ELSE BEGIN SP=01 SPP=01 ENO1
            SP=MATRIXAD(MOLO,J2,I2+3)=SP1

```

```

SP0NBNMTRIXPAU(MHLD0,J2,I2,I3)+SPP;
ENDI;
ENDI;
I2MAX(MHLD0,J2)+I2;
ENDI;
ENDI;
FOR LGREATER+1 STEP 1 UNTIL 3 DO BEGIN
    I2+01;
FOR J2>LGREATER+3 STEP 1 UNTIL LGREATER+1 DO
IF J2>0 THEN BEGIN
    T2L1>NLGREATR+1,J2)+I2;
FOR S2>0+1 DO
FOR L2>ABS(J2-S2) STEP 1 UNTIL J2+ S2 DO
IF L2>S2(LGREATR+2) AND L2SLGREATR THEN BEGIN
    I2+01 I2+I2+1;
FOR J3>LGREATR+2 STEP 1 UNTIL LGREATR+2 DO
IF J3>0 THEN BEGIN
    I3LOWER(LGREATR,J3)+I3);
FOR S3>0+1 DO
FOR L3>ABS(J3-S3) STEP 1 UNTIL J3+S3 DO
IF L3>S3(LGREATR+1) AND L3SLGREATR+1 THEN BEGIN
    I3+I3+1;
    IF ABS(J2+J3)+S1 AND ABS(L2-L3)+S1 AND (J2+J3)=0 AND S2=S3 THEN BEGIN
        STLS+ SORT((2+J2+I2)*
                    #2#00(L2+J2+L3,J3,S2))#2#00(LGREATR+1,L2,LGREATR,L3,I2)
                    X(I2+J2+J3));
    IF I2+J2+J3=1 THEN STLS+=STLS;
    IF L3=L2 THEN STLS+=STLS;
    END ELSE STLS=0;
    STLS+LGREATR,(I2+I1)+STLS;
ENDI ENDI ENDI ENDI ENDI;
WRITE(PRINTER,FL);
L0NFBLOCK+001 MHLD0+13 IJMAX+01 IJMIN+01;
FOR IJ01 STEP 1 UNTIL 17 DO T2D(IJ01)+1;
FOR IJ+2 STEP 1 UNTIL NHAX+1 DO BEGIN
    IF MHLD0(IJ) THEN BEGIN
        FOR IJ+IJMIN STEP 1 UNTIL IJMAX DO
        FOR I1+1 STEP 1 UNTIL IMAX(IJ) DO
        INDEX(IJ+I1)+1;
        IF MHLD0(IJ) THEN 01;
        LOWERBLOCK+L0NFBLOCK+(IJMAX+1);
        IJMAX+01 IJMIN+101;
        FOR IJ+1 STEP 1 UNTIL 10 DO IMAK(IJ)+01;
    ENDI;
    IJ>ENTIER(IJ+1));

```



```

IF IJ>IJMAX THEN IJMAX+1;
IF IJ<IJMIN THEN IJMIN+1;
BLOCK(IJ)+L0NFBLOCK+1;
IMAK(IJ+IJMAX+1)+1;
FOR IJ>IJMAX+1 STEP -1 WHILE TESTP(IJ,IJ+1) DO BEGIN
    IJ+1+I1+T2D(IJ,IJ+1);
    IJ+1+I1+420(IJ,IJ+1);
END;
T2D(IJ+1)+T4N;
T2D +1+T4N;
IJ+1+T4N;
INDEX(IJ+1);
END;
WHITE (PRINTER,FL);
BLOCK+1+01 INDEX(IJ+1)+1;
V3D(IJ+1)+50RT(6); V3D(IJ+1,2)+01;
FOR N+1 STEP 1 UNTIL NHAX;
DO REGIS SUM1+01 SUM2+01 SUM3+01 WRITE (PRINTER,FL),F4);
SIZE2+2#MAX(L1+1)+ENTIER(IJ+1));
I2L0NFB00+I2L0NFB(IJ+1,J1));
FOR I2+1 STEP 1 UNTIL SIZE2 DO
    V10(I2)+V3D(BLOCK(IJ),INDEX(N+1,I2));
FOR N+1 STEP 1 UNTIL NHAX DO
IF ABS(L1+1)-L4(N)+1 AND ABS(J1+1)-J4(N)+1 AND (J1+N)+J(N)+0
AND ABS(NEFF1)+NEFF(N)+0 THEN NEFF
THEN BEGIN
    LGREATR+MAX(L1+1,L1+1);
    SIZE3+2#MAX(L1+1)+ENTIER((J4(N)));
    I3L0NFB00+I3L0NFB(I4(N)+J4(N));
    T5+01;
    IF L1+1>LGREATR THEN
        FOR I2+1 STEP 1 UNTIL SIZE2 DO
        FOR I2+1 STEP 1 UNTIL SIZE3 DO
        05+05+V10(I2)+STL3#00(LGREATR,I2+I3L0NFB00,I2+I2L0NFB00)+X
        V3D(BLOCK(IJ),INDEX(N+1,I3));
    ELSE
        FOR I3+1 STEP 1 UNTIL SIZE3 DO
        FOR I2+1 STEP 1 UNTIL SIZE2 DO
        05+05+V10(I2)+STL3#00(LGREATR,I3+I3L0NFB00,I2+I2L0NFB00)+X
        V3D(BLOCK(IJ),INDEX(N+1,I3));
    JS=(05+1)*2/((4*NLGREATR+2+1)*(2#J4(N)+1));
    TT+T4(N)+T4N; TT+T4(N); SUM1+SUM1+05; SUM2+SUM2+05/TT;
    LAMBDA+001; S+3+SUM3+05*TT;
    A+2.02005*(IA+JS*TT+3);
    A+AR(2#J4(N)+1)/C2#J4(N)+1);
    WRITE (PRINTER,FS,N+1,03+TT,A);

```

```

        WRITE (READF2,F0,N,N,05,77)
        ENOJ
        WRITE (PRINTER08L),F3,N,SUM1,SUM2,SUM3)
        WRITE (READF2,F6,N,N,SUM1,SUM2))
        TIMEIT(PRINTER)
        WRITE (READF2,F7,N,COREIN1),L(N),K(N),J(N),TIN1))
        FNO J REINIO(READF2) J END )
        LOCK (READF2)
        END,
EXP      IS SEGMENT NUMBER 0517, PRT ADDRESS IS 0207
LN       0018      0206
SORT     0019      0076
OUTPUT(=) 0020      0062
BLOCK CONTROL 0021      0009
INPUT('') 0022      0094
I TO THE I 0023      0216
GO TO SOLVER 0024      0079
ALGOL WRITE 0025      0014
ALGOL READ   0026      0019
ALGOL SELECT 0027      0018
NUMBER OF ERRORS DETECTED = 0           LAST CARD WITH ERROR HAS SEQ # 8
PRT SIZE = 2001 TOTAL PGM SEGMENT SIZE = 2800 WORDS; DISK SIZE = 160 SEGS; NO. PGM, SEGS = 28
ESTIMATED CORE STORAGE REQUIREMENT = 7029 WORDS.
19619137 REON1307, MAY 10, 1967    PROCESSOR TIME = 99.42 SECONDS    I/O TIME = 99.87 SECONDS

```

LABEL 00000000LINE 001671307 COMPILE GIANT/FIASCO SYNTAX

0R07PACC ALGOL

APPENDIX C

CALCULATION OF THE OPTICAL RADIATION EMITTED BY A CYLINDRICAL ARC OF KNOWN TEMPERATURE PROFILE

by. R. Liebermann

INTRODUCTION

In order to compare measurable physical properties of an emitting plasma with theory, a computer program has been written to calculate at the surface of a cylindrical arc discharge:

- (1) the spectral radiance (normal to the surface) due to radiant contribution from along the line of sight of the diameter which has a spatial temperature gradient, and
- (2) the spectral radiant emittance due to contributions from all radiating volume elements of a homogeneous temperature arc column.

The above calculations involve self-absorption processes within the arc column and therefore are solutions of a radiant heat transfer equation.

A. Radiant Heat Transfer Equation

With the assumption that the plasma is in local thermal equilibrium (LTE) the spectral radiance is related to the properties of the medium through the radiant heat transfer equation

$$-\frac{d I_v}{d \tau_v} = I_v - B_v \quad (1)$$

which describes the spatial gradient of intensity along the line of sight at some point x where I_v is the spectral radiant intensity at frequency v in the proper direction, B_v is the corresponding black body intensity and τ_v is the optical depth as measured from $x = -\infty$ to x . We define the optical depth as

$$\tau_v(T) \equiv \int_{-\infty}^x \kappa'_v(T) ds \quad (2)$$

where $\kappa'_v(T)$ is the spectral absorptivity coefficient (including stimulated emission) due to free-free, bound-free, and bound-bound radiative processes. The solution of 1 is given as

$$I_v(\bar{\tau}_v) = \int_0^{\bar{\tau}_v} B_v(\tau_v) \exp \{ -\bar{\tau}_v + \tau_v \} d\tau_v \quad (3)$$

where

$$\bar{\tau}_v \equiv \int_{-\infty}^L \kappa'_v(T) ds \quad (4)$$

with L corresponding to that location along the line of sight (at the surface of the arc column) having spectral radiance $I_v(\bar{\tau}_v)$. In 3 it was assumed for $x \leq 0$ that no contribution to $I_v(\bar{\tau}_v)$ is made (i.e., no external radiation field is present).

1. Spectral Radiance

If our interest is radiance at the arc column's surface due to contributions from along the line of sight of the diameter, equation 3 by an assumption of radial symmetry can be placed in the following form.

$$I_v(\bar{\tau}_v) = I_v(r=R) = \int_0^{\bar{Z}} B_v(Z) \left[\exp \{ Z \} + \exp \{ -Z \} \right] \exp \{ -\bar{Z} \} dZ \quad (5)$$

where Z is an optical depth measured from the center of the arc column to some radial point r along the radius which has a maximum dimension R . The correspondence is $Z = 0$ at $r = 0$ and $Z = \bar{Z}$ at $r = R$ thus

$$\bar{Z} = \int_0^R \kappa'_{\nu} (T(r)) dr ; Z = \int_0^r \kappa'_{\nu} (T(r)) dr \quad (6)$$

For programming purposes Equation 5 is the better form of 3. In order to solve 5 it is first necessary to have prior knowledge of the temperature profile $T(r)$ and for a given gas vapor pressure a method by which κ'_{ν} can be determined such that solutions of 6 are obtainable. Part D of this section describes the general theory involved for determining $\kappa'_{\nu}(T)$.

Utilizing the theory of Part D we are then prepared to numerically integrate Equations 6 and thus 5. The method of approach was as follows. For a specified temperature profile and frequency the integrand of 6 was determined at division points in r and interpolated in r^2 between division points. Using a linear expansion of κ'_{ν} in r^2 a closed form integration was performed between division points and a summation yielded $Z(r)$. In similar fashion the black body term in the integrand of 5 was calculated at division points in r and linearly expanded in Z^2 . A closed form integration of 5 was then possible between division points of $Z(r)$ and was summed to yield $I_{\nu}(\tau_{\nu})$. Although the latter integration can be performed for all values of the parameters serious errors (due to cancellation effects) may develop when ΔZ is small between end points of the intervals. Hence for $\Delta Z < .01$ the solution was expanded in terms of ΔZ whereas for $\Delta Z > .01$ the closed form was used. Solution of 5 was then repeated for other selected ν values of the specified band pass to yield a representative spectrum.

2. Spectral Radiant Emittance

If our interest is spectral emittance at the arc column's surface due to contributions from all radiating volume elements with the

discharge assumed homogeneous in temperature then Equation 3 which yields the spectral radiance along a particular line of sight reduces to

$$I_v(T, S) = B_v(T) \left[1 - \exp \{ - \bar{\tau}_v \} \right] \quad (7)$$

where now from Equation 4

$$\bar{\tau}_v = K'_v(T) S \quad (8)$$

S being the distance through which radiation travels along a particular line of sight and is a function of arc geometry.

The spectral radiant emittance at the surface of the arc column can be calculated using 7 by applying the cosine law and integrating over solid angle. Using the geometry shown in Reference 1 the spectral radiant emittance is given as

$$F_v(T) = B_v(T) \left[\pi - 4 \int_0^{\pi/2} \int_0^1 \exp \left\{ \frac{-K'(T) D u}{u^2 + (1-u^2) \sin^2 \phi} \right\} u du d\phi \right] \quad (9)$$

where D is the column diameter

The radiant emittance is then determined by

$$F(T) = \int_0^\infty F_v(T) dv \quad (10)$$

Equations (9) and (10) were solved using straightforward numerical techniques.

B. Input to Arc Intensity Program

The input required for the above calculations is fully described within the program itself which is shown in Part E of this Section. In brief the basic required input is as follows:

- (1) Spectroscopic data involving bound-bound transitions such as
 - (a) oscillator strengths
 - (b) electron impact line shifts and widths
 - (c) excitation energies
 - (d) statistical weights
- (2) thermodynamic properties such as tables of
 - (a) electron number densities
 - (b) neutral particle number densities
 - (c) internal partition functions
 - (d) ionization lowering values
- (3) temperature profile
- (4) specified wavelength band pass.

C. Output of Arc Intensity Program

The output of the program provides plots as well as printouts of the spectral radiance and spectral radiant emittance. In addition plots of spectral absorptivities are obtainable. Samples of these plots are shown in Figures 3, 4, and 5. For particulars on how to obtain these plots see program Part E.

D. Spectral Absorptivities

The net absorption coefficient κ' which is the difference between true absorption and induced emission coefficients is in a spectral line for a given frequency ν and temperature T (assuming LTE)

$$\kappa'_{\nu}(T) = \pi r_o c f_{mn} N_n \left[1 - \exp \left\{ \frac{-hv}{kT} \right\} \right] L(\nu) \quad (11)$$

where π , r_0 , c , h and k are the usual constants, f_{mn} is the absorption oscillator strength for transitions from state n to m (n being the lower energy level state), N_n is the population density of the initial state, and $L(v)$ is the line profile normalized such that

$$\int_{-\infty}^{\infty} L(v)dv = 1 \quad (12)$$

where $L(v)$ is a function of the lines, shifts, widths etc. all a function of temperature and pressure.

For conditions of LTE the population density N_n can be expressed in terms of N_o (the total number of atoms or ions in question) by use of the Boltzmann relation

$$N_n = \frac{g_n N_o}{U_o} \exp \left\{ \frac{-E_n}{kT} \right\} \quad (13)$$

where g_n is the statistical weight of the initial level, E_n is the excitation energy of the initial level, U_o is the atomic (or ionic) internal partition function and T is the absolute electron temperature.

The line profile $L(v)$ is course dependent on the mechanisms of line broadening. The stark effect due to electron impact has the Lorentz dispersion profile given as

$$L(v) = \frac{1}{\pi\omega} \left[\frac{1}{\left[\frac{v - (v_o + d)}{\omega} \right]^2 + 1} \right] \quad (14)$$

where ω is the half width of the line at half intensity and d is the electron impact shift. v_o is the observed frequency of the line in an unperturbed condition.

When resonance broadening mechanisms are of importance, one must add to the electron impact half width ω the resonance half width ω_R which from first order approximation can be expressed for resonance lines as

$$\omega_R = \frac{3r_0 c}{4\pi} \left(\frac{g_1}{g_2} \right)^{1/2} \frac{f N_g}{v_0} \quad (15)$$

where g_1 and g_2 are respectively the lower and upper states' statistical weight factors of the resonance line, N_g is the ground state population density and f is the absorption oscillator strength of the transition (actually f as defined here is the average value for the resonance multiplet transition obtained by a sum of the multiplet's individual f 's over final states which are then averaged over initial states). In equation 15, N_g are neutral perturbers of the same kind (radiating atoms). For the case when perturbers of unlike kind are of such abundance (e.g. a strong concentration of another gas specie is present) then Van der Waals broadening may be of some importance and should be included in the dispersion profile.

Besides line broadening due to charge perturbers (Stark effect) or neutral atoms (Resonance and Van der Waals effects) there exists other broadening mechanisms which must also be considered, namely Doppler broadening, which results in a Gaussian line shape profile. This type of profile is dominant when collisions are negligible and the velocities of the radiating systems have a thermal distribution. The Gaussian line shape is given as

$$L_D(\Delta v) = \left(\frac{\ln 2}{\pi} \right)^{1/2} \frac{1}{\omega_D} \exp \left[-\frac{\ln 2}{\omega_D^2} (\Delta v)^2 \right] \quad (16)$$

with $\Delta v = v - v_0$ and where ω_D is the Doppler half (half) width

$$\omega_D = \left[\frac{2kT \ln 2}{Mc^2} \right]^{1/2} v_0 \quad (17)$$

M being the mass of the radiating system. When collision effects cannot be neglected (e.g. when ω , ω_R etc. are of the same order of magnitude as ω_D) then joint effects of Doppler and the more important pressure

broadening mechanisms should be considered. The observed line shape is then the so called Voigt profile provided the broadening processes are statistically independent. From 17 it is obvious that lines occurring in the UV regions will tend to be more of a Voigt profile type.

The net absorption coefficient κ'_v as expressed in 6 is not only due to bound-bound transitions but also includes bound-free and free-free processes as well. Therefore, one must add to a sum of Equation 11 these other processes to obtain representative values of 5 in the spectral regions where bound-bound transitions are not dominant. For conditions of LTE the bound free absorptivity $\kappa_{bf}(v, T)$ can be expressed in terms of a sum over excited states designated by quantum numbers n and l having corresponding photoionization cross-sections σ_{nl} and population density $N_{n,l}$ whose edge frequencies v_{nl} are less than or equal to v

$$\kappa_{bf}(v, T) = \sum_{n,l} \left. \sigma_{nl} N_{nl} \right\} \quad v_{nl} \leq v \quad (18)$$

The net bound-free absorptivity is then expressed as

$$\kappa'_{bf}(v, T) = \kappa_{bf}(v, T) \left[1 - \exp \left\{ \frac{-hv}{kT} \right\} \right] \quad (19)$$

Solution of 18 is a formidable task since σ_{nl} for each level requires numerical solutions of the Schrodinger equation.* A simplified approach is to separate 18 into two distinctive regions i.e., into levels which are hydrogen like and into levels which are non hydrogen like thus

$$\kappa_{bf}(v, T) = \sum_{n,l} \sigma_{n,l} N_{n,l} + \sum_{n,l} \sigma_{n,l}^H N_{n,l}^H \quad (20)$$

* See for example Ref. 1.

where in general for the hydrogen like terms $n \gg 1$. The sum over the hydrogenic levels can be simplified further as follows. Starting with a sum rule analogous to that for bound-bound transitions

$$\int_{v_{nl}}^{\infty} \sigma_{nl}^H dv = \pi r_o c f_{nl} \quad (21)$$

and using the proportionality $\sigma_{nl}^H \sim v^{-3}$ the hydrogenic photoionization cross section σ_{nl}^H is

$$\sigma_{nl}^H = 2\pi r_o c \frac{v_{nl}^2}{v^3} f_{nl} \quad (22)$$

where f_{nl} corresponds to the excited n, l state's continuum oscillator strength. Using the Rydberg formula for hydrogenic energy levels, the binding energy E_B of the excited level is ($E_{nl} - E_n$)

$$E_B = h\nu_{nl} = E_\infty - E_{nl} = \frac{E_H Z^2}{n^2} \quad (23)$$

where Z refers to the ionization stage, n is the principal quantum number, E_∞ is the ionization potential, E_{nl} is the excitation energy of the excited level and E_H is the Rydberg constant. From 23 we see that the rate at which the binding energy changes with respect to unit change in principal quantum number for $n \gg 1$ is

$$\Delta E_B \approx \frac{-2E_H Z^2}{n^3} \quad (24)$$

We now define an average hydrogenic cross section σ_n for all l states with same quantum number n as

$$\sigma_n \equiv \sum_l (2l+1) \sigma_{nl}^H / \sum_l (2l+1) \quad (25)$$

where l is the orbital-angular momentum quantum number. Thus using the hydrogenic relations

$$\left. \begin{aligned} \sum_l (2l+1) f_{nl} &= .5n \\ \text{and} \quad \sum_l (2l+1) &= n^2 \end{aligned} \right\} \quad (26)$$

$n = \text{constant}$

Equation 25 takes the form

$$\sigma_n = 4\pi^2 \frac{\alpha a_0^2}{5} \left(\frac{e_H}{h\nu} \right)^3 z^4 \quad (27)$$

where α and a_0 are the usual constants. Equation 25 is the familiar hydrogenic cross section less the Gaunt factor G_{bf} . Using Equation 13, and noting for atomic gases, whose higher levels are hydrogen like but degenerate in J (total angular momentum quantum number) that

$$g_n = \sum_l (2J+1)_n = 2n^2 g_1 \quad (28)$$

where g_1 is the statistical weight factor of the ground state of the parent term; and using the relationship of Equation 24 the hydrogenic sum term of 20 becomes

$$\sum_{n,l} \sigma_{nl}^H N_{nl}^H = \frac{-4\pi^2 \alpha a_0^2 g_1}{U_0 E_u} \left(\frac{e_H}{h\nu} \right)^3 z^2 N_0 \sum_n \exp \left\{ \frac{-E_n}{kT} \right\} \Delta E_B \cdot G_{bf} \quad (29)$$

For hydrogen the excitation energy E_n is approximately equivalent to E_{nl} . However, for other gases whose higher levels are hydrogen like but degenerate in J then E_n should be averaged over these J, ℓ states which have $E_{J\ell}$ excitation energies such as

$$E_n = \sum_J (2J+1) E_{J\ell} / 2n^2 g_1 \quad (30)$$

Thus with E_n as defined in 30 obeying Equation 23 wherein E_{nl} is replaced by E_n then 29 takes the form of

$$\sum_{nl} \sigma_{nl}^H N_{nl}^H = \frac{-4\pi^2 \alpha a_0^2 g_1}{U_o E_F} \left(\frac{E_H}{h\nu} \right)^3 Z^2 N_o G_{bf} \exp \left\{ \frac{-E_\infty}{kT} \right\}.$$

$$\sum \exp \left\{ \frac{E_B}{kT} \right\} \Delta E_B \quad (31)$$

with the assumption that $G_{bf} \approx \text{constant}$ for $n \gg 1$.

The sum on the right of 31 may for practical purposes be taken as an integral with lower limit $E_B = h\nu_n$ and upper limit $E_B = 0$. Hence for $\bar{\nu}_n$ representing the maximum edge frequency of the merged levels where $n \gg 1$ with $\bar{\nu}_n \leq \nu$ then

$$\sum_{nl} \sigma_{nl}^H N_{nl}^H = \frac{4\pi^2 \alpha a_0^2 g_1}{U_o} \left(\frac{kT}{E_H} \right) Z^2 N_o \left(\frac{E_H}{h\nu} \right)^3 \exp \left\{ \frac{-E_\infty}{kT} \right\} \left[\exp \left\{ \frac{h\nu_n}{kT} \right\} - 1 \right] G_{bf} \quad (32)$$

$$= 1.82 \times 10^{24} \frac{g_1 T}{U_o} Z^2 \frac{N_o}{\nu^3} \exp \left\{ \frac{-E_\infty}{kT} \right\} \left[\exp \left\{ \frac{h\nu_n}{kT} \right\} - 1 \right] G_{bf}$$

or for the case when ν is less than the maximum edge frequency of the merged levels ($\nu < \bar{\nu}_n$) then

$$\sum_{nl} \sigma_{nl}^H N_{nl} = 1.82 \times 10^{24} \frac{g_1 T}{U} Z^2 \frac{N_o}{v^3} \exp \left\{ \frac{-E_\infty}{kT} \right\} \left[\exp \left\{ \frac{hv}{kT} \right\} - 1 \right] G_{bf} \quad (33)$$

Equations 32 and 33 are equivalent to those presented by Biberman, Norman and Ulyanov⁽²⁾ less their correction factor which for our high n levels is approximately one and equivalent to the Gaunt factor. It is of interest to note that in the form of 31 if the right hand sum is taken as an integral with lower limit set to $E_B = 0$ and upper limit $E_B = -\infty$ representing unbound electrons we obtain at once the familiar free-free absorptivity expression

$$\kappa_{ff} = 1.82 \times 10^{24} \frac{g_1 T N_o Z^2}{U_o v^3} \exp \left\{ \frac{-E_\infty}{kT} \right\} \cdot G_{ff} \quad (34)$$

where the G_{ff} term has been introduced and is the free-free Gaunt factor. Thus equation 20 takes the form (including the f-f absorption)

$$\kappa_{bf+ff} = \sum_n \sigma_n N_{nl} + 1.82 \times 10^{24} \frac{g_1 T N_o Z^2}{U_o v^3} \exp \left\{ \frac{-E_\infty}{kT} \right\} \left[G_{ff} + G_{bf} \left(\exp \left\{ \frac{hv'}{kT} \right\} - 1 \right) \right] \quad (35)$$

whereby previous definitions $v' = \bar{v}_n$ if $v \geq \bar{v}_n$ and $v' = v$ if $v < \bar{v}_n$. In equation 35 the non-hydrogenic sum term then only includes such levels having edge frequencies v_E which meet the requirement that $\bar{v}_n < v_E \leq v$. In the above derivations the assumption that G_{ff} is constant independent on temperature and frequency is valid provided $T < 2$ ev (see Ref. 3) however when T is of greater value than G_{ff} increases and varies somewhat with frequency. Likewise when n is of some lower value then G_{bf} is no longer a constant but varies with

quantum number and frequency. The accuracy of 35 is thus better enhanced when the sum term includes the majority of the excited levels. Such calculations involving the sum term have been made by Ref. 2 and ⁴ who have utilized the techniques proposed by Ref. 1 for determining photoionization cross sections for ionized gases other than hydrogens. However their results differ somewhat in that they have chosen different normalization factors. In essence (using their results) Equation 35 remains the same with the exception of replacing the factor $Z^2 G_{bf}$ with a ζ (Zeta) factor, and in addition when using the ζ factor of Ref. 4. v' is to be replaced by v for all values. Their sum term then only includes a limited number of lower excited levels (including the ground state).

Since several b-b transitions usually occur for a given lower excited state near the frequency of its continuum photoionization edge (the upper excited state being near the ionization limit) there results a pseudo continuum (i.e. the lines in question merge with the continuum causing in appearance a false photoionization edge at a slightly lower frequency). When these b-b transitions are not included in the sum of Equation 11 near such corresponding photoionization edges then serious errors may develop in solutions of radian heat transfer problems. Therefore in order to avoid such difficulty (when all such b-b transitions are not fully resolved) one should assign a correction term to the photoionization edge v_E to yield an apparent edge v'_E such as

$$v'_E = v_E - \Delta E_S / h \quad (36)$$

where h is the usual constant and ΔE_S is the so called advance of the series limit (see Ref. 5), and let the photoionization edge cross-section $\sigma(v'_E)$ for this particular level be defined at v'_E . In addition the lowering of the ionization potential ΔE_∞ should be included in the calculation of v_E such as

$$h\nu_E = E_\infty - \Delta E_\infty - E_{nl} \quad (37)$$

where E_∞ is the ionization potential and E_{nl} is the excitation energy of the level in question.

REFERENCES

1. C. H. Church, et.al., "Final Report on Contract Nonr 4647(00)", 15 November 1965, AD 473 996. See also A. Burgess and M. Seaton, Mon. Not Roy. Astron. Soc. 120, 121 (1960).
2. L. M. Biberman, G. Norman and K. Ulyanov, Optics and Spectroscopy 10, 297 (1961).
3. J. M. Berger, Ap. J. 124, 550 (1956).
4. D. Schluter, Z. Astrophys. 61, 67 (1965) and private communication.
5. H. Griem, Plasma Spectroscopy, McGraw Hill Book Co., New York (1964).


```

READ(HEADF1//A,N,C)
IF ATNUM=SA THEN
  READ(HEADF1//A,FOR I=1      (I< NMAX DO (N=A,A,A,J[I],
  E[1])))
ELSE
  READ(HEADF1//A,FOR I=1 STEP 1 UNTIL NMAX DO (N=A,A,A,A,J[I],
  E[1]))+
    HEPIND(READ(I)) LOCK(HEADF1) +
FOR I=1 STEP 1 UNTIL NMAX DO J[I]=J[I]+1
  READ(HEADF2//A,N,C,F,G)
  I=0
  LAMMIN=LAMMIN+R
  LAMMA=LAMMA+R
  NUWING=1/LAMMIN
  NUMAX=1/LAMMA
  DEDU32=R*A
  C=.587234*NUWING/(1+NUWING*R)  F=NUWING*R
  IF F>1 THEN R=.587234*R ELSE R=.587234*NUWING/(1-F)
START1
  READ(HEADF2//A,N,C,F,G)(EXIT)
  IF N>N1 THEN
    IF YYRC THEN IF YYSR THEN
      BEGIN
        REAL A
        READ A
        IF ATNUM=0 THEN IF N=1 OR N>2 OR N=4 THEN D5=USM(.3)
        I=1+1
        A+TVA(.3)
        LAMMA+=A
        GFMN([1]+D5*XK(2*A([1]+1)/329211.93))
        NUO([1]*A
        N1([1]-N)+I([1])<=E([1])&E(N)
        WRITE (PRINTER,F3.2,*,FM=1,LAMBDA/NOC([1]),GFMN([1],E([1]))
        END OF IF STATEMENT
      GO TO START1
    EXIT 1 REWIND(HEADF2)  LOCK(HEADF2)
    ZZ=MAX+1
    READ(HEADF3//A,N,C,F,G)
START21
  I=0
START22
  READ(HEADF3//A,N,C,F,G)(EXIT)
  IF B=0 THEN GO TO START22
  IF B=1 THEN
    BEGIN
      IT=IT+1  T=TEMPITY+C+(IT,N)*F+U((IT+N)*G)
      WRITE(PRINTER,F3.2,*,FM=1,LAMBDA/NOC([1]),GFMN([1],E([1]))
      END
    COMMENT DETERMING FREQUENCY AND WAVELENGTH ARRAYS WHICH INCLUDE ALL
    PEAK LINE VALUES FOR ALL TEMPERATURES LISTED IN PROFILE 1
    REAL NUW=REAL SYSL(1000)
    REAL NUWA=INTEGER N1
    LABEL EXIT21  REAL DELN=1  INTEGER JMAX  JU=1
    REAL DELLAC
    REAL WIA(2*Q3)
    JQD=1
    FOR Q=1 STEP 1 UNTIL QMAX DO
      BEGIN
        IT=ENTIER((3*ALIA+IT*T(G))/1000)
        IF IT>N THEN ITONT=IT
        WIAQ3=IT
        NUW=IT
        NUWA=(C((IT+1)/H)*.3)*WIA
        FOR I=1 STEP 1 UNTIL IT
          DELN=1/(1+(1+Q3)*(1-Q3)+(Q*(IT+1)*WIA*0*(IT+1,N))*Q3)
          QD=1/Q3
          A=NUW*QD
          IF A>WIA THEN
            IF A> MAX THEN
              BEGIN
                JU=1
                JU+=1
                SNL(JU)=1
                END
              END OF I LOOP
            END OF Q LOOP
            JMAX=J
            NU([1]+1)/(LAMB([1]+LAMMIN))
            DELLAC=(LAMMA+LAMMIN)/NLAM
            FOR K=1 STEP 1 WHILE LAMB(K)<LAMMAX DO

```


APPENDIX D

WHITTAKER AND GAMMA FUNCTIONS - DESCRIPTION OF TWO ALGOL PROCEDURES

By G. Basi
Computer Sciences R & D

ABSTRACT

This report describes the development and testing of two computer algorithms WOG and GAMMAC required in connection with computation of spectral properties of plasma arcs being carried out for Dr. C. H. Church of Quantum Electronics R & D. The algorithm WOG computes the irregular Whittaker function $W_{\eta, l+1/2}$ for real positive non-integral η , and for l a non-negative integer. GAMMAC computes the function $f(z)$ for z real or complex. A very good accuracy has been obtained from both of these algorithms. GAMMAC is used in WOG, which calculates one of the four confluent hypergeometric functions needed in the calculation of transitions between eigenstates described by the Coulomb wave functions.


```

SYMBOL(I=LY+,I+,14+BC03+0,24) ; SC 381 17411
NUMBER(2,68+LY+,I+,14+BC04+0,2) ; SC 381 17911
SYMBOL(I=LY+,I+,14+BC04+0,24) ; SC 381 18413
NL BEK(1,72+LY+,I+,14+BC04+0,3) ; SC 381 18413
LINE(LAMB,FINU,NMAX,I,TRY) ; SC 381 18711
PLOT(LX+3,0,-3) ; SC 381 19011
END OF I LOOP PLOTS ;
EXIT61 ;
END OF SPECTRAL EMISSANCE CALCULATIONS AND PLOT ROUTINE ;
IF PLOTEST THEN SC 381 19412
BEGIN SC 381 19510
COMMENT ABSORPTIVITY PLOT ROUTINE ;
ROOLEAN TRY;
ALPHA ARRAY YALF(014)=AALF(013)+BCD(014) ;
FILL YALF() WITH "SPE", "CTRAL" ;
"TAUSHP", "TIVITY", "(1/CM)" ;
FILL XALF() WITH "WAVELN", "NGTH", ("ANGSTR", "UNS") = 1 ;
FILL BCDF(0) WITH "STCHMR", "ATMURE", "EM", "DEN", "G", K = 1 ;
TRY+TRUE ;
FOR I=1 STEP 1 UNTIL MAXX DO SC 311 45410
BEGIN SC 311 45411
AXIS(0,0+XALF+24+LX+0,44IN+0X) ;
0+PLOT<1>(I,I+1) ;
FOR N=0 STEP 1 UNTIL NMAX DO SC 311 45413
FINU(N)+RT(CN) ;
RSCALE(FINU,NMAX,I+1,LY, VMIN,DT) ;
AXIS(-.25+3*YALF+30,LY,90+YMIN,DT) ;
SYMBOL(ILY+,5,I+BC01,0,30) ;
NUMBER(2,68+LY+,5,I+14+BC01+0,0) ;
LINE(LAMB,FINU,NMAX+1,TRY) ;
PLOT(LX+3,0,-3) ;
END OF I LOOP ;
END OF ABSORPTIVITY PLOT ROUTINE ;
END;
END;
END;
END;
PLOT(0,0,0,0+10);
END;
END;
CDS IS SEGMENT NUMBER 0052; HRT ADDRESS IS 0160
Exp 0053 0174
Ly 0054 0173
SIS 0055 0161
SURT 0056 0056
OUTPUT(=) 0057 0133
BLOCK CONTROL 0058 0005
INPUT(=) 0059 0201
X TO THE I 0060 0175
GU TO SOLVEN 0061 0245
ALGOL WHITE 0062 0014
ALGOL READ 0063 0015
ALGOL SELECT 0064 0016
NUMBER OF ERRORS DETECTED = 0 LAST CARD WITH ERROR HAS SEQ # SC 301 1810
PHI SIZE = 3481 TOTAL PGM SEGMENT SIZE = 2979 409651 DISK SIZE = 160 SEGMENTS PGMS. SEGS = 95
ESTIMATED CORE STORAGE REQUIREMENT = 7265 WORDS,
DATE IS THURSDAY MAY 11, 1967 PROCESSOR TIME = 66.73 SECONDS END TIME = 79.40 SECONDS

```

APPENDIX D

WHITTAKER AND GAMMA FUNCTIONS - DESCRIPTION OF TWO ALGOL PROCEDURES

By G. Basi
Computer Sciences R & D

ABSTRACT

This report describes the development and testing of two computer algorithms WOG and GAMMAC required in connection with computation of spectral properties of plasma arcs being carried out for Dr. C. H. Church of Quantum Electronics R & D. The algorithm WOG computes the irregular Whittaker function $W_{\eta, l+1/2}$ for real positive non-integral η , and for l a non-negative integer. GAMMAC computes the function $F(z)$ for z real or complex. A very good accuracy has been obtained from both of these algorithms. GAMMAC is used in WOG, which calculates one of the four confluent hypergeometric functions needed in the calculation of transitions between eigenstates described by the Coulomb wave functions.

Summary

This report describes the development and testing of two computer algorithms WOG and GAMMAC required in connection with computation of spectral properties of plasma arcs being carried out for Dr. C. H. Church of Quantum Electronics R & D. The algorithm WOG computes the irregular Whittaker function $W_{\eta, \lambda+1/2}$ for real positive non-integral η , and for λ a non-negative integer. GAMMAC computes the function $F(z)$ for z real or complex. A very good accuracy has been obtained from both of these algorithms. GAMMAC is used in WOG, which calculates one of the four confluent hypergeometric functions needed in the calculation of transitions between eigenstates described by the Coulomb wave functions.

Introduction

Purpose of this study was to translate two subroutines WOG and GAMMAC from fortran into Algol and improve upon them. As received neither of the subroutines were in usable form, and considerable revision has been necessary. These algorithms will be used in a program to calculate the transitions between the eigenstates described by the Coulomb wave function.

The calculation of the transitions involves the use of confluent hypergeometric functions. Two of the four confluent hypergeometric functions are the solutions to Kummer's equation¹

$$x \frac{d^2y}{dx^2} + (b-x) \frac{dy}{dx} - ay = 0.$$

The two solutions of the above are Kummer's functions ${}_1F_1(a; b; x)$ and $U(a; b; x)$ defined as follows:

$$y = {}_1F_1(a; b; x) = \sum_{n=0}^{\infty} \frac{(a)_n}{(b)_n} \frac{x^n}{n!}$$

Where $(a)_n = a(a+1) \dots (a+n-1)$ for $n \geq 1$ and $(a)_0 = 1$

$(b)_n$ is similarly defined.

$$y = U(a; b; x) = \frac{\pi}{\sin \pi b} \left[\frac{{}_1F_1(a; b; x)}{\Gamma(1+a-b)\Gamma(b)} - \frac{x^{1-b} {}_1F_1(1+a-b; 2-b; x)}{\Gamma(a)\Gamma(2-b)} \right].$$

The other two confluent hypergeometric functions are the solutions to Whittaker's equation²

$$\frac{d^2y}{dz^2} + \left(-\frac{1}{4} + \frac{\eta}{z} - \frac{\ell^2 + \ell}{z^2} \right) y = 0.$$

Two solutions are Whittaker's functions $M_{\eta, \ell+1/2}(z)$ and $w_{\eta, \ell+1/2}(z)$. Whittaker's functions are defined as follows:

$$M_{\eta, \ell+1/2}(z) = z^{\ell+1} e^{-1/2z} {}_1F_1(\ell+1-\eta; 2\ell+2; z).$$

$$w_{\eta, \ell+1/2}(z) = \frac{\pi}{\sin(2\ell+1)\pi} \left[\frac{-M_{\eta, \ell+1/2}(z)}{\Gamma(-\ell-\eta)\Gamma(2\ell+2)} + \frac{M_{\eta, -(\ell+1/2)}(z)}{\Gamma(\ell+1-\eta)\Gamma(-2\ell)} \right]$$

1.1 Available programs

Two programs that calculate the generalized hypergeometric function

${}_pF_q(a_1, a_2, \dots, a_p; b_1, b_2, \dots, b_q; z)$ are available in Algol B5000.

These programs were written by Hammers³. One of these two programs computes a general hypergeometric function which has a complex or real argument and any number of real parameters. The other program computes the same function for any number of real or complex parameters.

There are three programs called BEAUTY, BEAST, and CHIC in Fortran II. These programs were written by Johnson and Sangren⁴ and calculate any generalized hypergeometric functions. Program BEAUTY can be used to calculate any generalized hypergeometric function with up to ten numerator and ten denominator parameters and one argument. Program BEAST can be used to compute analytical continuation of an ordinary hypergeometric function. The program called CHIC can be used for calculating 34 distinct hypergeometric series in two variables.

Two other programs WOG and HLIGAM are obtained from McGuire⁵. Both these programs were obtained in Fortran. Program WOG calculates the irregular Whittaker function $W_{\eta, \ell+1/2}(z)$ for $\eta > 0$, real, and non-integral. Program HLIGAM calculates the same function where η is a pure imaginary number.

Both of these programs call for another program--GAMMAC-- which calculates the function $\Gamma(z)$ for any z real or complex. GAMMAC was obtained in Fortran from Dr. McGuire.

2. Computation of GAMMAC

Procedure GAMMAC computes the value of $\Gamma(z)$ in the following way:

Let $z = (x, y)$ {i.e. $z = x+iy$ }. The notation $z_i = (x_i, y_i)$ will be used during the discussion and shall be understood for $i = 1, 2, 3, 4$. \bar{z} will denote the complex conjugate of any complex number z .

For positive real integral values of z , $\Gamma(z)$ is computed as $(z-1)!$, for non-positive real integral values of z , the procedure does not work. If $x < 0$, then the procedure uses the following recurrence relation to relate $\Gamma(z)$ to $\Gamma(z_1)$ where the real part of z_1 is positive.

or

$$\Gamma(z) = \frac{1}{z} \Gamma(z+1)$$

$$\Gamma(x, y) = \frac{1}{(x, y)} \Gamma(x+1, y).$$

Now if y_1 (which is the same as y), in z_1 is negative, the $\Gamma(z_1)$ is related to $\Gamma(z_2)$, where y_2 is positive, by the following relation

$$\Gamma(z_1) = \overline{\Gamma(\bar{z}_1)} = \overline{\Gamma(z_2)}$$

$$\text{i.e. } z_2 = \bar{z}_1, \text{ or } y_2 = -y_1 \text{ and } x_2 = x_1$$

with the use of the above relations the computation of $\Gamma(z)$ for general z reduces to the computation of $\Gamma(z_2)$ whose both real and imaginary parts are positive.

The next step is to relate $\Gamma(z_2)$ with $\Gamma(z_3)$ where $0 \leq y_3 < 1$. This is done by making use of Gauss' multiplication theorem. Gauss' multiplication theorem asserts that if $z_2 = nz_3$ where n is an integer then

$$\Gamma(z_2) = \frac{\Gamma(z_3)\Gamma(z_3 + \frac{1}{n})\Gamma(z_3 + \frac{2}{n}) \dots \dots \Gamma(z_3 + \frac{n-1}{n})}{(2\pi)^{\frac{1}{2}(n-1)} n^{\frac{1}{2} - z_2}}$$

In our case integer n is chosen to be the next greater integer than y_2 so that $y_2/n = y_3 < 1$. Next we relate $\Gamma(z_3)$ to $\Gamma(z_4)$ where z_4 is such that both x_4 and y_4 satisfy the inequalities $0 < x_4 \leq 1$, $0 \leq y_4 < 1$. In fact $y_4 = y_3$ and $x_4 = x_3 - [x_3]$ in case x_3 is a nonintegral real and if x_3 is an integer $x_4 = 1$, where $[x_3]$ is greatest integer contained in x_3 . The relation between $\Gamma(x_3)$ and $\Gamma(z_4)$ can conveniently be expressed as follows.

$$\Gamma(x_3) = (z_3 - 1)(z_3 - 2)(z_3 - 3) \dots (z_4)\Gamma(z_4)$$

Now the computation of $\Gamma(z)$ for any complex number z has been related to $\Gamma(z_4)$ where z_4 is such that $0 < x_4 \leq 1$, $0 \leq y_4 < 1$. $\Gamma(z_4)$ is determined by the Padé power approximation of $1/\Gamma(z)$.

The procedure GAMMAC was obtained in Fortran and has been translated into Algol. Some changes were made during the translation to make the program

more efficient and clear. A basic constant was defined to greater accuracy to reduce the error. At present it is as discussed above, and calculates the function $\Gamma(z)$ for z real or complex. The values were checked against the available tables and found to be accurate to eight significant figures in the region

$$x = -2.0 (.25) \quad 2.0$$

$$y = -2.0 (.25) - 2.5 \quad \text{and}$$

$$y = .25 (.25) \quad 2.0$$

3. Computation of Irregular Whittaker Function $W_{\eta, \ell+1/2}(z)$ for η real, positive and non-integral.

Program WOG calculates the irregular Whittaker function $W_{\eta, \ell+1/2}(z)$ for η real, positive and non-integral. The function is computed by two different expressions for smaller and larger values of $2R/\eta$, where $2R/\eta = z$. The expression used to compute the function for small values of z is given by Hartree⁶ and is as follows.

$$\begin{aligned} (-)^{\ell+1} \frac{W_{\eta, \ell+1/2}(z)}{\eta^{\ell} \Gamma(\eta-\ell)} &= \frac{\sin \pi \eta}{\pi} e^{-1/2z} (\eta z)^{-\ell} \\ &\left[- \sum_{m=0}^{2\ell} \frac{\Gamma(\eta+\ell+1)}{\Gamma(\eta+\ell+1-m)} \frac{(2\ell-m)!}{m!} z^m \right. \\ &+ \sum_{m=2\ell+1}^{\infty} (-)^{m-1} \frac{\Gamma(\eta+\ell+1)}{\Gamma(\eta+\ell+1-m)} \frac{z^m}{m!(m-2\ell-1)!} \\ &\left. \log z + \pi \cot \pi \eta + \psi(\eta+\ell+1-m) - \psi(m+1) - \psi(m-2\ell) \right] \quad (1) \end{aligned}$$

Some important aspects of the evaluation of this expression are worth mentioning. Computation of the multiplying factor makes use of the identity

$$\frac{1}{\eta^{2\ell+1}} \frac{\Gamma(\eta+\ell+1)}{\Gamma(\eta-\ell)} = \prod_{k=1}^{\ell} \left[1 - \left(\frac{k}{\eta} \right)^2 \right] \quad (A2)$$

In computing the finite sum in Equation (1), use is made of the identity

$$\prod_{k=1}^m \left[\frac{(\eta+\ell+1-k)}{k(2\ell+1-k)} \left(\frac{2\ell}{\eta} \right) \right] = \frac{\Gamma(\eta+\ell+1)}{\Gamma(\eta+\ell+1-m)} \frac{(2\ell-m)!}{m!(2\ell)!} z^m \quad (A5)$$

In summing the infinite series in Equation (1) the summation parameter is transformed by $k = m - 2\ell - 1$ where k goes from 0 to ∞ . The term when $k = 0$ is obtained separately. The expression containing ψ functions is computed in three different ways depending upon the value of η . In case $\eta < \ell$ and $\eta < 60$ the identities

$$\psi(n) = -\gamma + \sum_{k=1}^{n-1} \frac{1}{k} \quad (n \geq 2) \quad (2)$$

$$\psi(1+z) = -\gamma + \sum_{k=1}^{\infty} \frac{z}{k(k+z)} \quad z \neq -1, -2, -3, \dots \quad (3)$$

$$\psi(1-z) = \psi(z) + \pi \operatorname{Cot} \pi z \quad (4)$$

are used. If $\ell < \eta < 60$ the following additional relation is used,

$$\psi(n+z) = \frac{1}{(n-1)+z} + \frac{1}{(n-2)+z} + \dots + \frac{1}{z} + \psi(z) \quad (5)$$

In the case $\eta > 60$ the asymptotic expansion of the ψ function is used,

$$W(z) \sim \ln(z) - \frac{1}{2z} - \frac{1}{12z^2} + \frac{1}{120z^4} - \frac{1}{252z^6} + \dots \dots .$$

$$(z \rightarrow \infty \text{ in } |\arg z| < \pi). \quad (6)$$

When the argument z of the Whittaker function is large, the asymptotic expansion is used for the computation in place of Equation (1). This expansion is given by Whittaker and Watson.⁸

$$W_{\eta, \nu+1/2}(z) \sim e^{-\frac{1}{2}z} z^\eta \left\{ 1 + \sum_{n=1}^{\infty} \left\{ \frac{\{(v+1/2)^2 - (\eta-1/2)^2\}}{n! z^n} \right\} \left\{ \frac{\{(v+1/2)^2 - (\eta-3/2)^2\}}{z^\eta} \right\} \dots \right. \\ \left. \left\{ \frac{\{(v+1/2)^2 - (\eta-n+1/2)\}}{n! z^n} \right\} \right\} \quad (7)$$

Some test runs with McGuire's program gave results of rather low accuracy--two or three significant figures, and some steps were taken to improve this. The major source of error appeared to be the summation for the function in Equation (3), which is slowly convergent. McGuire truncated this summation at 50 terms. We have summed greater numbers of terms and also introduced a correction for the remainder term by consideration of the integral

$$\int_{x_0}^{\infty} \frac{dx}{x(x-a)} = \frac{1}{a} \ln \left(\frac{x_0}{x_0-a} \right)$$

By approximating to the integral in two different ways, we determine the error bounds for the remainder

$$\frac{1}{a} \ln \left(\frac{N-1}{N-1-a} \right) - \frac{1}{2(N-1)(N-1-a)} < \sum_{j=N}^{\infty} \frac{1}{j(j-a)} < \frac{1}{a} \ln \left(\frac{N-1/2}{N-1/2-a} \right)$$

The remainder term is approximated by the mean of the two bounds and good accuracy is obtained by taking $N = 1001$. In the case of the infinite sum involved

in (1), the series was being truncated when the term became less than 10^{-3} of the sum. In the modified version, the summation is truncated when the term becomes smaller than 10^{-8} of the sum and when at least 10 terms have been summed.

In computing the asymptotic expansion of Whittaker's function, the number of terms summed by McGuire was the greatest integer contained in $\ell + \eta$. The reason for this choice is not clear and it was found that improvement could be obtained by summing up to, but excluding, the smallest term (normal procedure with an asymptotic series). This method was, therefore, adopted.

With these modifications, a considerable increase in accuracy has been obtained, at the expense of some increase in computer time. Tables of the Whittaker's irregular function were not available. For checking the accuracy of the results Coulomb tables⁷ were used. Coulomb tables list the functions $P_{\ell}(\frac{1}{\eta^2}, R)$ and $Q_{\ell}(\frac{1}{\eta^2}, R)$. The relation between Whittaker's function and the functions $P_{\ell}(\frac{1}{\eta^2}, R)$ and $Q_{\ell}(\frac{1}{\eta^2}, R)$ is given by the equation

$$w_{\eta, \ell+\frac{1}{2}}\left(\frac{2R}{\eta}\right) = \frac{\left(\frac{-2}{\eta}\right)^{\ell+1} \Gamma(\ell+\eta+1)}{(2\ell+1)!} \left\{ Q_{\ell}\left(\frac{1}{\eta^2}, R\right) \sin \eta + P_{\ell}\left(\frac{1}{\eta^2}, R\right) \cos \eta \right\}$$

The results of the program have been found to agree with the results obtained by using the tabulated values to six or more significant figures for the ranges $\ell = 0, 1, 2, 1/\eta^2 = -2.0(.2)-.2, z = .5(.5)4.0$. From results obtained in these ranges, it appeared appropriate to switch the computation from the series (1) to the asymptotic form (7) at the value $z = 9$.

Our next step in the project of writing a computer program for the calculation of transitions between eigenstates will be to check the results for the other program called HLIGAM against the available Coulomb tables and make the possible changes if necessary to improve its accuracy. Procedure HLIGAM calculates the function

$$\frac{(i\eta)^{\ell+1}}{\Gamma(\ell+1+i\eta)} w_{i\eta, \ell+1/2} \left(\frac{2R}{i\eta} \right)$$

for $i\eta$ a pure imaginary number. Then both of these functions (one calculated by WQG and the other by HLIGAM) will be integrated to determine the transitions probabilities. The result of integration will be checked against the tables given by Peach⁹.

References

1. L. J. Slater, Confluent Hypergeometric Functions, Cambridge University Press P. 2. (1960).
2. L. J. Slater, Confluent Hypergeometric Functions, Cambridge University Press P. 9. (1960).
3. R. R. Hammers, "Technical Bulletin, Mathematical report series MRS-133. Burroughs Corporation, February 21, 1961.
4. M. L. Johnson and W. Sangren. Technical reports, GA-1704, GA-1543, GA-2739 General Atomic, Division of General Dynamic Corporation, September 6, 1960, October 10, 1960, and December 1, 1961.
5. Dr. E. J. McGuire. Through private communication. Radiation Phenomena Division 5242, Sandia Corp. Albuquerque, New Mexico.
6. Dr. D. R. Hartree, Proc. Camb. Phil. Soc. V. 24, P. 426 (1928).
7. M. Abramowitz and I. A. Stegun, Handbook of Mathematical Functions, AMS 55. National Bureau of Standards, June 1964.
8. E. T. Whittaker and G. N. Watson, A Course of Modern Analysis, Cambridge University, Press. Fourth Edition p. 343 (1952).
9. G. Peach "A Revised General Formula for the Calculation of Atomic Photoionization Cross-sections", Private Communication (to be published in Memoirs of the R.A.S.).

Appendix Program Usage

A1. GAMMAC (x, y, u, v); An algol procedure to compute $\Gamma(z)$ for real or complex values of the argument z .

Procedure GAMMAC (x, y, u, v) computes the function $\Gamma(z)$ for any argument z , real or complex. This procedure can be included in any main program by including the following two cards in the programme declarations

$\$\$ A$ GAMMAC

COMMENT HIGHER SEQUENCE CARD;

Both the cards must have some sequence number in the column 73-80. and the sequence number on the comment card must be higher than that on the $\$\$ A$ GAMMAC card. The formal parameters x and y are the input parameters. x and y are both real and respectively are the real and imaginary part of the complex number z , whose gamma function is required. u and v are the output parameters and respectively are the real and imaginary parts of the complex number $\Gamma(z)$.

For example if one wants to calculate $\Gamma(z_1)$ and store the value at z_2 where $z_i = (x_i, y_i)$ for $i = 1, 2$, are complex numbers then one would do so by including a card, at the desired place, in the main program with the following information on it.

GAMMAC (x_1, y_1, x_2, y_2);

Either one or both of the input parameters x and y can be real valued arithmetic expressions. There is no loss of efficiency caused by using the expression as an actual input parameter since it is called by value.

Limitations. The procedure has the following limitations.

For the non-positive integral values of the argument an error message of divide by zero would occur since the gamma function is singular at such points. For the rest of the negative real values of the argument procedure calculates $\Gamma(z)$ except very close to the negative integers where an exponent overflow message would occur. For positive real values of the argument procedure computes $\Gamma(z)$ for $z \leq 53.3$. For larger values of z an error message of exponent overflow occurs. For very small values of z ($z < 8.758 @-47$) an error message of divide by zero occurs since computer sets such numbers to zero.

For pure imaginary argument $|z| > 66..$ the value of $|\Gamma(z)|$ is so small that it is set to zero by the computer.

For $z =$ a complex number on the diagonal $x = y$ or $x = -y$ and $x > 0$. While computing $\Gamma(z)$ of z such that $x > 42.00$ an error message of maximum argument of exponent would occur. On the diagonals $x = y$ and $x = -y$ for $x < 0$ the value of $\Gamma(z)$ is so small for $x < -22.60$ that it is set to zero by the computer.

A2. WOG (L, ETA, R, W); An algol procedure to compute the irregular

Whittaker function $\frac{W_{n,\ell+1/2}(\frac{2R}{n})}{\Gamma(n+\ell+1)}$

The procedure WOG(L,ETA,R,W) calculates the function

$$\frac{W_{n,\ell+1/2}(\frac{2R}{n})}{\Gamma(n+\ell+1)}$$

A deck of cards for this procedure, to be included in the main program, may be obtained from the writer. The formal parameters L, ETA and R correspond to the variables ℓ , n and R in the Whittaker function $W_{n,\ell+1/2}(\frac{2R}{n})$. Either one or any number of these input variables L, ETA, and R can be a real valued arithmetic expression. There is no loss of efficiency caused by using an expression as an actual parameter since it is called by value. W is the output parameter, which has the value of the function $W_{n,\ell+1/2}(\frac{2R}{n})$ as computed by the procedure.

One of the infinite series involved in computation is a function of ℓ and n but not R. This summation is the most time-consuming part of the computation. To increase efficiency when successive values of W are to be calculated with constant ℓ and n , varying R, the procedure has been written so that this particular sum is preserved between calls. It is recomputed only when either ℓ or n changes. Therefore it is recommended that the user arrange his program so that consecutive calls on the procedure WOG are made, as far as possible, with constant ℓ and n (i.e. variation of R should be the innermost loop).

Limitations. This procedure is limited to the real values of R, to n positive and nonintegral, and to ℓ integral only.

1513A107 FRIDAY, APRIL 13, 1967

NPL ALGOL VERSION OF 10/20/66

```

        EXIT
END;

PROCEDURE GAMMAPEX(Y,X,B);
  VALUE X,Y;
  REAL X,Y,B;
BEGIN
  COMMENT THIS PROCEDURE CALCULATES GAMMA(X+Y) WHEN X IS POSITIVE
  IF Y IS POSITIVE THEN IT CALCULATES GAMMA OF THE NUMBER ITSELF
  ELSE IT CALCULATES THE GAMMA OF THE CONJUGATE NUMBER AND TAKES
  THE CONJUGATE OF THAT;
  REAL A,B,X,Y,A1,B1,C,D,S,Q,C,D,P,T,R,T1;
  INTEGER I,J,K,L;
  BOOLEAN RQUL,FAL;
  LABEL FA1E;
  K = 2*0.0062827/AR3;
  IF Y <= 0 THEN RQUL = TRUE ELSE RQUL = FALSE; Y = -Y;END;
  GAMMA(X,Y,B);
  GO TO EXIT;END;
  J = 1 + 1 + ENTIER(Y);
  XNO X/J;
  X10 Y/J;
  GAMMA(X,Y,B);
  A1 = 1/PJ;
  IF P NOT STEP E UNTIL 1 DO
  BEGIN
    A = ARG(A1);
    GAMMA(X,Y,B);
    A2 = SINH(Y*A);
    T = S*EXP(A);
    S = A2;
  END;
  C1 = R01*SIGN(A1);
  C2 = LNU(J);
  C3 = AR2;
  C4 = Y*RC2;
  C5 = EXP(C3)/C1;
  C = C5*COS(C4);
  D = C5*SIN(C4);
  A2 = C5*B;
  V = C5*A;
  IF NOT RQUL THEN V = (-V);
  EXIT;
END;

PROCEDURE GAMMAPOL(Y,X,B);
  VALUE X,Y;
  REAL X,Y,B;
BEGIN
  COMMENT THIS PROCEDURE CALCULATES THE GAMMA FUNCTION OF A REAL OR
  COMPLEX ARGUMENT Z = A + i*B; X AND Y RESPECTIVELY ARE THE REAL
  AND IMAGINARY PARTS OF THE ARGUMENT. THE QUANTITIES R AND I
  RESPECTIVELY ARE THE REAL AND IMAGINARY PART OF THE VALUE OF
  THE FUNCTION. THIS PROCEDURE CALLS FOR ANOTHER PROCEDURE
  GAMMA WHICH MUST ALSO BE INCLUDED IN THE MAIN PROGRAMME;
  REAL R,I,B,S,Q,C,D,P,T,R,T1;
  INTEGER I,J,K,L;
  LABEL FA1E;
  Y = 0 THEN IF X AND I = 0 THEN
  G1N;
  IF A <= 0 THEN R = Y/0 ELSE
  BEGIN
    R = 1;
    FOR B = 1+1 STEP -1 UNTIL 1 DO
    A = A + B;
  END;
  R = A;
  I = 0;
  GO TO FA1E;
  IF A >= 0 THEN GAMMA(X,Y,B);
  Y = SIGN(-B)*ENTIER(Y*RC2);
  A = NO;
  GAMMA(X,Y,B);
  J = NO;
  FOR B = 0 STEP 1 UNTIL 1 DO
  BEGIN
    A = A+B;
    W = A*B*Y*2;
    Q = (A*B*Y*W)/W;
    T = (A*B*Y*W)/W;
    P = P1;
  END;
  EXIT;
END;

```

ESTIMATED CORE STORAGE REQUIREMENT = 02440 RECORDS.
15134:39 ESTDATE APRIL 16, 1987 PROCESSING TIME = 11.70 SECONDS I/O TIME = 21.42 SECONDS

COMPUTED VALUES OF ENERGY LEVELS, ν_{eff}

16.3.		16.4.5.6.7.8.	
1.0	1.0	7.1.352312231644300	7.1.34447294288000
1.0	5.4	7.1.351878240000000	7.1.35121122978000
1.0	2.2	7.2.301333738400000	7.1.35359124930000
1.0	9.4	7.2.301252843330000	7.1.34447119174000
1.0	2.4	7.2.312055453580000	7.1.35123333940000
1.0	6.8	7.1.311565020318000	7.1.34101115580000
1.0	3.2	7.1.372116425640000	7.1.35204149850000
1.0	6.8	7.1.362233794400000	7.1.35500954744000
1.0	1.4	7.1.3139153573034000	7.1.34225513171000
1.0	8.0	7.0.778435926400000	7.1.35620258406000
1.0	2.0	7.1.353204001070000	7.1.3484743314378000
1.0	4.0	7.1.371200319940000	7.0.00748210348000
1.0	3.0	7.1.511263105818000	7.1.37412364478000
1.0	6.4	7.1.370525934918000	7.1.37293794440000
1.0	8.0	7.1.72432984864000	7.1.30161373555000
1.0	8.0	7.1.148309141738000	7.1.31300931413600
1.0	1.4	7.1.51159457618000	7.2.25227825300000
1.0	9.4	7.1.217007764200000	7.1.30511115340000
1.0	7.2	7.1.202485517840000	7.1.30942119495000
1.0	8.0	7.0.456291163918000	7.1.15721488240000

TABULATED VALUES OF EQUITY, etc.

REAL	IMAGINARY
-1.1593122654746e-00	-1.1548487035908e+01
-7.6181275950000e-00	-7.61811390800e-01
-9.2161139373000e-00	-9.21611390800e-01
-1.2993524900000e+01	-1.2993524900000e+00
-2.2332558448700e-00	-2.2332558448700e-01
-7.3840452550000e-00	-7.3840452550000e-01
-1.1720149497500e-00	-1.1720149497500e-01
-5.1437157155000e-00	-5.1437157155000e-01
-1.1193159472900e-00	-1.1193159472900e-01
-9.776493888100e-00	-9.776493888100e-01
-1.2562460149000e-00	-1.2562460149000e-01
-3.9720201190000e-00	-3.9720201190000e-01
-2.9112124194358e-00	-2.9112124194358e-01
-7.7077052005000e-00	-7.7077052005000e-01
-8.7245295078000e-00	-8.7245295078000e-01
-9.1483363220000e-00	-9.1483363220000e-01
-3.75711584.00000e-01	-3.75711584.00000e-01
-1.1217730000000e+01	-1.1217730000000e+01
-7.4178655170000e-00	-7.4178655170000e-01
-9.8542014450000e-00	-9.8542014450000e-01

93319914 59048

APPENDIX E

RADIATIVE TRANSPORT IN A XENON ARC

by

B. W. Swanson

I. INTRODUCTION

The problem of interest has been to determine the steady state temperature profile in a Xenon arc, which requires a solution of the energy equation

$$\frac{\partial^2 S}{\partial r^2} + \frac{1}{r} \frac{\partial S}{\partial r} - \vec{\nabla} \cdot \vec{F} + \sigma(P, S)E^2 = 0 \quad (1)$$

where $\vec{F}(r)$ is the radiative flux vector, T the plasma temperature, σ the electrical conductivity, P the pressure and E the electric field. The Schmitz function S is defined by the equation

$$S(T) = \int_{T_W}^T K(T)dT \quad (2)$$

and the divergence of F is given by

$$\vec{\nabla} \cdot \vec{F} = \frac{dF}{dr} + \frac{F}{r} \quad (3)$$

where the radiative flux F is found from the equation

$$F(r) = \int_0^\infty \int_{\omega=4\pi}^\infty I_\lambda(r, \vec{\omega}) \vec{\omega} d\omega d\lambda \quad (4)$$

In equation 4, $\vec{\omega}$ is a unit direction vector and $I_\lambda(r, \vec{\omega})$ is the monochromatic intensity of radiation.

The first phase of this program consisted of writing a computer program for calculating the radiative flux¹, which can be expressed as

$$F(r) = -4 \int_{\lambda_{\min}}^{\lambda_{\max}} \int_0^{\pi} \int_0^R R_M(\phi) K_\lambda(s) B_\lambda(s) G_1[\beta_\lambda(s)] \cos \phi ds d\phi d\lambda \quad (5)$$

In equation 5, $K_\lambda(T)$ is the spectral absorptivity, λ_{\min} and λ_{\max} the wavelength band of interest, B_λ is the Planck function, $\beta_\lambda = \int_0^s K_\lambda(\zeta) d\zeta$ and the function G is given by

$$G_n(x) = \int_0^{\frac{\pi}{2}} e^{-\frac{x}{\sin \theta}} (\sin \theta)^n d\theta \quad (6)$$

and accounts for the attenuation of radiation by self absorption. The geometry for the evaluation of equation 5 is shown in figure 1.

Since the numerical evaluation of the triple flux integral is expensive the second phase of the program sought a faster flux approximation method. An analysis was made which permitted an a'priori integration with respect to wavelength to reduce computation time. The approximate flux integral is given² by the equation

$$\hat{F}(r) = -4 \int_0^{\pi} \int_0^R R_M(\phi) K_a(s) B(s) G_1 \left[\int_s^R K_a(\zeta) d\zeta \right] \cos \phi ds d\phi \quad (7)$$

where

$$B(s) = \int_{\lambda_1}^{\lambda_2} B_\lambda[T(s)] d\lambda \quad (8)$$

and the mean absorption coefficient $K_a(s)$ is defined by the equation

$$K_a(s) = \left[\frac{b}{b + \tau_p(s)} \right] \left[\frac{b + \tau_p(s)}{b + \tau_R(s)} \right] K_p(s) + \left[\frac{\tau_p(s)}{b + \tau_p(s)} \right] K_R(s) \quad (9)$$

The term b is a constant of the order of unity which can be varied to improve the approximation. The terms τ_R and τ_p are the Rosseland and Planck optical lengths along the ray from point M to point R in figure 1 and are given by

$$\tau_R(s) = \int_0^s K_R(\zeta) d\zeta \quad (10)$$

$$\tau_p(s) = \int_0^s K_p(\zeta) d\zeta$$

where the Planck and Rosseland absorption coefficients are given by

$$K_p(T) = \int_{\lambda_1}^{\lambda_2} \frac{K_\lambda(T) B_\lambda(T) d\lambda}{B(T)} \quad (11)$$

$$K_R(T) = \int_{\lambda_1}^{\lambda_2} \frac{1}{K_\lambda(T)} \frac{dB_\lambda}{dT} d\lambda$$

and

$$B(T) = \int_{\lambda_1}^{\lambda_2} B_\lambda(T) d\lambda \quad (12)$$

The form of the approximation is such that under optically thin conditions when τ_p and τ_R are much less than unity, the mean absorption coefficient K_a approaches the Planck absorptivity K_p and equation 7 is exact. Under optically thick conditions, when τ_p and τ_R are much greater than unity, K_a approaches the Rosseland mean K_R and equation 7 is a good approximation.

The subject of this report, which is the third phase of the program, consists of the numerical solution of equation 1 utilizing the exact and approximate flux programs.

II. XENON PROPERTIES

The initial data needed for a numerical solution consists of the electrical conductivity, thermal conductivity and spectral absorptivity as functions of temperature and pressure. The temperature dependence of the S integral is shown in figure 2 for a pressure of 11 atmospheres, and the electrical conductivity σ is shown as a function of S in figure 3. The variation of spectral absorptivity with temperature is shown in Table I. An inspection of the table reveals that the spectral absorptivity in the ultra violet region is orders of magnitude greater than that in the visible region. Therefore, the flux computer program consists of an exact flux program for the U. V. and an approximate flux program for the visible. The wavelength bands defining these regions are given by the equations

$$\text{U.V. } \left\{ \begin{array}{l} \lambda_{\min} = .0612 \times 10^{-4} \text{ cm} \\ \max = .0952 \times 10^{-4} \text{ cm} \end{array} \right.$$

$$\text{Visible } \left\{ \begin{array}{l} \lambda_1 = .1034 \times 10^{-4} \text{ cm} \\ \lambda_2 = 2.0 \times 10^{-4} \text{ cm} \end{array} \right.$$

III. NUMERICAL ANALYSIS

A steady state solution of the energy equation can be obtained by solving the "transient" equation

$$\frac{\partial S}{\partial t} = \frac{\partial^2 S}{\partial r^2} + \frac{1}{r} \frac{\partial S}{\partial r} - \left[\frac{dF}{dr} + \frac{F}{r} \right] + \sigma(s) E^2 \quad (13)$$

until a steady state solution is achieved. The following calculation procedure was followed:

Table I - Spectral Absorptivity of Xenon (cm^{-1})

$\lambda \times 10^4$ cm	T [°K]				
	3000	6000	10000	14000	18000
2.0	1.25@-14	4.909@-05	.2502	3.046	2.406
.7500	2.616@-14	1.679@-05	.0523	.5612	.4115
.4615	1.224@-12	1.052@-04	.1352	.9441	.5476
.3333	8.184@-12	9.594@-05	.0768	.5461	.3027
.2609	6.775@-11	1.076@-04	.0511	.3594	.1872
.2143	5.557@-10	1.194@-04	.0345	.2446	.1193
.1818	9.842@-10	9.506@-05	.0225	.1598	.0761
.1579	6.446@-10	6.226@-05	.0147	.1049	.0501
.1395	4.449@-10	4.297@-05	.0107	.0725	.0347
.1250	3.198@-10	3.089@-05	.00731	.0521	.0250
.1132	2.376@-10	2.295@-05	.00543	.0387	.0186
.1034	1.81@-10	1.751@-05	.00414	.0295	.0142
.0952	2.269.0	1.134.0	614.1	145.9	13.07
.0882	2.094.0	1.047.0	56.0	135.7	12.07
.0822	1.920.0	959.7	519.8	124.4	11.07
.0769	1.746.0	872.6	472.6	113.1	10.06
.0723	1.572.0	785.5	425.4	101.8	9.06
.0682	1.397.0	698.4	378.3	90.51	8.05
.0645	1.223.0	611.3	331.1	79.22	7.05
.0612	1.049.0	524.2	283.9	67.94	6.04

- (a) specify arc radius and central core temperature.
- (b) specify an initial temperature profile
- (c) calculate a radial flux profile
- (d) define E by the equation

$$E = \sqrt{\frac{-\nabla^2 S(o)}{r} + 2 \frac{dF(o)}{dr}}$$

- (e) select a time step Δt and solve for a new S profile
- (f) repeat steps c,d, and e until the solution converges to a steady state

The field E is so defined as to keep the central temperature essentially constant. This procedure was adopted to avoid large central temperature variations which would greatly affect the flux and its divergence. The finite difference equation used to replace equation 13 is

$$\frac{S_i^{n+1} - S_i^n}{\Delta t} = \frac{1}{\Delta r^2} [(1 + \frac{\Delta r}{2r_i}) S_{i+1}^{n+1} + (1 - \frac{\Delta r}{2r_i}) S_{i-1}^{n+1} - 2S_i^{n+1}] - [\frac{F_{i+1}^n - F_{i-1}^n}{2\Delta r} + \frac{F_i^n}{r_i}] + \sigma(S_i^n)(E^n)^2 \quad (14)$$

where the subscript i denotes a radial position. Equation 14 is an implicit difference equation, which for linear equations, is known³ to be unconditionally stable. Now let $\theta = \frac{\Delta t}{\Delta r^2}$ and define the coefficients $C_{i,j}$ by the equations

$$\begin{aligned} C_{i,i-1} &= -\theta(1 + \frac{\Delta r}{2r_i}) \\ C_{i,i} &= (1 + 2\theta) \\ C_{i,i+1} &= -\theta(1 + \frac{\Delta r}{2r_i}) \end{aligned} \quad (15)$$

Then equation 14 can be written as

$$c_{i,i-1} s_{i-1}^{n+1} + c_{i,i} s_i^{n+1} c_{i,i+1}^{n+1} = b_i^n \quad (16)$$

where

$$b_i^n = \sigma(s_i^n)(E) - \left[\frac{F_{i+1}^n - F_{i-1}^n}{2\Delta r} + \frac{F_i^n}{r_i} \right] \quad (17)$$

Let \vec{s}^n and \vec{b}^n define the vectors

$$\vec{s}^n = \begin{pmatrix} s_1^n \\ s_2^n \\ \vdots \\ s_i^n \\ \vdots \\ s_N^n \end{pmatrix}; \quad \vec{b}^n = \begin{pmatrix} b_1^n \\ b_2^n \\ \vdots \\ b_i^n \\ \vdots \\ b_N^n \end{pmatrix} \quad (18)$$

Then the finite difference equations can be written in matrix form as

$$\langle C \rangle \vec{s}^{n+1} = \vec{b}^n \quad (19)$$

The k^{th} row of $\langle C \rangle$ contains only the coefficients $c_{K,K-1}$, $c_{K,K}$, $c_{K,K+1}$ and the matrix is tri-diagonal. The matrix $\langle C \rangle$ can be "inverted" very efficiently by Gaus's elimination method. The first equation ($i=1$) is used to eliminate s_1^{n+1} from the second equation ($i=2$), the new second equation used to eliminate s_2^{n+1} from the third equation and so on until finally the new last but one equation can be used to eliminate s_{N-2}^{n+1} from the last equation, giving only one equation with only one unknown s_{N-1}^{n+1} . The unknowns $s_{N-1}^{n+1}, s_{N-2}^{n+1}, \dots, s_1^{n+1}$ can then be found in turn by back substitution. The method provides a fast computational procedure for large numbers of equations. In the numerical solution,

50 radial increments were employed. The flux program was used to evaluate the flux at 9 points and intermediate values were obtained with the use of a quadratic interpolation program.

IV. NUMERICAL SOLUTIONS

Numerical solutions were obtained for a pressure of 11 atm. and central arc temperatures of 10,000°K and 18,000°K. For the first example, several iterative S profiles are shown in figure 4. S_0 denotes the initial profile, and S_{29} denotes the final profile obtained after 29 time increments. The final solution has a maximum error ϵ of .03% where ϵ is defined as

$$\epsilon = \frac{\partial S}{\partial t} \quad (20)$$

In figure 5 are shown several iterative flux profiles. For the final S profile (S_{29}), the approximate flux calculations were compared with exact calculations over the range $\lambda_1 - \lambda_2$ and were found to agree to within 1%. In figure 6 is shown the final temperature profile corresponding to S_{29} . The temperature profile is very flat with a narrow conduction layer near the tube wall. The total current was evaluated from Ohm's law as

$$I = 2\pi E \int_0^R r \sigma [S(r)] dr \quad (21)$$

In figure 7 is given the variation of E with "time", showing a convergence to 20.69 volts/cm.

The iterative S profiles for the second example are shown in figure 8. A total of 80 time increments was required for convergence and the final profile S_{80} differs markedly from the initial S_0 profile. The final solution S_{80} has a maximum error of 0.2%. In figure 9 are shown the initial and final flux profiles. A comparison of approximate and exact flux calculations over the range $\lambda_1 - \lambda_2$ gave agreement to within

10%. Therefore the "final" solution S_{80} must still be considered an approximation to the exact solution. The temperature profile corresponding to S_{80} is shown in figure 10. Lowke and Capriotti⁵ have shown that the curvature of the temperature in the central core region is due to self absorption effects. Also, the thermal conduction edge is smaller than in the first example. The iterative variation of E is given in figure 11 showing convergence to a final value of 68.95 volts/cm and the corresponding current is 5795 amps. In summary, these examples indicate that the numerical method employed is stable and provides a convenient method for obtaining steady state solutions to the energy equation. Furthermore, with slight modification, the method can be used to calculate actual thermal transients in radiative plasmas, for applications where transient effects are important.

ACKNOWLEDGEMENTS

The author gratefully acknowledges the assistance of Mr. R. Lieberman who modified and consolidated existing flux programs; Mr. B. Wang who programmed the finite difference equations; and discussions with Mr. J. Vine and Dr. J. Lowke.

NOMENCLATURE

$$B_\lambda \quad \text{Planck function } B_\lambda = \frac{2c^2 h}{\lambda^5 [\exp(\frac{ch}{\lambda KT}) - 1]}$$

$$B(T) \quad B(T) = \int_{\lambda_{\min}}^{\lambda_{\max}} B_\lambda(T) dT$$

b constant in equation 9

$$B_i^n \quad B_i^n \equiv \sigma (S_i^n) (E^n)^2 - [\frac{F_{i+1}^n - F_{i-1}^n}{2\Delta r} + \frac{F_i^n}{r_i}]$$

$$\vec{B}^n = \text{col}(B_1^n, B_2^n, \dots, B_i^n, \dots, B_N^n)$$

$$C_{i,i-1} = -\theta(1 + \frac{\Delta r}{2r_i})$$

$$C_{ij} \quad C_{i,i} = (1 + 2\theta)$$

$$C_{i,i+1} = -\theta(1 - \frac{\Delta r}{2r_i})$$

$$< C > \quad \text{matrix } < C > = (C_{ij})$$

E Electric Field (volts/cm)

Eⁿ value of E for nΔt (volts/cm)

\vec{F} radiative flux vector (watt/cm²)

$$\vec{F} = \vec{r} F(r)$$

$$F(r) \quad F(r) = \int_{\lambda_{\min}}^{\lambda_{\max}} \int_{\omega=4\pi} I_\lambda(\vec{r}, \vec{\omega}) \vec{\omega} d\omega d\lambda; \text{ equation 5}$$

$\hat{F}(r)$ approximate flux; see equation 7

$$G_n(x) \quad G_n(x) = \int_0^{\frac{\pi}{2}} e^{-\frac{x}{\sin\theta}} (\sin\theta)^n d\theta$$

I current (amperes)

$I_\lambda(\vec{r}, \vec{\omega})$ intensity of radiation at r in direction $\vec{\omega}$ (watts/cm³)

K(T) thermal conductivity (watt/cm⁰K)

K_a mean absorption coefficient in equation 9 (cm⁻¹)

K_R Rosseland mean absorption coefficient (cm⁻¹)

$$K_R^{-1} = \int_{\lambda_1}^{\lambda_2} \frac{1}{K_\lambda} \frac{dB_\lambda}{dT} d_\lambda / \frac{dR}{dT}$$

K_P Planck mean absorption coefficient (cm⁻¹)

$$K_P = \int_{\lambda_1}^{\lambda_2} K_\lambda(T) B_\lambda(T) d\lambda / B(T)$$

N number of radial subdivisions

n number of "time" steps

P arc pressure (atm)

R	tube radius (cm)
r	radial coordinate (cm)
r_i	i^{th} radial position (cm)
Δr	$\Delta r = r_i - r_{i-1}$ (cm)
S(T)	$S = \int_{T_w}^T KdT$ (watt/cm)
s	position along a ray (cm)
S_i^n	value of $S(r_i)$ at the n^{th} time step
T	temperature ($^{\circ}\text{K}$)
T_w	wall temperature ($^{\circ}\text{K}$)
Δt	time step
β_λ	$\beta_\lambda = \int_0^S K_\lambda(\zeta) d\zeta$
θ	$\theta = \Delta t / \Delta r^2$
K_λ	spectral absorptivity (cm^{-1})
λ	wavelength (cm)
λ_1	$\lambda_1 = .1034 \times 10^{-4}$ cm
λ_2	$\lambda_2 = 2 \times 10^{-4}$ cm

$$\lambda_{\min} \quad \lambda_{\min} = .0612 \times 10^{-4} \text{ cm}$$

$$\lambda_{\max} \quad \lambda_{\max} = .0952 \times 10^{-4} \text{ cm}$$

σ electrical conductivity (mho/cm)

$$\tau_R \quad \text{Rosseland optical length; } \tau_R = \int_0^S K_R(\zeta) d\zeta$$

$$\tau_p \quad \text{Planck optical length; } \tau_p = \int_0^S K_p(\zeta) d\zeta$$

ϕ spherical coordinate measuring azimuth angle of a ray in figure 1.

$\vec{\omega}$ unit direction vector of a ray

REFERENCES

1. B. W. Swanson, "Radiative Flux in a Non-Isothermal Non-Grey Cylindrical Arc", Westinghouse Scientific Paper 65-1D8-GASDY-P2, November 1, 1965.
2. B. W. Swanson, "Radiative Flux Approximation in a Non-Grey Cylindrical Arc", Westinghouse Research Report 65-8D8-GASDY-R1, August 16, 1965.
3. R. D. Richtmyer, Difference Methods for Initial-Value Problems Interscience Publishers Inc., 1957.
4. G. D. Smith, Numerical Solution of Partial Differential Equations Oxford University Press, 1965 (page 20).
5. J. J. Lowke, E. R. Capriotti, "The Influence of Radiation on High Pressure Arcs", Westinghouse Research Report 66-1E2-GASES-R1, October 28, 1966.

Curve 575240-A

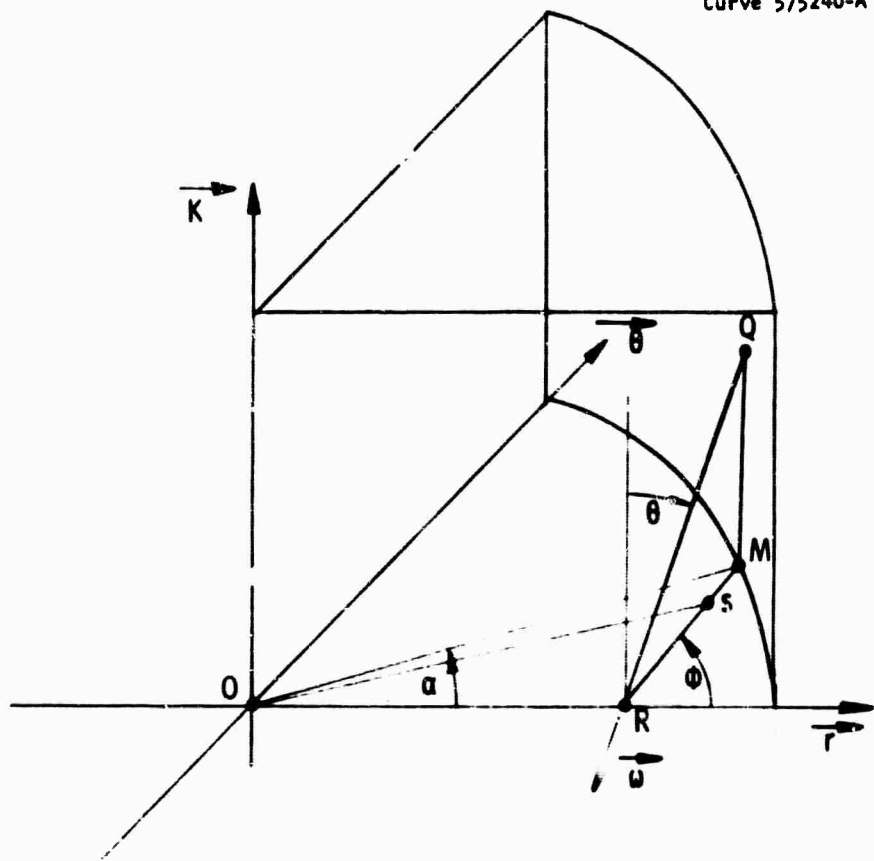


Fig. 1 - Arc geometry with $\theta' = 0$

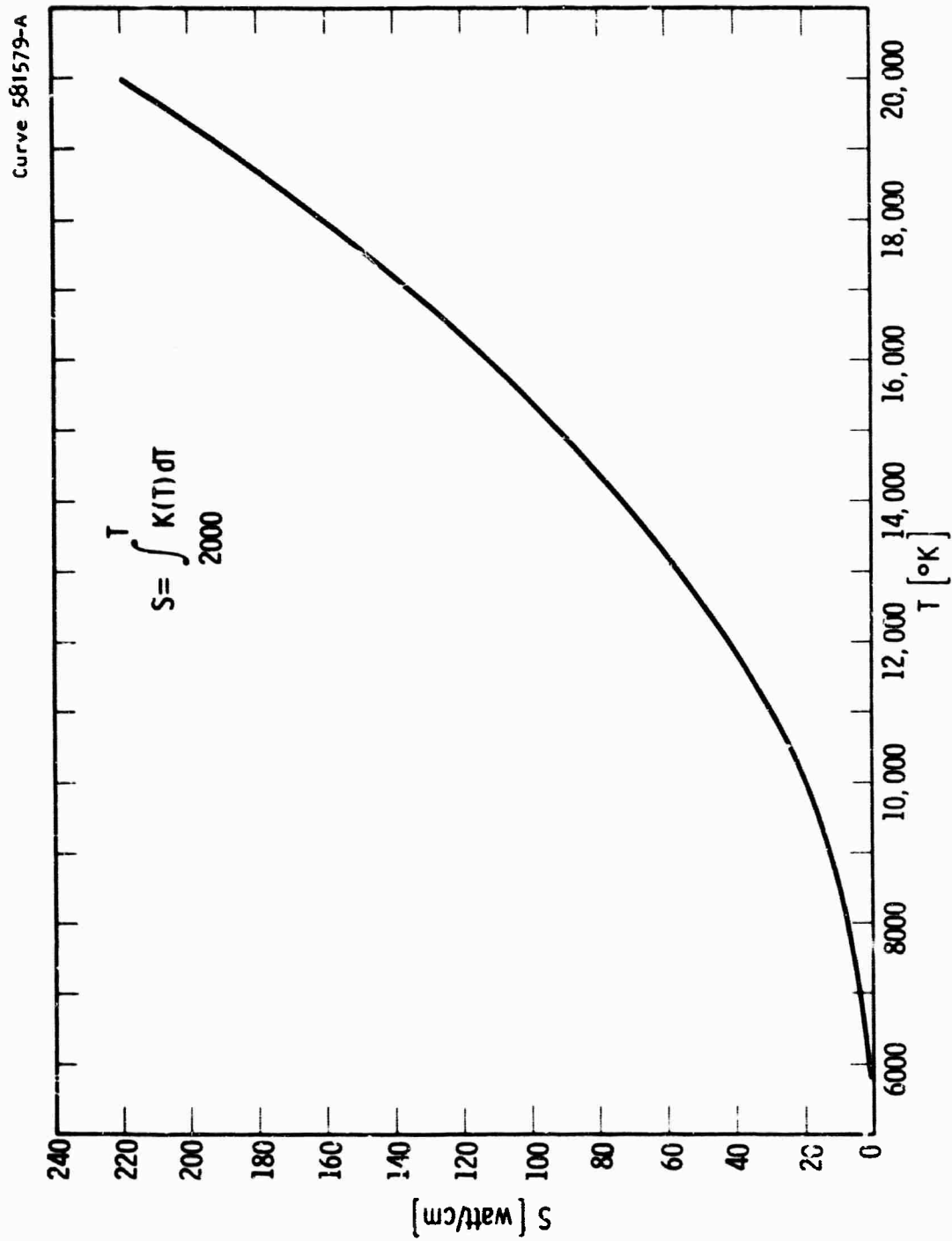


Fig. 2—S(T) vs T for Xenon at 11 atm pressure

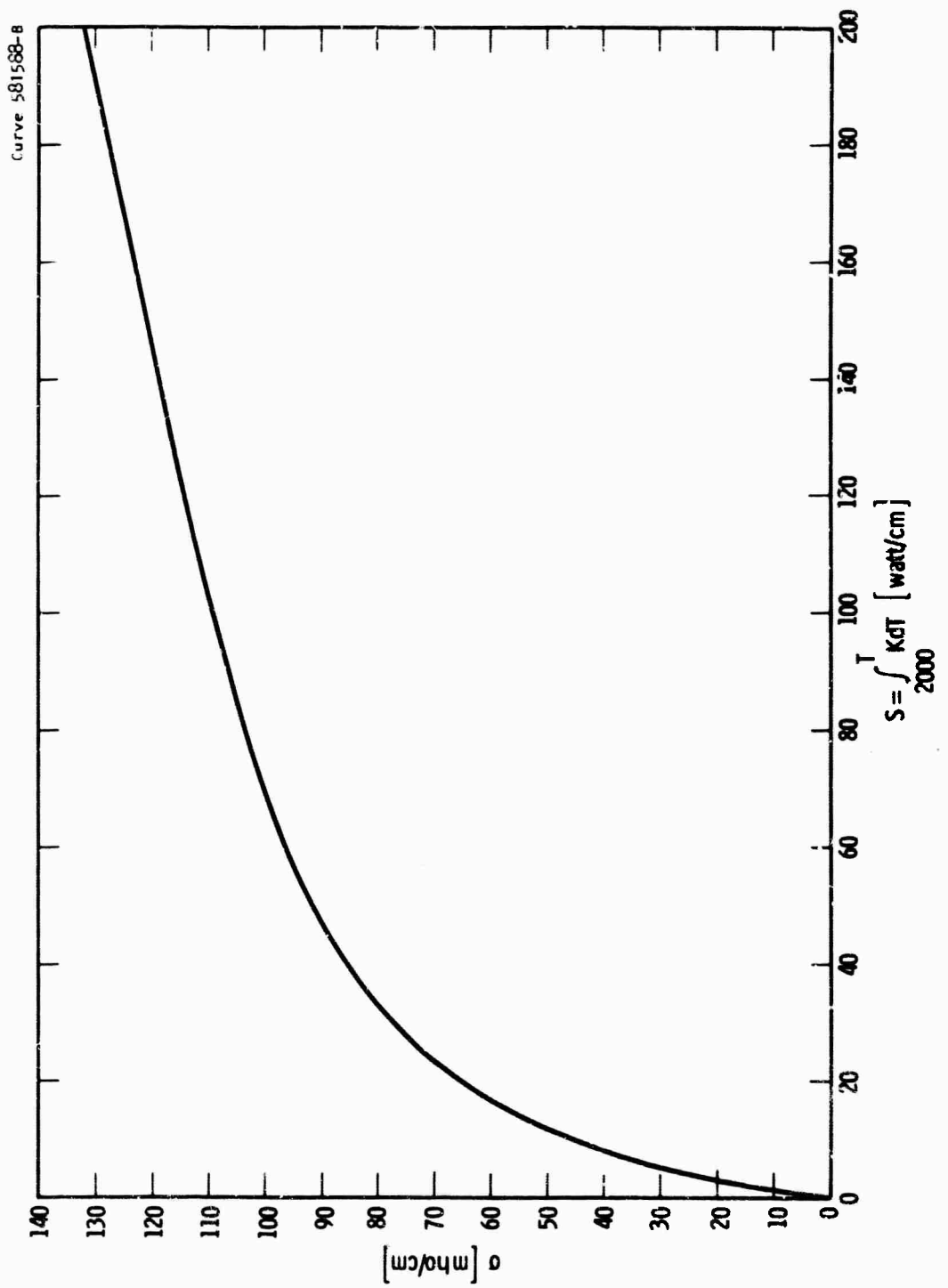


Fig. 3— σ vs S for Xenon at 11 atm pressure

Curve 581580-A

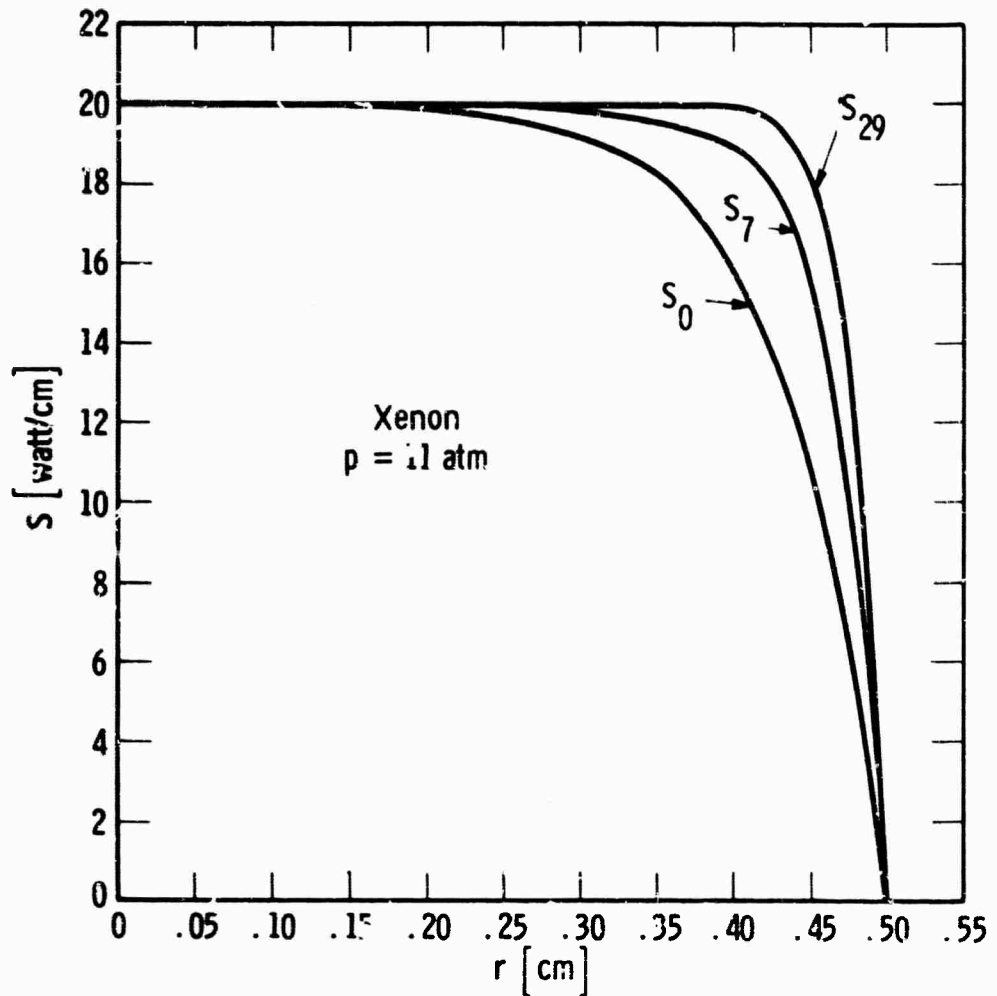


Fig. 4-Iterative S profiles

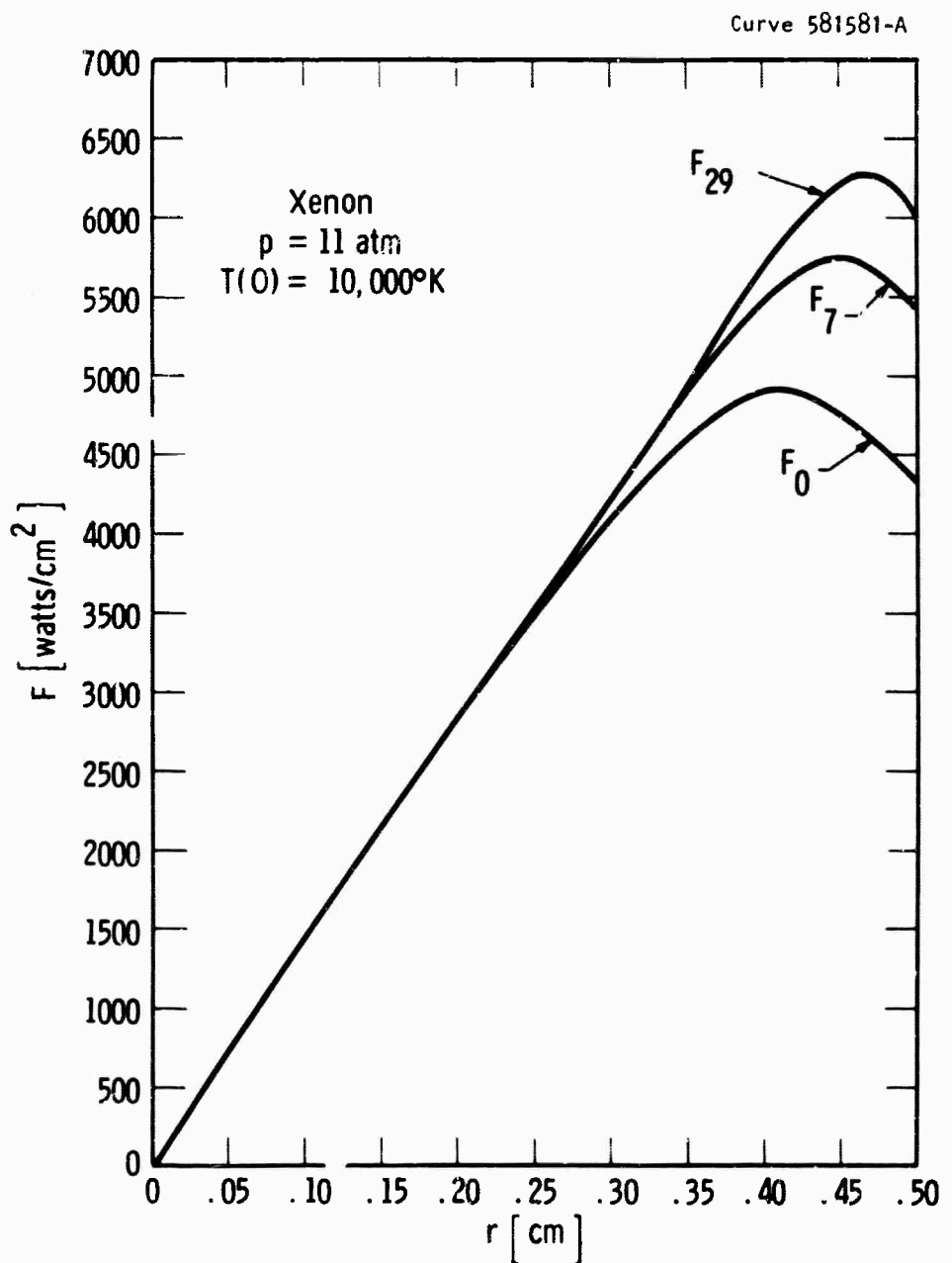


Fig. 5—Iterative flux profiles

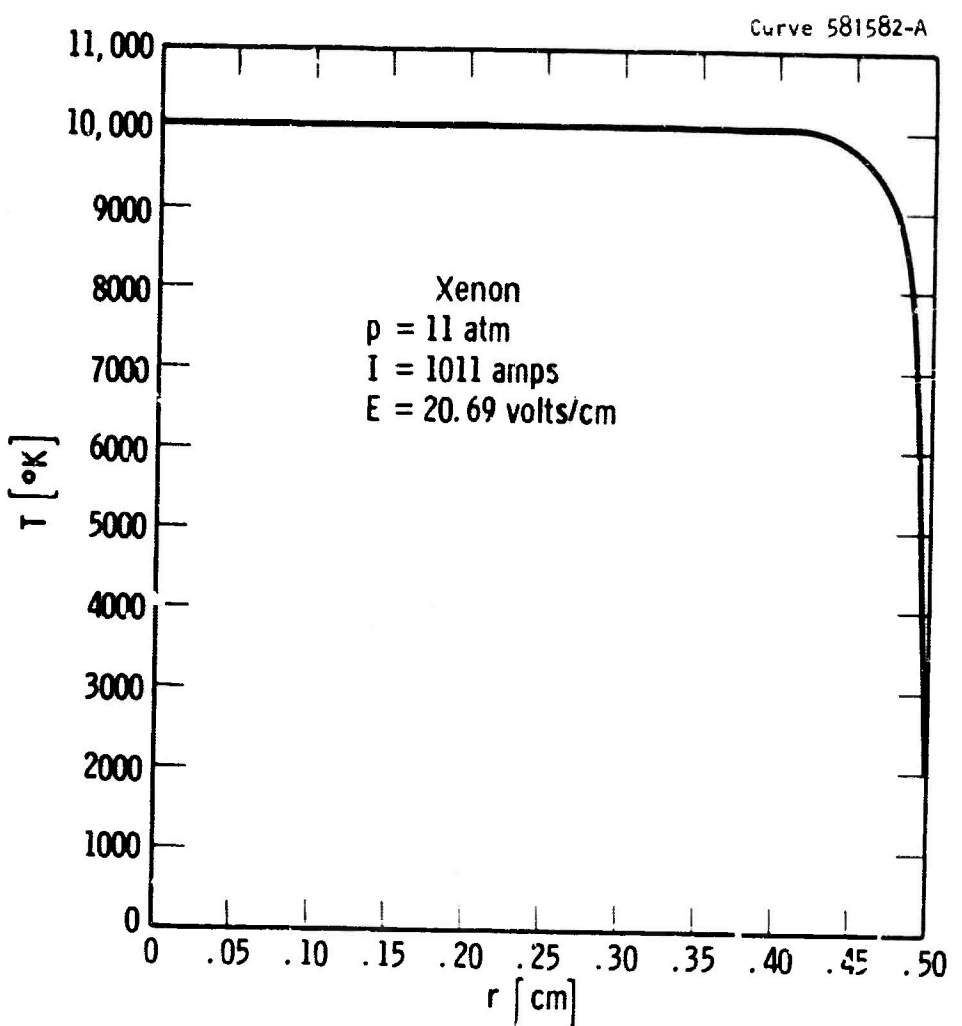


Fig. 6—Steady state temperature profile

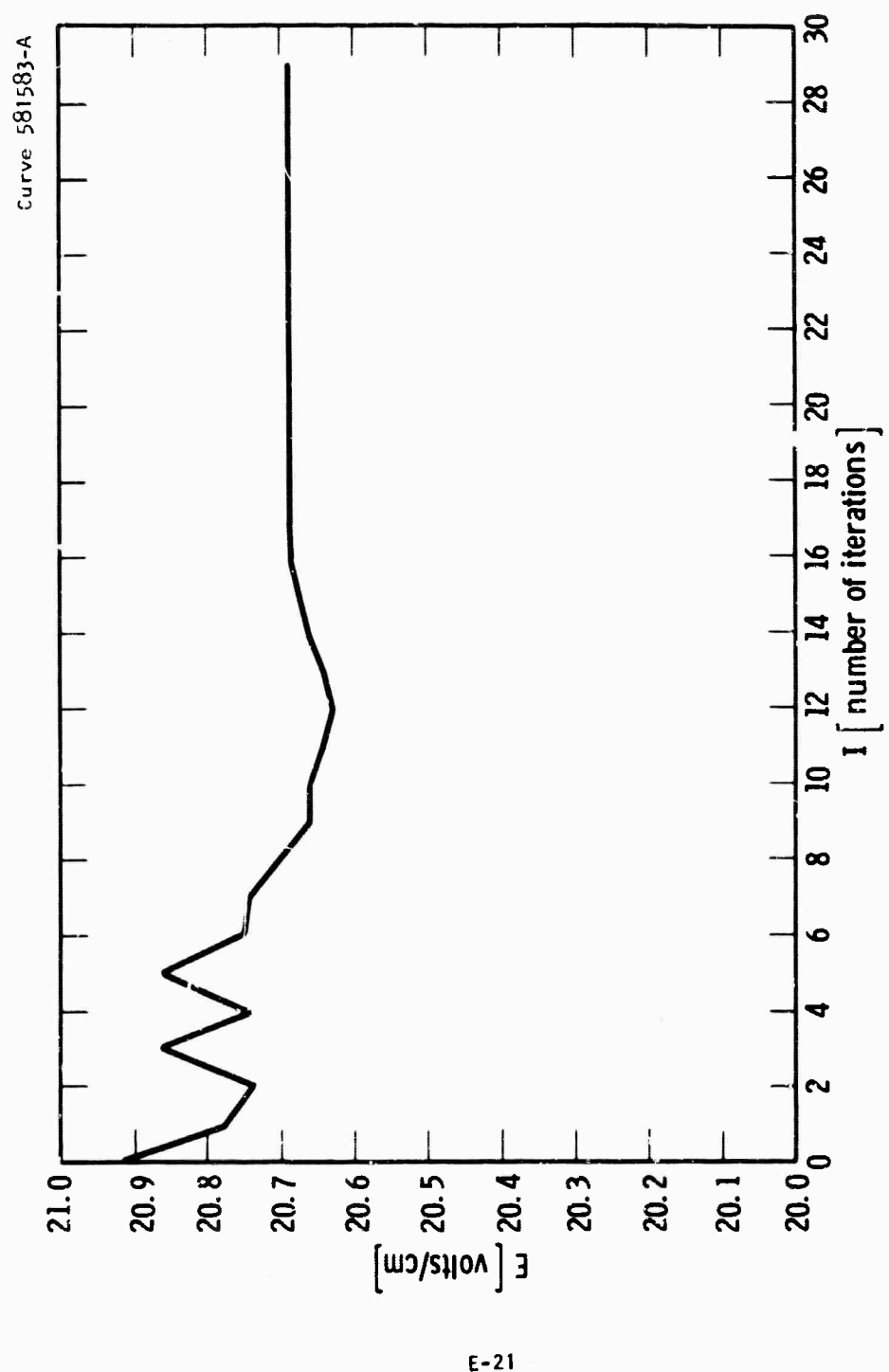


Fig. 7—Variation of E with iteration

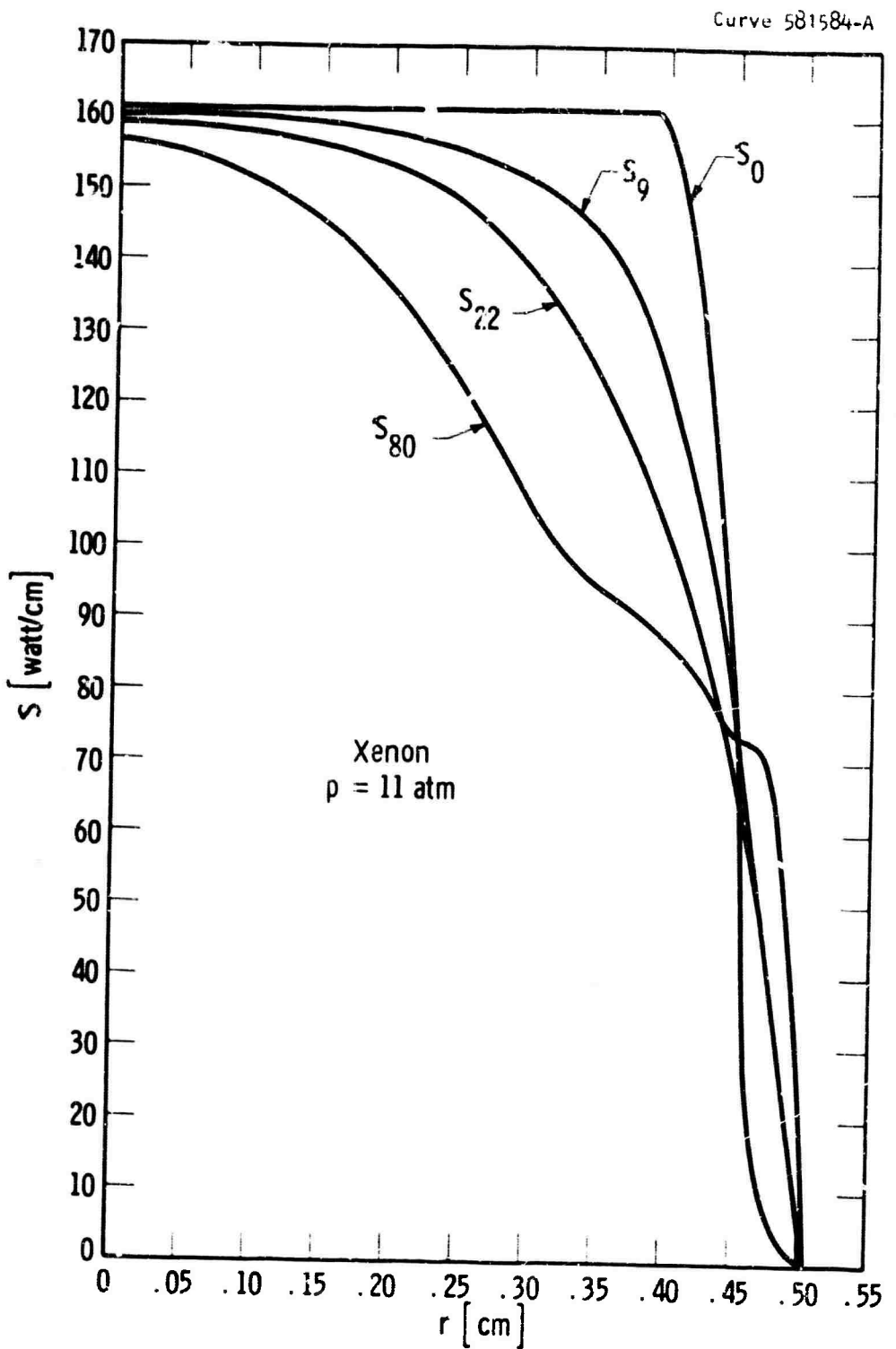


Fig. 8-Iterative S profiles

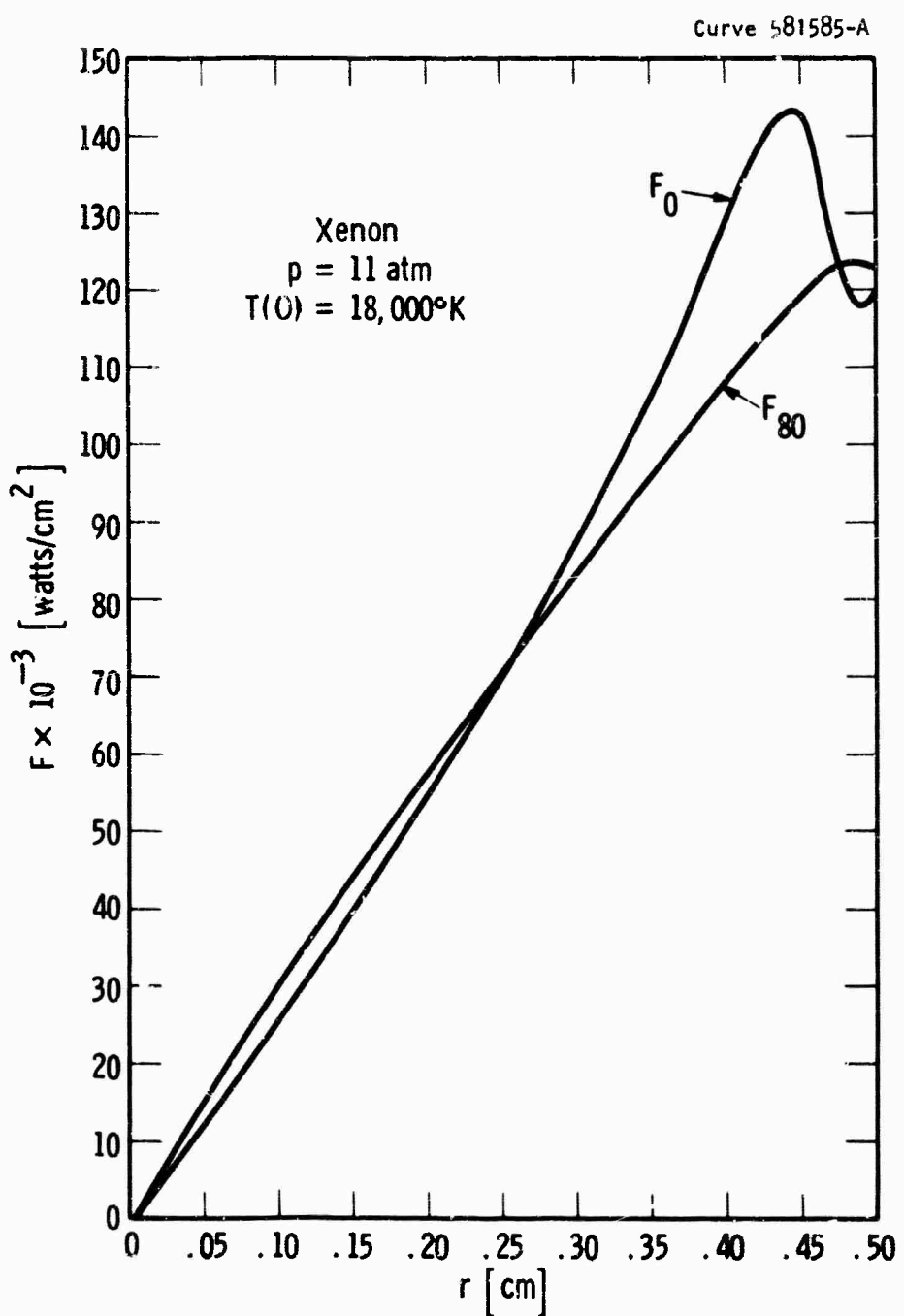


Fig. 9-Iterative flux profiles

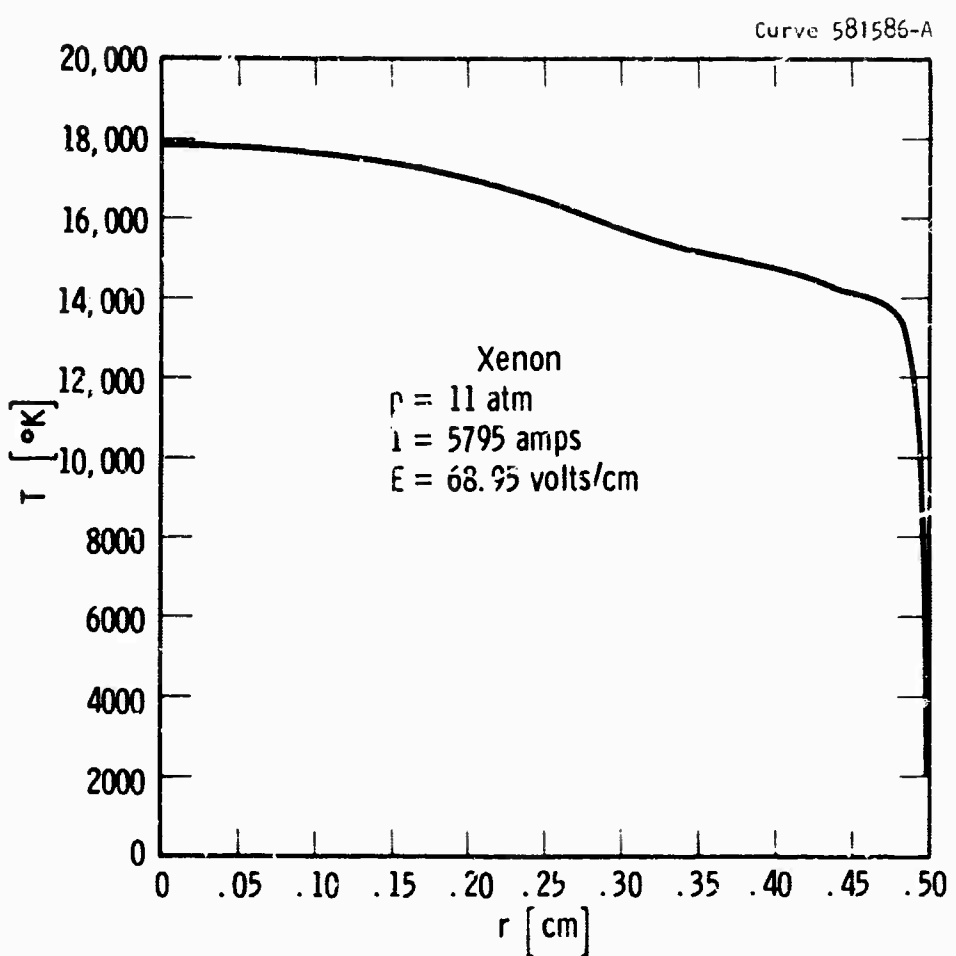


Fig. 10—Steady state temperature profile

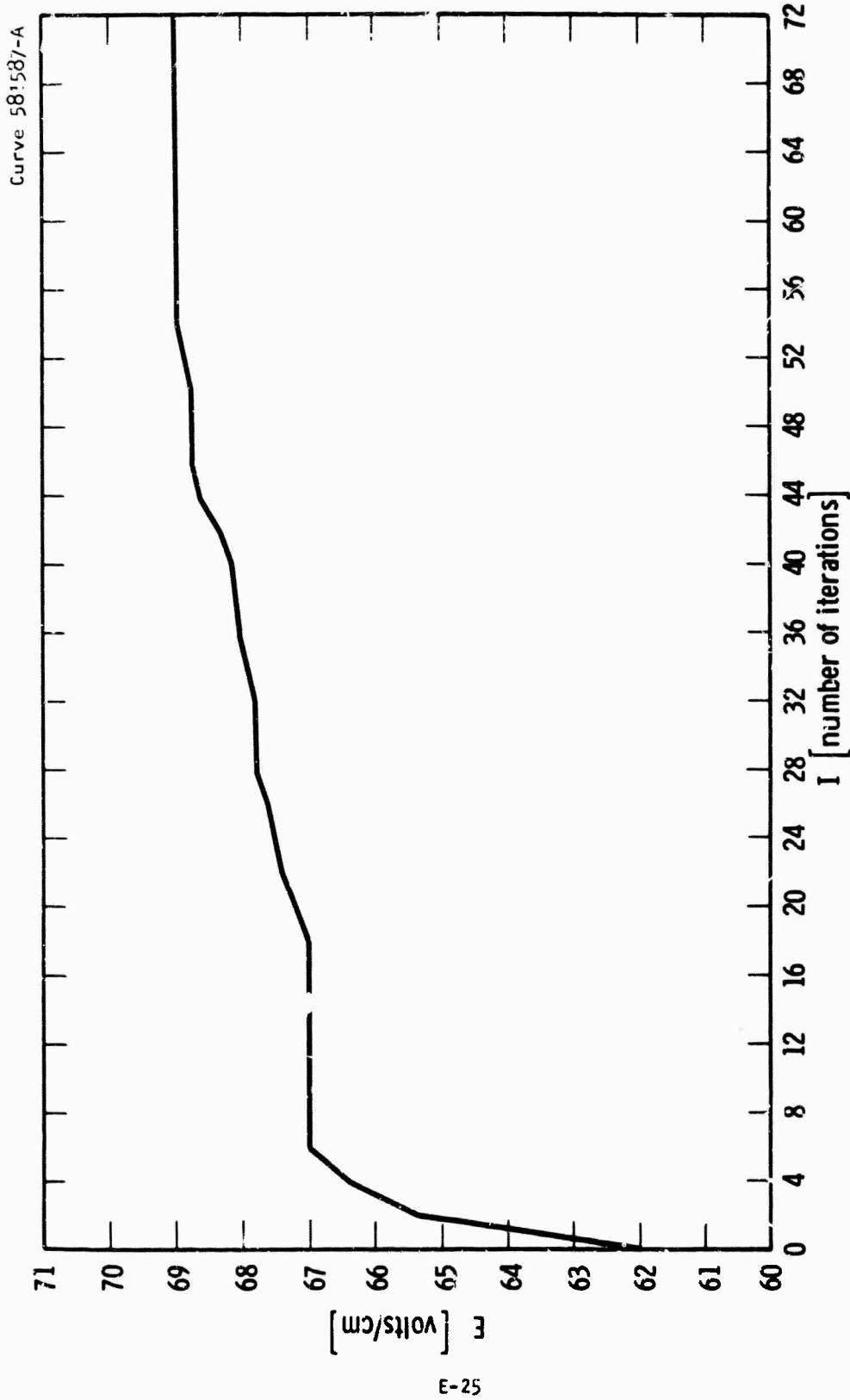


Fig. 11—Variation of E with iteration

16150129 WEDNESDAY JUNE 29 1988

NRL ALGOL VERSION OF 5/25/87

BEGIN

	SC	II	010
COMMENT	SC	21	010
THIS PROGRAM CALCULATES THE TEMPERATURE PROFILE OF AN ELECTRICAL ARC COLUMN HAVING CYLINDRICAL SHAPE AND INFINITE LENGTH AND POSSESSING SYMMETRICAL SPATIAL VARIANCES AROUND ITS AXIS. THE PROGRAM DETERMINES THE PROFILE BY AN ITERATIVE PROCESS USING A TIME DEPENDENT DIFFERENTIAL ENERGY BALANCE EQUATION WHICH INCLUDES RADIAVE AS WELL AS THERMAL TRANSPORT MECHANISMS.	SC	21	010
THE PROGRAM CONTAINS NINE READ STATEMENTS. THEY ARE LISTED BELOW IN ORDER OF CALL.	SC	21	010
(1)	SC	21	010
R0-----(REAL) THE ARC COLUMN RADIUS (UNITS-- CM) .	SC	21	010
N -----(INTEGER) NUMBER OF STEPS IN R (RADII'S)	SC	21	010
(2)	SC	21	010
DT-----(REAL) TIME STEP SIZE (UNITS -- SEC.) .	SC	21	010
NT-----(INTEGER) NUMBER OF TIME STEPS TO BE RUN	SC	21	010
(3)	SC	21	010
T -----(ARRAY) INITIAL RADIAL TEMPERATURE PROFILE, CONTAINS 51 VALUES STARTING WITH THE CENTRAL TEMPERATURE AND STEPPING IN EQUAL INCREMENTS OF RADIUS TO NR (UNITS--DEG. KELVIN)	SC	21	010
(4)	SC	21	010
KT-----(ARRAY) AN ARRAY GIVING THE VALUES OF THE INTEGRAL OF THERMAL CONDUCTIVITY WITH RESPECT TO TEMPERATURE (UNITS--WATTS/CM) .	SC	21	010
SBY-----(ARRAY) AN ARRAY OF ELECTRICAL CONDUCTIVITIES (UNITS--MHOS/CM)	SC	21	010
NOTE	SC	21	010
THE ABOVE TWO ARRAYS ARE READ IN SIMULTANEOUSLY AT CORRESPONDING TEMPERATURE VALUES .	SC	21	010
(5)	SC	21	010
NPNT----(INTEGER) NUMBER OF PTS IN MAKING NUMERICAL APPROXIMATIONS IN THE FLUX PROCEDURE (USUALLY AD IN AS SIX) .	SC	21	010
APPROXDS---(REAL) APPROXIMATE STEP SIZE TO BE TAKEN ALONG EACH OF THE THE ABOVE PTS (USUALLY READ IN AS .05) .	SC	21	010
(6)	SC	21	010
RT-----(REAL) FIRST TEMPERATURE VALUE OF THE KAPPA TABLE DEFINED BELOW	SC	21	010
RT-----(REAL) TEMPERATURE STEP SIZE OF KAPPA TABLE	SC	21	010
ET-----(REAL) LAST TEMPERATURE VALUE OF THE KAPPA TABLE	SC	21	010
NOTE THE ABOVE THREE TERMS HAVE UNITS OF DEG. KELVIN	SC	21	010
(7)	SC	21	010
RFREQ---(REAL) FIRST FREQUENCY VALUE OF THE KAPPA TABLE	SC	21	010
RFREQ---(REAL) FREQUENCY STEP SIZE OF THE KAPPA TABLE	SC	21	010
EFREQ---(REAL) LAST FREQUENCY VALUE OF THE KAPPA TABLE	SC	21	010
Z-----(INTEGER) FREQUENCY INDEX (WITH S CORRESPONDING TO RFREQ) WHICH DEFINES THE SPECTRUM TO BE USED IN	SC	21	010


```

F20 + ( E2 * XA1 ) + ( E1 * X ) + E0 )  

F31 + ( E3 * XA1 ) + ( E2 * X ) + E1 )  

F32 + E3 * E2 )  

FLAG + (( G + 1 * DY + Y0 ) * E3 / F10 + ( E3 * DY + 1 * E1 * E0  

/ F31 / F32 ) + E1 * E2 / ( E3 + E0 ) + (( DY + G ) * E2 / F10  

/ F31 + ( 2 * DY + G ) * E1 / F20 + F32 ) + E0 * E1 / ( E2 + E1 )  

END LAG ;  

      5 IS 44 LONG, NEXT SEG 2  

REAL PROCEDURE LAG ( X, XD, DX, Y, N )  

COMMENT  

X = DESIRED INDEPENDENT VALUE  

X0 = FIRST INDEPENDENT VALUE OF Y TABLE (FOR Y(0))  

DX = TABLE STEP FOR INDEPENDENT  

Y = NAME DEPENDENT VARIABLE VALUE TABLE (MUST BE SINGLE SUBSCRIPT)  

N = MAX INDEX OF Y TABLE ( > 0 )  

VALUE X = X0 + DX * N  

REAL X = X0 + DX : INTEGER N : ARRAY Y(0:N)  

BEGIN  

  INTEGER I : REAL S :  

  TOINTICK(S+(X-X0)/DX))  

  IF S<1 THEN LAG(Y(I)) ELSE  

LAG((Y(I)+1)-Y(I)) - (N-1)*Y(I))  

      6 IS 44 LONG, NEXT SEG 2  

END LAG ;  

REAL PROCEDURE ULAG(X, YA, Y, N)  

COMMENT ORDER 3 LAGRANGE INTERPOLATION, NO EQUAL STEPS, SINGLE DEPENDENT  

& INDEPENDENT VARIABLE, EXTRAPOLATE IF NOT X(0) < X < X(N-1).  

X = DESIRED INDEPENDENT VALUE  

XA = NAME INDEPENDENT VARIABLE VALUE TABLE (SINGLE SUBSCRIPT)  

Y = NAME DEPENDENT VARIABLE VALUE TABLE (SINGLE SUBSCRIPT)  

N = MAX INDEX OF BOTH XA & Y TABLES (> 3 & 1)  

  VALUE OF N  

  REAL X:  

  ARRAY YA, Y(0:N)  

  INTEGER N:  

BEGIN  

  INTEGER I:  

  REAL E0, E1, E2, E3, F10, F20, F31, F32;  

  E0=SIGN(XA(0));  

  FOR I=0 STEP 1 WHILE(I<=N-1) DO (SIGN(XA(I+1))-E0);  

  F10=(E1*(XA(I+1)-X)+(E0*(XA(I)-X)));  

  F20=(E2*(XA(I+2)-X)+E1*(E0));  

  F31=(E3*(XA(I+3)-X)+E2*(E1));

```

```

      F32+ E3-E21          00011200 SC 71 2311
      ULAV=(Y(1)+E3/E10/F20+Y(1)-E3)H0/F31/F32)=E1+E2/(E3+E0)+(E11
      +1)*E2/F10/F31=Y(1+2)*H1/F20/F32)=E0+F3/(E1-F2)
      END ULAVG          00011300 SC 71 2A12
                                         00011400 SC 71 3111
                                         00011500 SC 71 3713
                                         7 18 A4 LONG, NEXT SEG 2
PROCEDURE FLUX(SP,FP,R) ;           SC 21 2610
VALUE R : REAL N ;                 SC 21 2610
ARRAY SP,FP(01) ;                 SC 21 2610
COMMENT PROCEDURE FOR EVALUATING FLUX GIVEN S FUNCTION           SC 21 2610
BEGIN                           SC 21 2610
BOOLEAN APPE ;                  SC 21 2610
                                         START OF SEGMENT 0000000000 8
INTEGER N,J,PHI;                SC RI 010
LABEL APP10,X,EXACT,EXIT ;       SC RI 010
REAL X,SUM1,SUM2,SP,A,B,TN,RSNXY,TBN,AVVM,LANRDA,TNN,TEMP,YNT,XLN,
      NRHT,PHI,      K,KRINT,K2INT ; SC RI 010
ARRAY FX[0112] ;               SC RI 010
ARRAY RT,TP,XPAPG(0151); ARRAY M,TPI(0117) ; SC RI 113
DNN REAL RFREQ,LFREQ,DFREQ ;   SC PI 610
DNN REAL APPX0DS ;             SC BS 610
DNN REAL OPHT,Z=LANMAX,BT,ET,C7,RTX,EXT,XT,LIT1LEP;
REAL D ;                         SC BI 610
DNN INTEGER NT,NKT ;           SC BS 610

DNN ARRAY LF1=DLANRDA(01190) ;   SC BI 610
DNN APPAY CANSUS(0111+0+10) ;   SC BI 013
DNN APPAY G(01300),XAPPAL(0150+0135),NAX(0111) ; SC PI 1912
DNN ARRAY PR(0136),K,KR,XP(0135) ; SC PI 1913
REAL TAUR2,TAUR2,XP2,XR2,YAUP,TAUP,COUNTS,KPT,XHT,TAUA,PRB ; SC BI 2A13
IF COUNT >1 THEN GO EXACT ;
READ(READER1//,N1,APPX0DS);
RPH1 = 3.1415926536/NPH1 * MP1 + 3.1415926536 * RPH1,A ; SC RI 3613
READ(PASSG,301+6(+1)) (EXIT) ; SC PI 3913
READ(READER1//,RT,FT)(EXIT) ; COMMENT TEMP AT WHICH KAPPA IS GIVEN ;
READ(READER1//,RFPEQ,DFPEQ,DFPEQ,Z)(EXIT) ; SC BI 4411
LANMAX = (FFPEQ-DFPEQ)/DFREQ + 1 ; SC RI 5A13
FOR N = 1 STEP 1 UNTIL LANMAX DO LAN(N)= SP10/(CBFPEQ+(N-5)*DFPEQ) ; SC BI 7710
NT = (ET-RT)/DT ; SC PI 4312
FOR N=1 STEP 1 UNTIL LANMAX DO
READ(READER1//,TUP,J+0 STEP 1 UNTIL NT DO KAPPAN(J))(EXIT) ; SC BI 4710
READ(READER1//,RT,FT,DKT)(EXIT) ; SC BI 1D10
MKT = (ET-RT)/DT ; SC BI 11713
FOR J = 2 STEP 1 UNTIL LANMAX DO DLANRDA(J)=LAN(J-1) ; SC BI 11912
DLANRDA(1)= DLANRDA(2) ; SC RI 12610
BEGIN                           SC BI 12712
      REAL FR1,RPHT,PHI,TAN2PH1,TANPH1,SYNPH1,COSPH1,COSALPH1,SINALPH1
                                         START OF SEGMENT 0000000000 9

```

```

        LENGTH,NDSI
        INTEGER NR,NPHI !  

        NR=0 !  

        FOR FRI = +1, -2, +35, +5, +6, +7, +8, +85, +9, +95, 1 DO
          BEGIN
            NR = NR +1 ! NPHI=0 !
            LPHI = IF FRI < 0 THEN DPHI+5 ELSE 1.9707963248 +DPHI+5 !
            FOR PH1=PHI STEP DPHI UNTIL NPHI DO
              BEGIN
                NPHI=NPHI+1 !
                TAN2PHI=(TANPHI+1*SINPHI*SIN(PHI))/COSPHI+COS(PHI)*S2 !
                COSALPHI=(F1*TAN2PHI-S0*(1+TANPHI*(1-FR1*2)))/(1+TAN2PHI) !
                SINALPHI=S0*(1-COSALPHI*2) !
                IF ABS(SINALPHI/(COSALPHI-FR1)-TANPHI) >,0000001 THEN
                  BEGIN
                    COSALPHI*(FR1*TAN2PHI)+S0*(1+TAN2PHI*(1-FR1*2)))/(1+TAN2PHI) !
                    SINALPHI=S0*(1-COSALPHI*2) !
                  END ! LENGTH *SINALPHI/SINPHI !
                NDS=ENTIER(LENGTH/APPROX05)+1 !
                NSINR=NPHI+LENGTH=(NSINR+NPHI)+LENGTH/NDS)/2#,0 !
                CTNR=NPHI+1+COSPHI !
                END ! MAX(NR)+NPHI ! END !  


```

9 IS 87 LONG, NEXT SEG 8

```

EXCT 5
FOR N=0 STEP 1 UNTIL 50 DO
  BEGIN
    RTIN=NR/50 !
    TR(N)=LAG(CSR(N+1))-ST(NAT, NAT, RTR) !
    END !
    TR151=TR150 !
    N=0 !
    FOR X=5,0,+1, -2, +35, +5, +6, +7, +8, +85, +9, +95, 1 DO
      BEGIN
        R1(N)=NR !
        TR1(N)=ULAG(XR,RT,TR,50) !
        N=N+1 !
      END !
    FOR N =1 STEP 1 UNTIL 51 DO
      BEGIN
        ACRIT=1 !
        SUMF = 0 !
        FOR PHI = 1 STEP 1 UNTIL MAX(F) DO
          BEGIN
            SUMD = 0 !
            HDSI(N,PHI) = HDSI(N,PHI) + DSIN(N,PHI) !
            FOR J =1 STEP 1 UNTIL LAMMAX DO FIPARGE(J)=0 !

```

```

VM = 0 :                                     SC  B1 19912
FOR S=1/2 STEP 1 UNTIL 0.00
  BEGIN
    ASHAY = SORT((A - )+2*XMAX R           +S+2 : J
    TM = LAG(ASHAY,0,4/50,10,51) :
    TRH = 1.44022/TM :
    ZH0U = 1
    FOR J = 2 STEP 1 UNTIL LAMMAX DO
      BEGIN
        LAMDA = LAM(J) :
        KLM = LAG(TM,BT,NT,KAPP/(J+1),NT) :
        TTR = 1.19250-12/(LAMDA+5*(EXP(TRH/LAMDA)-1)) :
        TEMP = KLMM/2+EXPAPG(J) :
        EXPAPG(J) = XMAX + EXPAR(J) :
        IF TEMP < 30 THEN
          BEGIN
            YTH = KLMM*TRH*LAG(TEMP,0,1,6,300) :
            ZH = -YTH*BLAMDA(J) +2H :
            END TEMP30 :
        END OF LAMDA LOOP :
        VM = ZH + VM :
      END OF S LOOP :
      SUM = VMAX + SUM :
    END OF PHE LOOP :
    SUM = SUMR + SURF :
  END OF PHE LOOP :
  FRIEN = SURFRADPHT :
END OF N LOOP :
IF ZH = THEN APPF = FALSE ELSE APPF = TRUE :
IF APPF THEN BEGIN
  IF COUNT >1 THEN GO APPROX :
  BEGIN
    COMMENT FORMING TABLES OF PP(T),KR(T),XP(T) FOR APPROX SOLUTIONS :
    REAL KRINT,XPINT :
    START OF SEGMENT ***** 10
    ARRAY PPB(0:150,0:113) :
    FOR J=1 STEP 1 UNTIL 20
      BEGIN
        LAMDA=BLAM(J) :
        TRH = 1.44022/LAMDA :
        TEMP=BLAMDA :
        ET = 1 :
        FOR K = 0 STEP DT UNTIL ET DO
          PPB(J,(K+1)+1,1.19250-12/(TEMP*(EXP(TRH/K)-1))) :
          PPB(J,(K+1)+2)=PPB(J,(K+1))+PPB(J,(K+1)) :
          PPB(J,(K+1)+2)=PPB(J,(K+1)) :
        END OF PPB TABULATION :
      END :
    END :
  END :
  END :

```

```

FOR I = 0 STEP 1 UNTIL NT DO          SC 101 1613
  BEGIN
    KB1100 J
    FOR J= 1 STEP 1 UNTIL Z DO        SC 101 3910
      BB110 = PBC(J)*HOLAMBO(J) * KME11 J
    END OF JN TABULATION J           SC 101 3910
    PRINT(J+2*KBINT*KBINT+1) J
  FOR I = 0 STEP 1 UNTIL NT DO          SC 101 4011
    BEGIN
      KPRINT(KPRINT+0) J
    FOR J = 1 STEP 1 UNTIL Z DO        SC 101 4110
      BEGIN
        KPRINT(KPRINT+IPBB(J)+I+1)=PBC(J+I+1)/12*DT)*HOLAMBO(J+I)
        TEMP= IF A = KAPPAB(J+I)0 THEN A ELSE B=30 J
        KPRINT + KPRINT + PBC(J+I)*TEMP*HOLAMBO(J) J
      END OF J LOOP J
      IF I = 0 THEN KRC0 = (KPC0)+(KPC1)=BB(0)/DT/KPRINT ELSE
      KRC1=(BB1101+BB1101)/(2*DT)/KPRINT J
      KPC1=KPRINT/BB1101 J
    END OF I LOOP J
    COMMENT BB1101,KPRINT,KRC1 J TABLES NOW FORMED J
    LITTLEB = 1 J
  END J

```

	10 IS	95 LONGA	NEXT SEG	R
APPROX J	SC	81	24010	
BEGIN COMMENT APPROX SOLUTION J	SC	81	24010	
ARRAY KAPRAX,TWLO12001 J	SC	81	24010	
	START OF SEGMENT	*****	11	
FOR N =1 STEP 1 UNTIL 11 DO	SC	111	211	
BEGIN	SC	111	310	
AP(N) J	SC	111	310	
SUMF = 0 J	SC	111	410	
FOR PH1= 1 STEP 1 UNTIL MAX(N) DO	SC	111	413	
BEGIN	SC	111	613	
SUMF = 0 J	SC	111	613	
X0DSIN=PH1 J =0C(N,PH1) & 0NSIN=PH1 J	SC	111	912	
VPH = 0 J	SC	111	1413	
TAUR2 = 0 J	SC	111	1512	
TAUR1 = 0 J	SC	111	1611	
RSHXY=SUMF*(4+2*TAUR1*(S+D+15HX)+S+2) J	SC	111	1710	
TMMOLAM(RSHYT =0,R/50,TAUR1) J	SC	111	2311	
KPP= LAU(TEMP,HT,DT,KPRINT) J	SC	111	2612	
KB2= LAU(TEMP,HT,DT,KPRINT) J	SC	111	2911	
TAUP = KPP*HX/2 J	SC	111	3210	
TAUR = KB2*HX/2 J	SC	111	3313	
COUNTS =INT((S+25HX)/APPROX01*2)	SC	111	3512	

```

K0,ANX 0
FOR S=0 U      =,1XX STEP =X UNTIL K      =0
      BEGIN
      COUNTS + COUNTS = 1 ;
      NSHAY + SORT(A+P +2*XSHAYB +5*P) ;
      TEMP + THECOUNTS1+(A*NSHAYT+0,R/50,TR,51) ;
      KPT+LAG(TEMP,RT,DT,KP,NT) ;
      KRT+LAG(TEMP,RT,DT,KR,NT) ;
      TAUP2+     XKPT + TAUP2 ;
      TAUR2+     XKRT + TAUR2 ;
      KA(COUNTS)+LITTLEFR/(TEMP+LITTLEFR+TAUP2+LITTLEFR+TAUR2)/
                  TEMPXKPT + TAUP/TEMPXKRT ;
      TEMP+LAG(SORT(A+2*XHAYR(TEMP+P/X/2)+TEMP+P),0,R/50,TR,51)
      ;
      KP2+ LAG(TEMP,RT,DT,KP,NT) ;
      KR2+ LAG(TEMP,RT,DT,KR,NT) ;
      TAUP+KP2*X+TAUP ;
      TAUR+KR2*X+TAUR ;
      KA2(COUNTS)+LITTLER/(TEMP+LITTLER+TAUP2)*(LITTLER+TAUR2)/
                  TEMPXKP2 + TAUP2 /TEMPXKR2 ;
END OF PRE S LOOP ;
TEMP+LAG(SORT(A+2*XHAYR(S+A/4)+5*P),0,R/50,TR,51) ;
KPT +LAG(TEMP,RT,DT,KP,NT) ;

```



```

KRT +LAG(TEMP,RT,DT,KR,NT) ;
TAUP+(KP2*XKP2)/2KA/A ;
TAUR+(KRT*KR2)/2KR/A ;
KA2(LITTLER/(TEMP+LITTLER+TAUP)*(LITTLER+TAUR)/TEMPXKPT
    * TAUP/TEMPXKRT)/2 ;
TAUA +U ;
COUNTS+0 ;
FOR S= A/2 STEP X UNTIL 0      =0
      BEGIN
      COUNTS+1+COUNTS ;
      NSHAY+ SORT(A+P +2*XSHAYB +5*P) ;
      KLM + KA(COUNTS) ;
      BRR + LAG(THECOUNTS1,RT,DT,BR,NT) ;
      TEMP +TAUA+     KA(COUNTS1)A + TAUA ;
      IF TEMP >30 THEN ZH=G ELSE ZH=KLHRRRRLAG(TEMP+0.1,G+300) ;
      VHO ZH + VH ;
END OF S LOOP ;
SUM +     VHO*OSH ;
SUMF+     SUMFA*OSH ;
END OF PM1 LOOP ;
FRX(N)+     SUMFRADPM1 + FRX(N) ;
END OF M1 LOOP ;
END OF APPDOK FLUX ;

```

```

END OF APPF ;                                     11 15 170 LONG, NEXT SEG 6
FRX(0)+FR(1)+0 ;                               SC 81 26110
FOR J=2 STEP 1 UNTIL 91 DO ;                   SC 81 26110
FR(J)+ULAS(N+J-1),R1,FRX,11) ;               SC 81 26311
COUNT + 10 ;                                 SC 81 26A10
EXIT ;                                         SC 81 27012
IF COUNT # 10 THEN ;                           SC 81 27111
WRITE(PNINTER,< "DATA CANON FOR FLUX PROCEDURE ARE INCOMPLETE > ) ; SC 81 27210
SC 81 27213

END OF FLUX ;                                12 15 11 LONG, NEXT SEG 8
SC 81 27611

PROCEDURE DELSO (N,SC) ;                      P 15 296 LONG, NEXT SEG 2
  VALUE N ;  INTEGER N ;
  ARRAY SC(0) ;                                SC 21 2610
BEGIN
  SC(1)=A*(S(1)*S(1))/((DR+2)) ;
  FOR I=2 SL N DO
    SC(I)=(S(I)+I)*S(I-1)*0.5/(DR*R(I)) +(S(I+1)*S(I-1)+S(I)*2)/(DR+2) ;
END OF DELSO ;                                SC 21 30113
SC 21 3210

PROCEDURE TRIAG (N, A,B,C,D) ;                SC 21 4013
  ARRAY A,B,C,D(); ;  INTEGER N ;
COMMENT PROCEDURE FOR INVERTING TRIDIAGONAL MATRIX OF N*N ; SC 21 4610
SC 21 4610

BEGIN  REAL Z;  INTEGER J ;                     SC 21 4610
Z(0)=0 ;                                         SC 131 010
Z(1)=B(1) ;                                    SC 131 211
FOR J=2 SL N DO ;                            SC 131 311
  BEGIN  R(J)=C(J-1)/Z(J-1) ;                  SC 131 410
  Z+B(J)=A(J-1)*R(J) ;                        SC 131 710
  D(J)=A(J)-B(J)*D(J-1)/Z(J) ;                SC 131 1012
  END ;
FOR J=1 SL N-1 DO ;                          SC 131 1510
  D(N-J)=D(N-J)-(B(N-J)*D(N-J+1)) ;          SC 131 1711
END TRIAG ;                                  SC 131 2112
SC 131 2712

PROCEDURE DVGVT (N,SM,F,DOV) ;                13 15 30 LONG, NEXT SEG 2
  ARRAY SM,F,OGV(0) ;  INTEGER N ;
COMMENT PROCEDURE FOR EVALUATING THE DIVERGENCE OF FLUX ; SC 21 4610
EGIN  REAL P,Z;  INTEGER I,J ;
P= F(2)*2/DR -(A(S(2)+S(1))/((DR+2)) * P*ARS(P))/E* SORT(P/SIGHA()); START OF SEGMENT ***** 14
DVGF(1)= F(2)*2/DR ;                         SC 1A1 010
  SIGHA(); + SIGHA(); N#2 ;
FOR I=2 SL N DO BEGIN ;                       SC 1A1 1012
  DVGF(I)=(F(I+1)-F(I-1))/(2*DR) + F(I)/R(I) ; SC 1A1 1310
SC 1A1 1410

```

```

      SEG(I2 + SIGNA(I)) * E+2 )           SC  141  1913
      DVGETI + SEG(I2 + DVGETI)  1           SC  141  2211
      END  I2  1                           SC  141  2412
      DVGETI + SIGNA(I) * E+2 = F(2)N2/DR  1   SC  141  2613
      END  DVGET  1                         SC  141  3110

      IA  IS  1A LONG, NEXT SEG  2
      00000000  SL  21  A610
      00000000  SC  21  A011
      COMMENT EXCHANGE (VERSION OF 4/1/64)1
      COMMENT PRELIMINARY CALCULATIONS  1
      TIME1(PRINTER) 1
      RETA + 1,0 1  H + 90  1
      READ(READER, /> RD, N)  1
      COUNT=0 1
      READ(READER, /> OTAT)  1
      NN + N + 1  1
      DR + NN/N  1
      FOR I = 1 SL  NN  DR  RETI + (I-1)*DR  1
      RHO + RETANOT /(DR+2)  1
      LDA + RETANOT /(2*DR)  1
      -(SII + DR*RSII)+ RB  1
      ACII + LDA/DR = RHO  1
      CCII + = ARHMO  1
      RETI + 1= ARHMO  1
      SC  21  9011
      SC  21  9512
      SC  21  0713
      SC  21  10010
      SC  21  10212
      SC  21  10A13
      SC  21  10613

      FOR I=2 SL  N  DO BEGTN
      ACII+ (LDA/R(I)+1) =RHO  1
      CCII + =(RHO +LDA/R(I))  1
      END  I  1
      READ(READER,/> FOR  I=1 SL  S1  DO  TETI  )  1
      READ(READER,/> FOR  I=0 SL  H  DO  (STFI), SHY(I)  )  1
      K=0 1  TH01 GO  1
      FOR  I=1 SL  NN  DO  STII + LAG(TETI), 2000, 200, NT, M)  1
      COMMENT MAIN PROGRAM AND NEW TIME SOLUTIONS S, TT HERE  1
      START 1
      WRITE(PRINTER, FNTL, FOR  I=1 SL  NN  DO  RETI)  1
      FOR  I=1 SL  NN  DO  SIGNA(I)+ ULAG(SEI),ST, SHY, M)  1
      IF  K # 0 THEN
      FOR  I=1 SL  NN  DO  TETI + LAG(SEI), ST, M, 2000, 200  1
      WRITE(PRINTER,PAGE1)  1
      WRITE(PRINTER, <X3, FAT TIME>, X12.4, X3,*SECOND*, //>, THK)  1
      SC  21  10910
      SC  21  1010
      SC  21  1310
      SC  21  11513
      SC  21  11810
      SC  21  13013
      SC  21  14513
      SC  21  14713
      SC  21  15413
      SC  21  19413
      SC  21  19510
      SC  21  1A011
      SC  21  17510
      SC  21  17513
      SC  21  1A213
      SC  21  14512
      SC  21  19611
      SC  21  19612
      SC  21  14913
      SC  21  20213
      SC  21  20411
      SC  21  21011

      15  IS  12 LONG, NEXT SEG  2
      FEUX (SF, RBL)  1
      IF  COUNT # 10  THEN  GO  EXIT  1
      DVGET (N + SIGNA(F) OGV)  1
      DLSH (ND, SC)  1
      FOR  (+1 SL  N  DO  SSEI + SC(I) + SF(I) = DVGETI  1
      WRITE(PRINTER, NO1)  1
      SC  21  19611
      SC  21  19612
      SC  21  14913
      SC  21  20213
      SC  21  20411
      SC  21  21011

```

```

        WRITE(PRINTER1, FNT1), FOR 1=1 SL NN DD TRIT1,6111,FILE1, T111;
SC 21 21371
SIGN1111,SC111, DNGR111, SEC111, SS111 > ) >
SC 21 22610
WRITE(PRINTER1,0) 1
SC 21 23811
WRITE(1PRINT1, <X3>, RE 01, F10.6, //>, F ) >
SC 21 24110
16 15 8 LONG, NEXT SEG 2
AT +0.0 ) >
SC 21 24811
FOR 2=1 SL NN DD REBIN
SC 21 24910
IFC+ IF 1=1 UN 10NN THEN 1 ELSE IF (1=1) MOD 2 =0 THEN ?
SC 21 25010
ELSE 4 ) >
SC 21 25413
AT + 41 + 283+1015926+EXR11)NSIGNAL13H1FC >
SC 21 24613
END INT 1
SC 21 26110
AT + A1DR/3 ) >
SC 21 26311
WRITE(PRINTER, </>,X3,PARC CURRENT 101, K12.5, //>, A1) >
SC 21 26510
17 15 12 LONG, NEXT SEG 2
TIME11(PRINTER1) >
SC 21 27311
IF K = NT THEN WRIT1PUNCH, <S(E12.5,% * )>, FOR 1=1 SL NN DD
SC 21 27411
18 15 7 LONG, NEXT SEG 2
T111 1 >
SC 21 24111
IF K = NT THEN GO TO EXIT 1 >
SC 21 24011
TH1K010 TH1K1 + DT 1 > K0 K01 1
SC 21 24912
FOR 1=1 SL N DD 0111 + C111 + D1V111RETANDT >
SC 21 20311
0111 + 1 + ARND 1 >
SC 21 24912
FOR 1=2 SL N DD 0111 + 1+ ZERHO 1 >
SC 21 30113
TRIDAG (N, 4, B,C, D) >
SC 21 30712

EXCHANGEC SxD ) >
SC 21 31111
GO TO START 1
SC 21 31313
EXIT1
SC 21 31611
TIME11 (PRINTER1) >
SC 21 31510
END.
SC 21 31610
2 15 319 LONG, NEXT SEG 1
COS IS SEGMENT NUMBER 0010, PRT ADDRESS IS 0164
EXR 0020 0160
STN 0021 0154
SORT 0022 0154
OUTPUT(N) 0023 0107
BLOCK CONTROL 0024 0004
INPUT(W) 0025 0164
GO TO SC1VER 0026 0164
ALGOL WRITE 0027 0014
ALGOL READ 0028 0014
ALGOL SELECT 0029 0014
NUMBER OF ERRORS DETECTED = 0 LAST CARD WITH ERROR HAS SEQ #
PRT SIZE = 1561 TOTAL PUN SEGMENT SIZE = 1604 WORDS1 D1EY 517F = 40 SEGS1 RD, PGH, SEGS = 30
ESTIMATED CORE STORAGE REQUIREMENT = 6630 WORDS.
10159142 WEDNESDAY, JUN 7, 1987 PROCESSOR TIME = 31.60 SECONDS I/O TIME = 31.62 SECONDS

```

APPENDIX F

Analysis of Xenon Discharges

J. J. Lowke
Westinghouse Research Laboratories
Pittsburgh, Pennsylvania 15235

I. INTRODUCTION

Calculations have been performed deriving temperature profiles of discharges in xenon flash tubes from given material functions for xenon, at a specified experimental value of current and electric field strength. The calculations include the effects of conduction, radiation, and self absorption of radiation. Comparisons are made of three different methods of doing these calculations. Results of these calculations indicate that for typical values of electric field strength and current the temperature profiles are radiation dominated if the pressure is equal to or higher than four atmospheres, the profiles are relatively flat, the influence of radiation at wavelengths less than 1000 \AA is negligible, and the effect of self absorption in the visible continuum is of only secondary importance in determining the central temperature.

An analysis has been made of the time dependence of the experimental data of electric field strength, current and radiation. The radiation measurements suggest that the xenon discharge should be treated as a time dependent problem rather than a wall stabilized, steady state arc, which is the basis of the present calculations.

II. TEMPERATURE PROFILE CALCULATIONS

Calculations of the temperature profile for a wall stabilized steady state arc for a given electric field strength, current and gas pressure have been made using (1) the Eddington Approximation, (2) a pseudo time dependent equation and an exact radiation flux calculation and (3) a pseudo time dependent equation and an exact radiation intensity calculation. It is considered that method (3) is the least expensive. However, for comparison of calculated values of central temperature and arc radius with experiment, a simple constant temperature model is adequate.

The input material functions for the calculations are those supplied by C. H. Church. The spectral absorptivities are an estimate of the continuum and neglect line radiation. Thermal and electrical conductivities are calculated using a program of De Voto. The effects of radiation were determined by dividing the spectrum into 20 equal frequency bands extending to 5×10^{16} Hz (600A).

1. Method using Eddington Approximation

This method is outlined in reference (1). The following equations are solved numerically.

$$\nabla \cdot (\vec{F}_c + \vec{F}_R) = \sigma E^2 \quad (1)$$

$$\vec{F}_c = -kV T \quad (2)$$

$$\vec{F}_R = \int \vec{F}_{R\nu} d\nu \quad (3)$$

$$\nabla \cdot \vec{F}_{R\nu} = 4\pi (\epsilon_\nu - J_\nu K_\nu) \quad (4)$$

$$\vec{F}_{R\nu} = -\frac{4\pi}{3K_\nu} \nabla J_\nu \quad (5)$$

The nomenclature is given in Table I.

Equation (5) is the only inexact equation and is known in astrophysics as the Eddington approximation. The equation is in effect a diffusion approximation for the radiation flux and is equal to a constant multiplied by the gradient of the radiation energy density, which is proportional to ∇J_ν . An iterative procedure is used to satisfy the boundary conditions which are as follows

$$\text{at } r = 0 \quad F_{R\nu} = 0 \quad \text{and } F_T = 0$$

$$\text{at } r = R \quad T = T_W \quad \text{and } J_\nu = \frac{2}{\pi^2} F_{R\nu} .$$

Table I

Nomenclature

\vec{F}_C	Conduction Flux Density	(watts cm^{-2})
\vec{F}_R	Radiation Flux Density	(watts cm^{-2})
k	Thermal Conductivity	(watts $\text{cm}^{-1}\text{°K}^{-1}$)
σ	Electrical Conductivity	(mho cm^{-1})
K_v	Spectral Absorbtivity	(cm^{-1})
ϵ_v	Spectral Emission Coefficient	(watts $\text{cm}^{-3}\text{ster}^{-1}\text{sec}$)
\vec{F}_{Rv}	Radiation Flux Density per unit Frequency	(watts cm^{-2}sec)
J_v	Radiation Intensity per unit Frequency	(watts $\text{cm}^{-2}\text{ster}^{-1}\text{sec}$)
T	Temperature	(°K)
E	Electric Field Strength	(volt cm^{-1})
I	Electric Current	(amps)
r	Radius	(cm)
T_w	Wall Temperature	(°K)
C_p	Specific Heat at Constant Pressure	(Joules $\text{gm}^{-1}\text{°K}^{-1}$)
ρ	Density	(gm cm^{-3})
ϵ	Integrated Emission Coefficient	(watts $\text{cm}^{-3}\text{ster}^{-1}$)
t	Time	(sec)
B_v	Planck Function	(watts $\text{cm}^{-2}\text{ster}^{-1}\text{sec}$)
p	Pressure	(Atmospheres)

Input values are the material functions k , σ , K_v and ϵ_v (which are functions of temperature), and the experimental values of I and E . R is determined from

$$2\pi R(F_C + F_R)_{r=R} = IE \quad (6)$$

The solution of these equations giving T , F_R and F_C as a function of radius for $E = 29$ volt/cm and $I = 1140$ amps at a pressure of 11 atmospheres is shown in Fig. 1.

2. Method using a pseudo time dependent equation and an exact radiation flux calculation

This method has been suggested by B. Swanson.

Rather than iterate to satisfy split boundary conditions as in the former method, an assumed initial temperature profile is modified using the time dependent equation to obtain the steady state solution.

The time dependent equation, neglecting effects of mass flow is given by equation (7)

$$C_p \rho \frac{\partial T}{\partial t} = \sigma E^2 - \nabla \cdot \vec{F}_C - \nabla \cdot \vec{F}_R \quad (7)$$

As we are only interested in obtaining the steady state solution, C_p^c is made equal to 1, a constant. \vec{F}_C is obtained using equation (2) and \vec{F}_R is obtained exactly using the integration procedure of Swanson.² A number of difficulties associated with this method are overcome as described below.

(1) The numerical solution of this equation is unstable for large step sizes in time. This instability is described by Richtmyer³ and in the present method of solving the equation, the size of the time step for stability has been empirically found to closely follow the requirement cited by Richtmyer that

$$\Delta t < \frac{(\Delta r)^2}{2F} \text{ where } F = k/\rho C_p . \quad (8)$$

Generally the small step size requirement makes computing times prohibitively large. However in radiation dominated arcs, the temperature of most of the arc is controlled by the terms $\sigma E^2 - \gamma \vec{F}_R$ of equation (7) and not by ∇F_C which causes the instability. By initially dividing the term $\nabla \vec{F}_C$ by a factor of the order of 30 and increasing the step size by the same factor the rate of convergence to the final profile is greatly increased. The multiplying factor is then removed to determine the outer small region of the profile, which is controlled by conduction. In this latter stage of the calculation it is only necessary to recalculate \vec{F}_R , which is the most time consuming part of the calculation, at say every twentieth time step, for \vec{F}_R is determined primarily by

the temperature of the inner region of the arc. With this simplification any initial temperature profile can be made to rapidly converge to the final solution.

(2) In the present problem, current and electric field strength are input values and the radius and the temperature profile are the output. After each time step the radius is recalculated using equation (9), where the temperature profile is regarded as a function of r/R

$$R^2 = I[2\pi E \int_0^1 x \sigma dx]^{-1} \quad (9)$$

where $x = r/R$.

In this way the correct current is maintained as the temperature profile is varied.

(3) It is found that the temperature profile can vary monotonically and very slowly in a way making it difficult to determine the error from the true steady state solution. To test for convergence, after calculating each new temperature profile, equations (1) and (2) are solved to obtain \hat{F}_R as a function of r . If the temperature profile is correct, the values of \hat{F}_R will agree with the values of \hat{F}_R obtained from the spectral absorbtivities using the Swanson exact integration procedure.

In the numerical results presented using this method the two values of \vec{F}_R agree to 1% in each case. The method was used for the conditions of Fig. 1 and the temperature profile is shown as the broken curve. The small difference in the profiles near the outer wall is considered to be due to an insufficiently small step size in method 2 and not due to the Eddington approximation. The step size in r/R near the wall in method 2 was 0.01 whereas in the Eddington method it was 0.0001.

The method was also used for $p = 4$ Atmospheres with $E = 29 \text{ volt cm}^{-1}$ and $I = 1140 \text{ amps}$ giving results insignificantly different from those shown in Fig. 2, which were obtained using method 3. Fig 3 gives results obtained using method 2 showing the variation of F_{Rv} with r at two different frequencies. The radiation flux integrated from the absorption edge at $v = 2.9 \times 10^{15}$ to $v = 5 \times 10^{15} \text{ Hz}$ attains a maximum of only 2% of the total radiation flux at $r/R = 0.87$ for the conditions of Fig. 2. The inclusion of lines in this region of the spectrum will only decrease the radiation flux as, from the Eddington Approximation, which is equation (5), K_v is increased in the region of lines and $J_v \sim B_v$ (see Fig. 4). Consequently it is concluded that, except for very high powers where the central temperature is greater than 14000°K , the effect of radiation for wavelengths less than 1000\AA can generally be neglected in the present calculations.

3. Method using a pseudo time dependent equation and exact radiation intensity calculations

For the conditions of the present problem it is of considerable advantage to express equation (7) in the form

$$C_p \rho \frac{\partial T}{\partial t} = \sigma E^2 - \nabla \cdot \vec{F}_c - 4\pi(\epsilon - \int J_v K_v dv) \quad (10)$$

where use is made of the continuity equation for radiation, equation (4). From Kirchoff's Law $\epsilon = \int B_v K_v dv$ and ϵ is simply a function of temperature. J_v can be obtained exactly from a modification of the Swanson integration procedure used to obtain \vec{F}_R .

The advantages of this modification to method 2 are

- a. The increment in temperature does not depend on the gradient of a computed quantity. In method 2 to determine $\nabla \cdot F_R$, F_R needs to be calculated to high accuracy and at many radial steps.
- b. For typical experimental conditions in xenon, $\int J_v K_v dv$ is small compared with ϵ , provided that ultraviolet radiation can be neglected. Then the integral need only be calculated at say every 100th step, instead of after every 20th step, as outlined in the latter part of Section

II 2 (1). In fact if the integral in the visible range of the spectrum is set at zero, the central temperature is decreased by only 200°K for Fig. 1 and 300°K for Fig. 2.

Instead of having E and I as the input, as in method 2, E and R are treated as the input and the value of I is calculated as output. The difficulty outlined in II 2 (2) is thus removed and the stability of the numerical solution is also improved.

The profile obtained using this method, with $E = 29$ and $R = 0.1$ as input at a pressure of 4 Atmospheres is shown in Fig. 2. Fig. 4 gives J_v as a function of frequency at two radial points.

4. Constant temperature model

In any comparison of theoretically derived temperature profiles with experiment one of the principal interests is to compare, for any value of I and E , the theoretical central temperature and radius with experimental observations. An assessment can then be made of the accuracy of the input material functions, σ and K_v , assuming that the experimental arc is well stabilized and in an effective steady state condition. For this purpose, for the experimental conditions considered in this paper, the central temperature and R can be computed to within 5% simply by assuming that the arc is at constant temperature, without computing the temperature profile.

For radiation dominated arcs, loss of energy by conduction at the center of the arc is negligible compared with radiation losses. Thus the input electrical energy equals the net emission of radiation energy, as expressed in equation (11), i.e.,

$$\sigma E^2 = 4\pi(\epsilon_v - \int J_v K_v dv) \quad (11)$$

At the center of a cylindrical plasma of radius R and uniform temperature T, J_v can be calculated using the two radiation equations (4) and (5) again given below

$$\nabla \cdot \vec{F}_{RV} = 4\pi(\epsilon_v - J_v K_v)$$

$$\vec{F}_R = - \frac{4\pi}{3K_v} \nabla J_v$$

As ϵ_v and K_v are constant the equations can be solved analytically to give

$$J_v(0) = B_v \left\{ 1 - 1/(I_0(y) + \frac{8}{\sqrt{3}\pi} I_1(y)) \right\} \quad (12)$$

where $y = \sqrt{3} K_v R$ and I_0 and I_1 are modified Bessel Functions.

In this way the integral in equation (11) can be evaluated, and the equation used to determine E for any given cylinder of radius R and temperature T . The current I is then obtained from the conductivity equation (13)

$$\frac{I}{E} = \pi R^2 \sigma \quad (13)$$

Curves computed using equations (11), (12) and (13) are given in Figs. 5, 6 and 7 for pressures of 2.5, 4 and 11 atmospheres respectively. The agreement of the central temperature and radius predicted for pressures of 4 and 11 atmospheres for $E = 29$ and $I = 1140$ with the temperature profiles of Figs. 1 and 2 is within 5%.

For $p = 2.5$ Atmospheres, the point at $E = 29$ volt cm^{-1} and $I = 1140$ amperes appears to be just in the folded region of the curves of Fig. 5 where multiple solutions are possible. The existence of multiple solutions has been investigated but for other input material functions and for a different gas and will be reported later. For xenon at 2.5 Atmospheres, for E greater than 30 and $I = 1140$ the only solution that exists is for a conduction dominated arc where the central temperature is controlled by thermal conduction and not by radiation. At $E = 29$ volt cm^{-1} $I = 1140$ amperes the only solution that was found was that of a conduction dominated arc with a central temperature above 19,000°K. At these temperatures the input material functions are unknown. No detailed search was made for the existence of a solution corresponding to a radiation dominated arc for this value of E and I .

III. COMPARISON WITH EXPERIMENT

1. Steady state condition

For a tube of $R = 0.63$ cm the peak values of I , E and temperature that have been measured are $E = 29$ volt cm^{-1} , $I = 1140$ amps, central temperature = $11,500^\circ\text{K}$ and pressure = 4.2 atmospheres.⁴ As these quantities apply for a time corresponding to $\frac{\partial T}{\partial t} = 0$ it should be appropriate to compare with the steady state theoretical solution. Upper and lower limits of the possible gas pressure are 11 and 2.5 Atmospheres.

Results obtained from Fig. 6, and for similar curves at 4 Atmospheres but with different values of σ and K_v are given in Table 2.

Table 2 ($p = 4$, $E = 29$, $I = 1140$)

σ	K_v	Input		Output	
		R	T	R	T
De Votto Values	Normal Continuum	0.4	13,300		
De Votto Values	2 x Continuum	0.42	11,700		
1/2 x De Votto	Normal Continuum	0.6	11,700		
1/2 x De Votto	2 x Continuum	0.62	10,800		

If lines are included in the spectral absorbtivity data, the integrated emission coefficient may be increased by a factor of two. However, as is seen from Table 2, the computed radius is still only 0.42 cm and σ would still need to be decreased for the arc to fill the tube.

Unfortunately measurements of the discharge radius are difficult to make. Furthermore no accurate experimental measurements of σ for xenon are known. It is seen that the theoretical predictions are in very approximate agreement with experiment, but if the discharge does indeed fill the discharge tube it would appear that the De Vott⁴ values of σ are too high. However an analysis of the time dependence of the experimental parameters suggests that the discharge does not fill the tube. Therefore it should not be concluded that we believe that the σ or ϵ data is in error.

2. Time dependence of the discharge

From the time dependence of the experimentally⁴ observed values of E , I and radiation intensity at 8232 \AA , the curves of Fig. 8 and 9 have been prepared. In Fig. 8 it is seen that the curves for differing discharge energies are in reasonable coincidence for the latter portion of the discharge time. However it is seen in Fig. 9 that the radiation intensity at a particular value of I varies markedly for discharges of differing input power. If the discharge were to be well stabilized and effectively in the steady state condition, the value of E and central temperature (and thus

the radiation intensity) would be determined for any value of R and I. If the experimental measurements are correct, it appears that the arc cannot be regarded as being wall stabilized and in the steady state at times after the peak radiation intensity.

It is known that the pressure inside of the discharge tube is determined not only by the core temperature, but is controlled to a large extent by the temperature of the gas near the tube wall. It is suggested that this gas is continually heated throughout the duration of the pulse, thus increasing the pressure. The central temperature, which is determined from equation (11), is thus lower at a given I for pulses of high power because the gas pressure is higher. In this way it may be possible to explain the radiation measurements of Fig. 9. It would then be expected that the radius of the central portion of the arc does not fill the tube, and increases throughout the duration of the pulse.

Measurements of the temperature profile at peak power are consistent with the theoretical predictions that the temperature profile is very flat.

IV. CONCLUSIONS

For the experimental parameters typical for the operation of xenon flash tubes, the following generalizations can be made.

1. The temperature profiles are very flat and are radiation dominated, provided the gas pressure equals or is greater than 4 Atmospheres.

2. Except for very high powers where the central temperature is above 14,000°K, the effect of radiation of wavelengths less than 1000Å can be neglected.
3. Self absorption effects in the visible continuum generally effect the central temperature by less than 1000°K.
4. The constant temperature model in which account is taken of absorption, can be used to predict the central temperature and outer radius of wall stabilized arcs to within 10%.
5. Of the three methods used to compute temperature profiles of steady state, wall stabilized arcs from input material functions, it appears that the time dependent method using an exact radiation intensity calculation is the most economic.
6. Experimental measurements indicate that the arc discharge is not wall stabilized and that time dependent studies are needed.

V. POSSIBLE FUTURE WORK

1. Experimental
 - (1) Time dependent studies of the radiation intensity as a function of radius are needed to determine whether the radius varies with time.
 - (2) Improved measurements of the pressure as a function of time.
 - (3) Measurements of temperature profiles of a cascade arc in xenon. Such a measurement would enable a determination of electrical conductivity, which is a crucial input parameter in the theoretical calculation of temperature profiles.

2. Theoretical

(1) If the pressure and E were known as a function of time, a time dependent study using equation (10) could be made to predict the current and the temperature profile as a function of time. The self-absorption integral of equation (10) could be neglected giving very considerable improvement in computation time and an error of only a few hundred degrees in the central temperature. It is proposed that for a given I the temperature of the gas near the quartz walls which contain the arc, is dependent on the total power fed into the pulse, but that the temperature profile of the arc core at late times is relatively insensitive to the initial temperature profile that is assumed for the calculations. The gas pressure as a function of time could be derived from the computed temperature profiles and compared with the input pressure as a function of time.

(2) A more involved computation could be carried out solving equations (14), (15) and (16)

$$\frac{C_p}{p} \left(\frac{\partial T}{\partial t} + \underline{v} \cdot \nabla T \right) - \nabla \cdot (k \nabla T) + v \frac{\partial \underline{v}}{\partial t} + v \underline{v} \cdot \nabla v - \sigma \dot{E}^2 - 4\pi - \frac{1}{\rho} \frac{\partial p}{\partial t} = 0 \quad (14)$$

$$\rho \frac{\partial \underline{v}}{\partial t} + \rho \underline{v} \cdot \nabla \underline{v} = -\nabla p \quad (15)$$

$$\frac{\partial p}{\partial t} + \nabla \cdot \rho \underline{v} = 0 \quad (16)$$

As p and ρ determine T ; p , ρ , v and T can be determined as a function of time and compared with experiments.

VI. ACKNOWLEDGEMENT

Acknowledgement is made for many discussions with A. V. Phelps, B. Swanson, M. A. Uman, C. H. Church, R. Lieberman and P. Duchhave.

VII. REFERENCES

1. J. J. Lowke and E. R. Capriotti, "The Influence of Radiation on High Pressure Arcs", Report 66-1E2-GASES-R1 (1966).
2. B. W. Swanson, "Radiation Flux in a Non-Isothermal Non-Grey Cylindrical Arc", Paper 65-8D8-GASDY-P1 (1965).
3. R. D. Richtmyer, "Difference Methods for Initial Value Problems", Interscience (1957).
4. P. Buchhave, Quantum Electronics Dept., Private Communication.

BLANK PAGE

Curve 581487-A

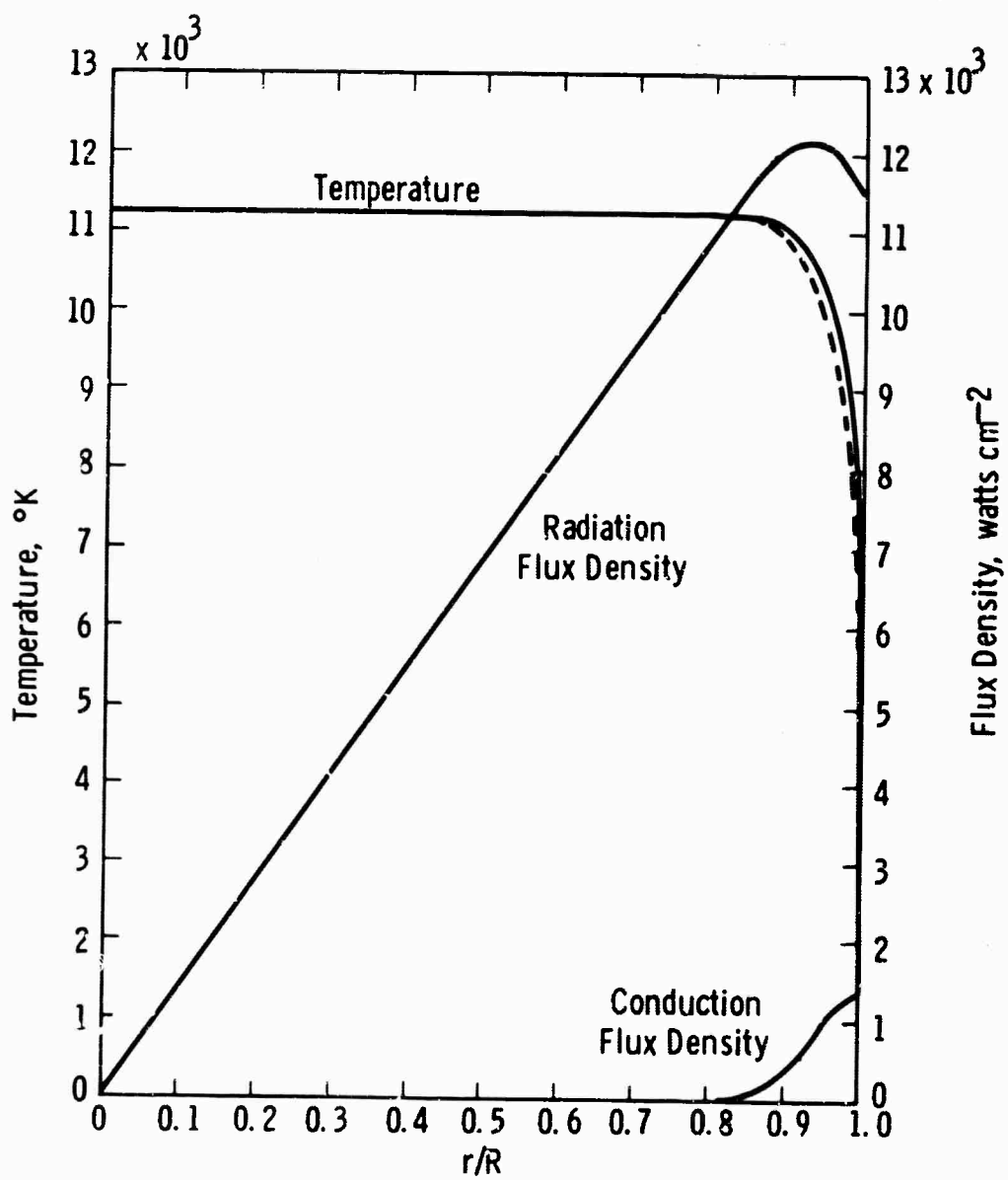


Fig. 1-Xenon arc profile

Input: $p = 11 \text{ Atm}$, $E = 29 \text{ V/cm}$, $I = 1140 \text{ Amp}$, $T_W = 2000^\circ\text{K}$
Output: $R = 0.410 \text{ cm}$

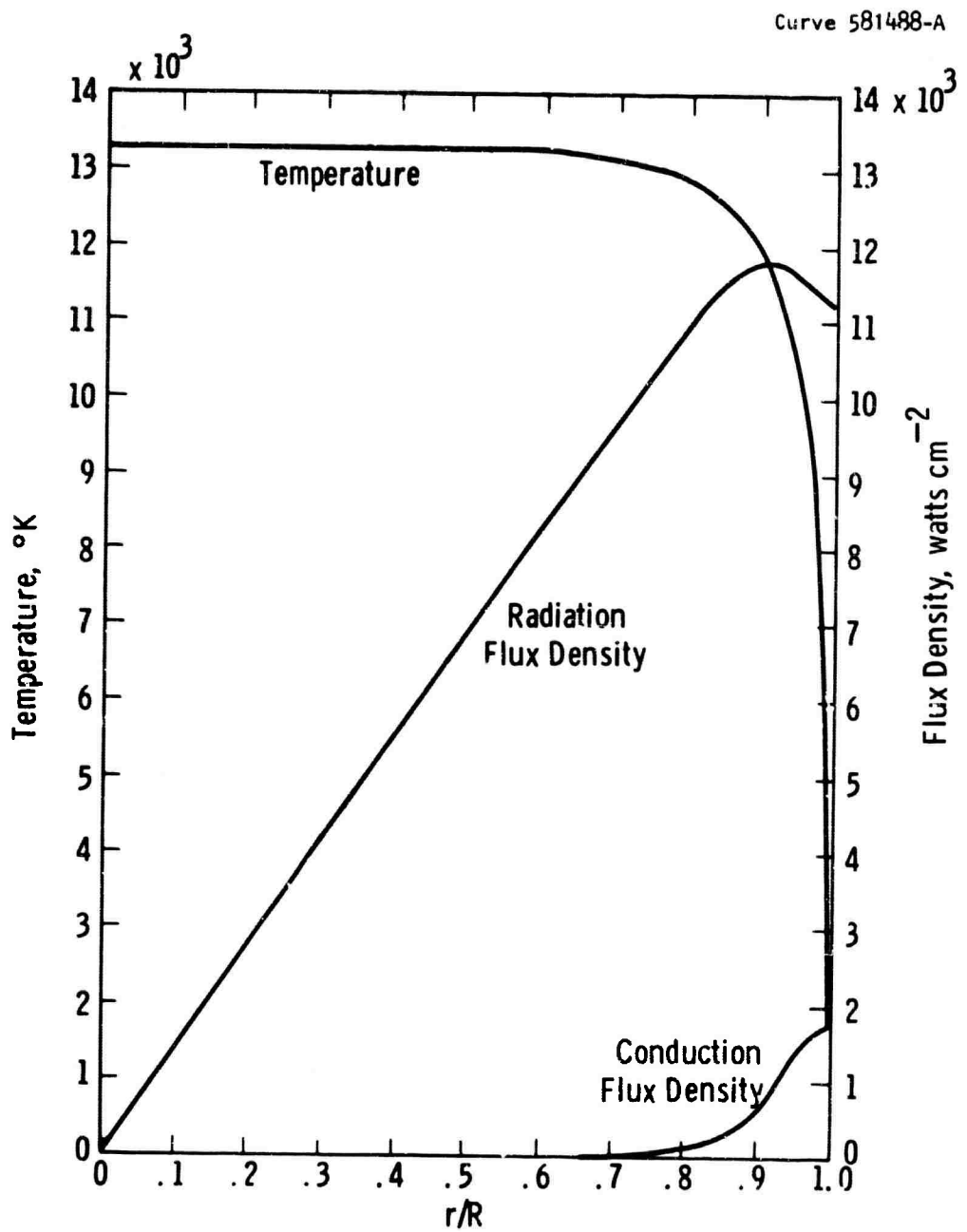


Fig. 2—Xenon arc profile

Input: $p = 4 \text{ Atm}$, $E = 29 \text{ V/cm}$, $R = 0.411 \text{ cm}$, $T_W = 2000 \text{ }^\circ\text{K}$
 Output: $I = 1145 \text{ Amps}$

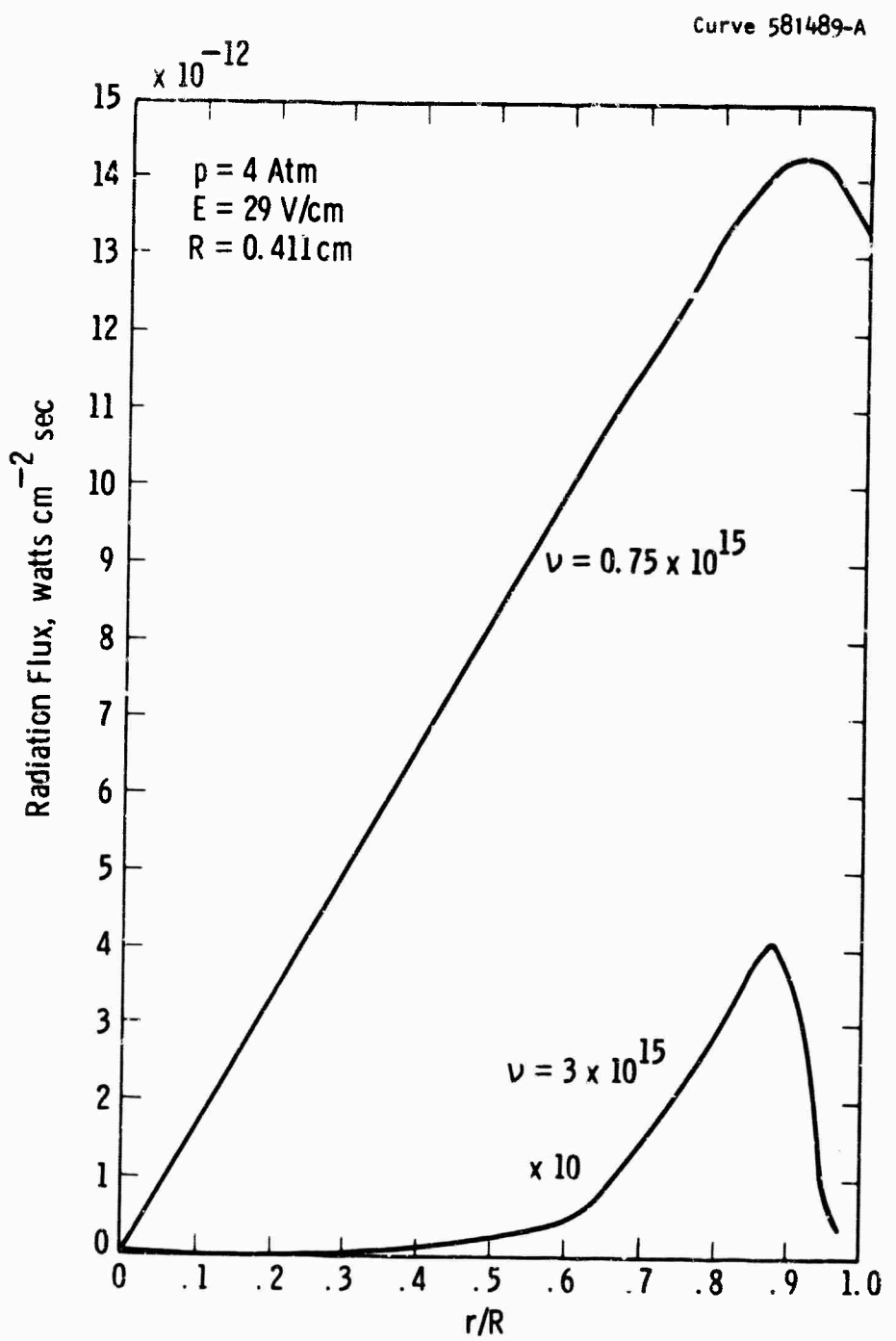


Fig. 3—Radiation flux

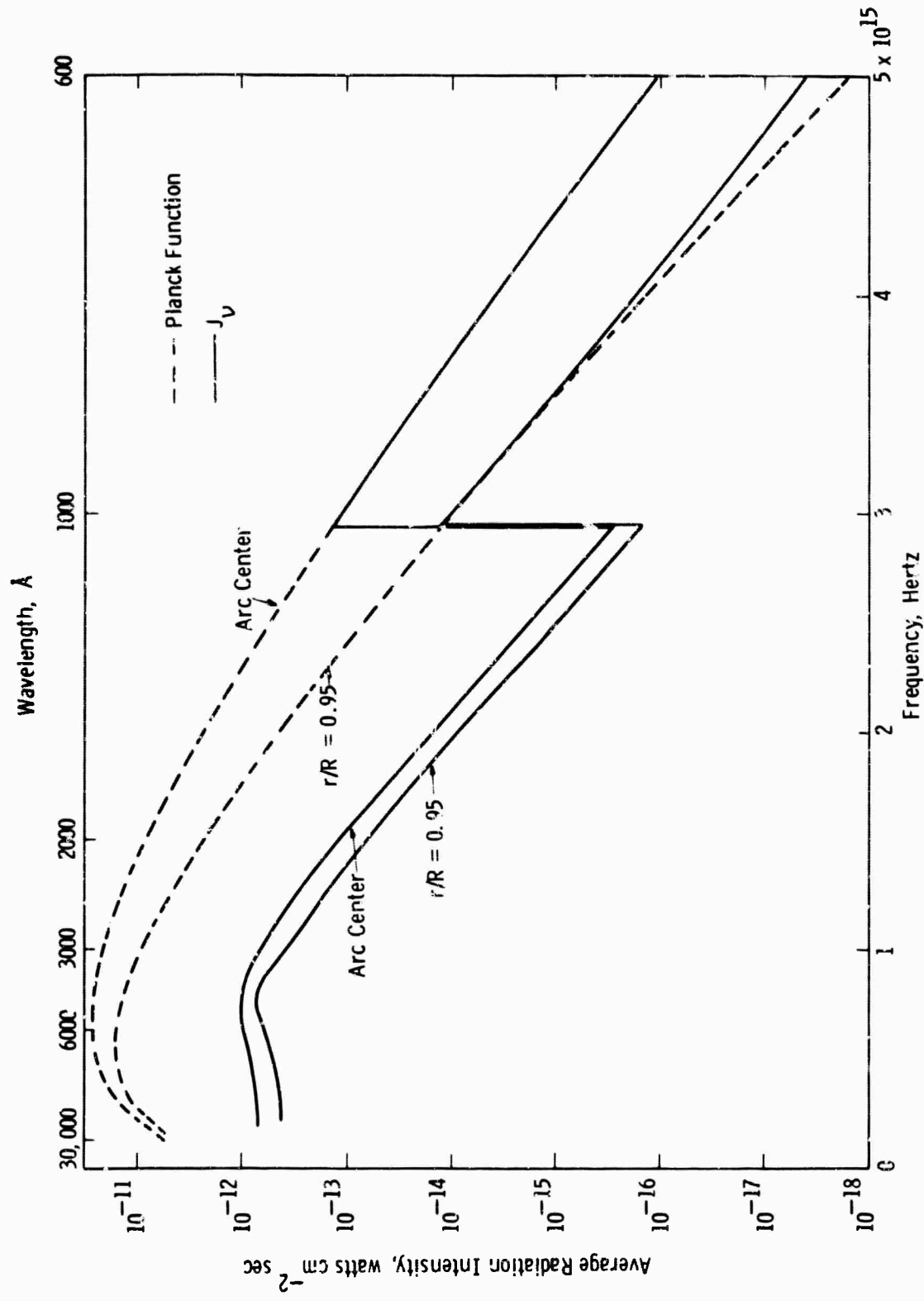


Fig. 4

Curve 581491-A

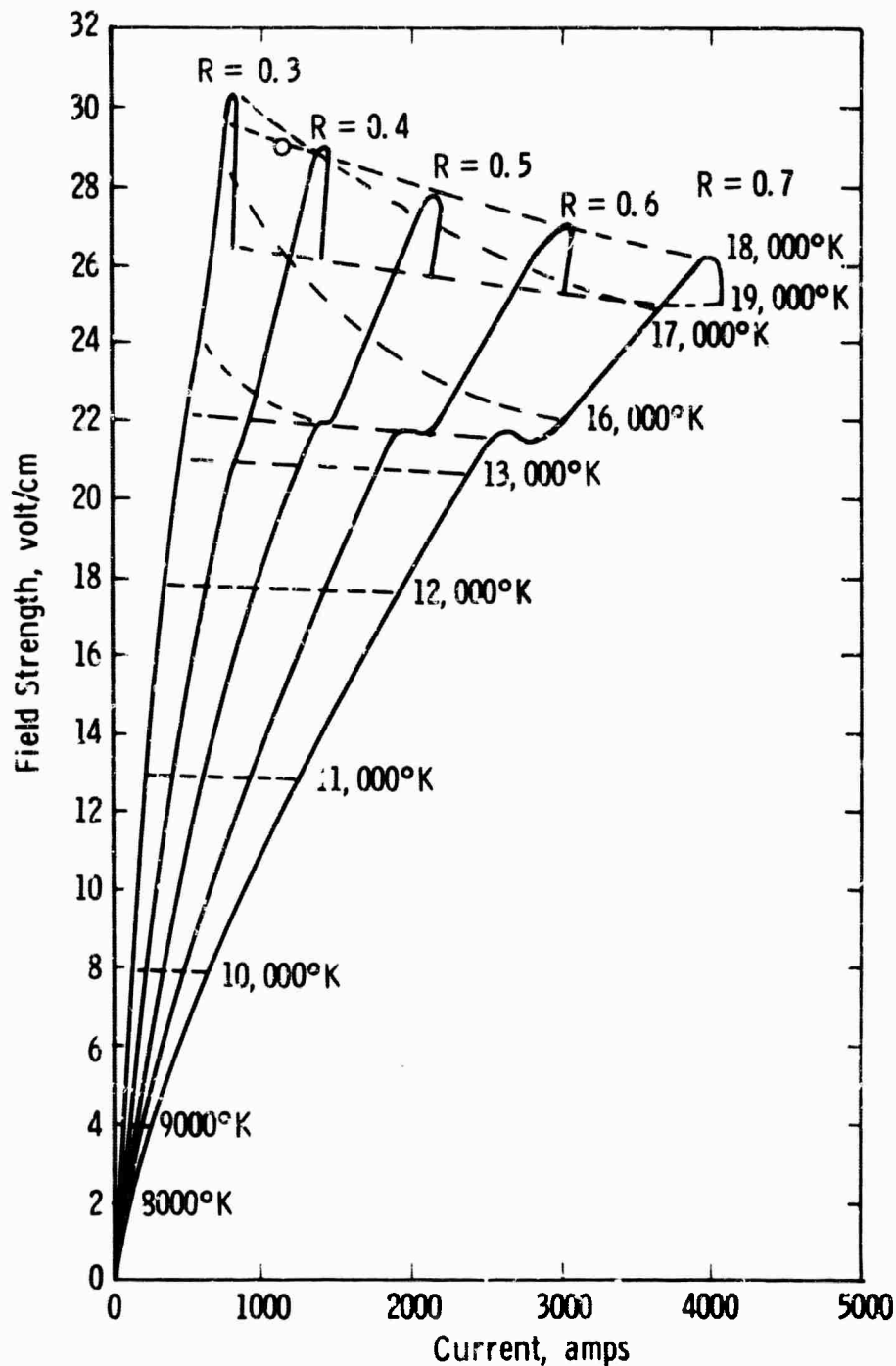


Fig. 5-Xenon, constant temp model, $p = 2.5$ atmospheres

Curve 581492-A

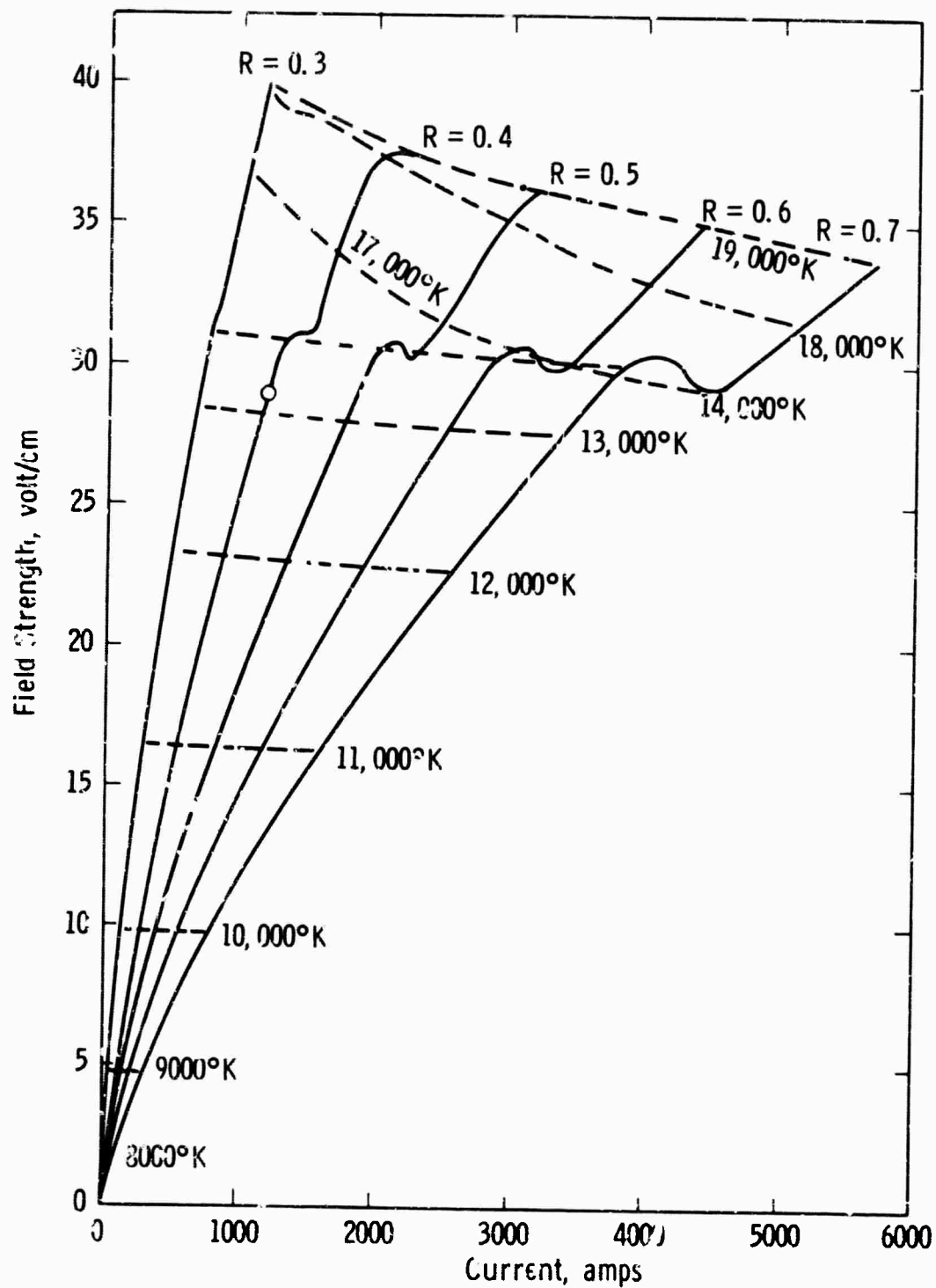


Fig. 6-Xenon, constant temp model, $p = 4$ atmospheres

Curve 581493-B

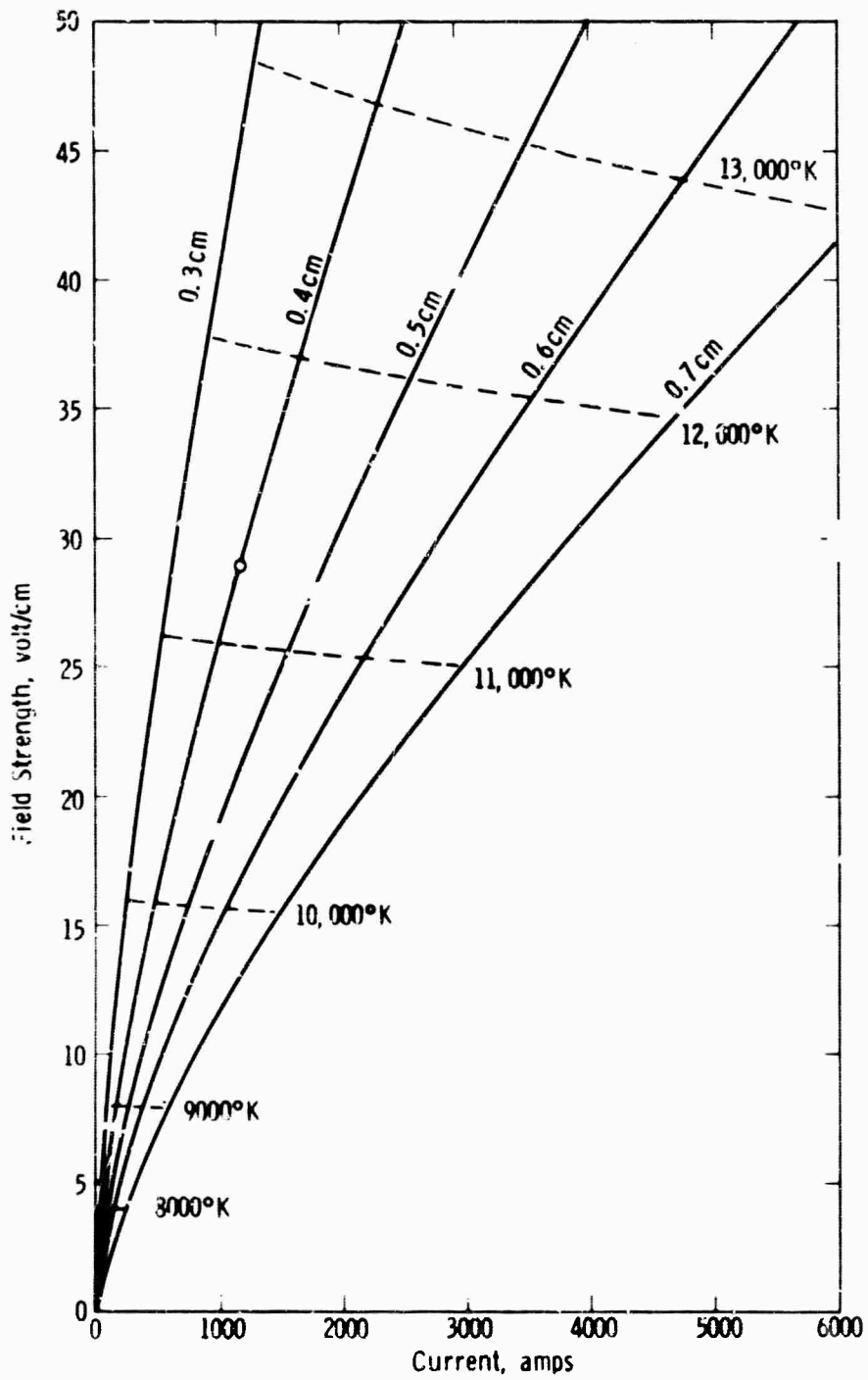


Fig. 7 -Xenon, constant temp model, $p = 11$ atmospheres

Curve 561494-A

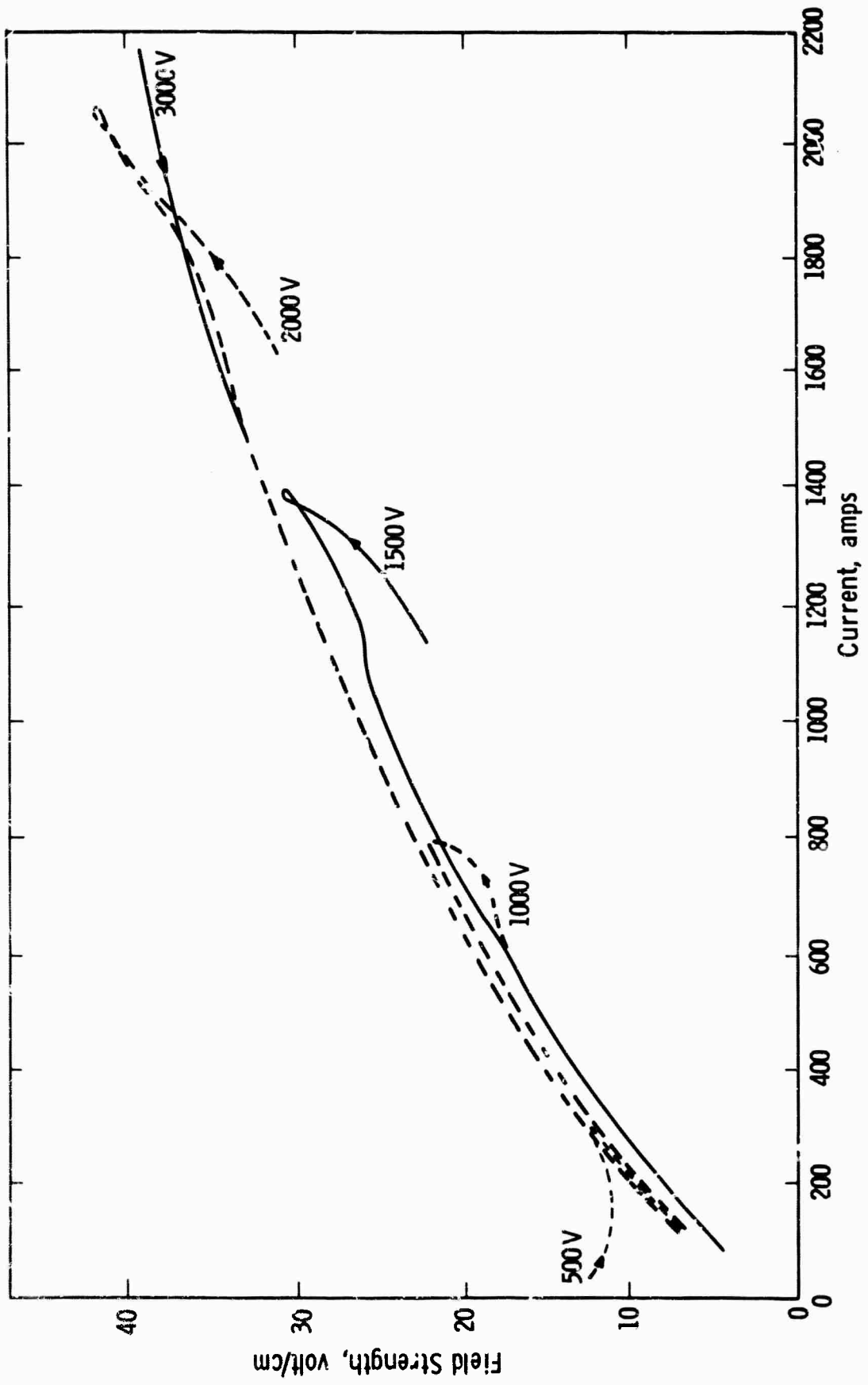


Fig. 8—Voltage/current characteristic $R = 0.63$

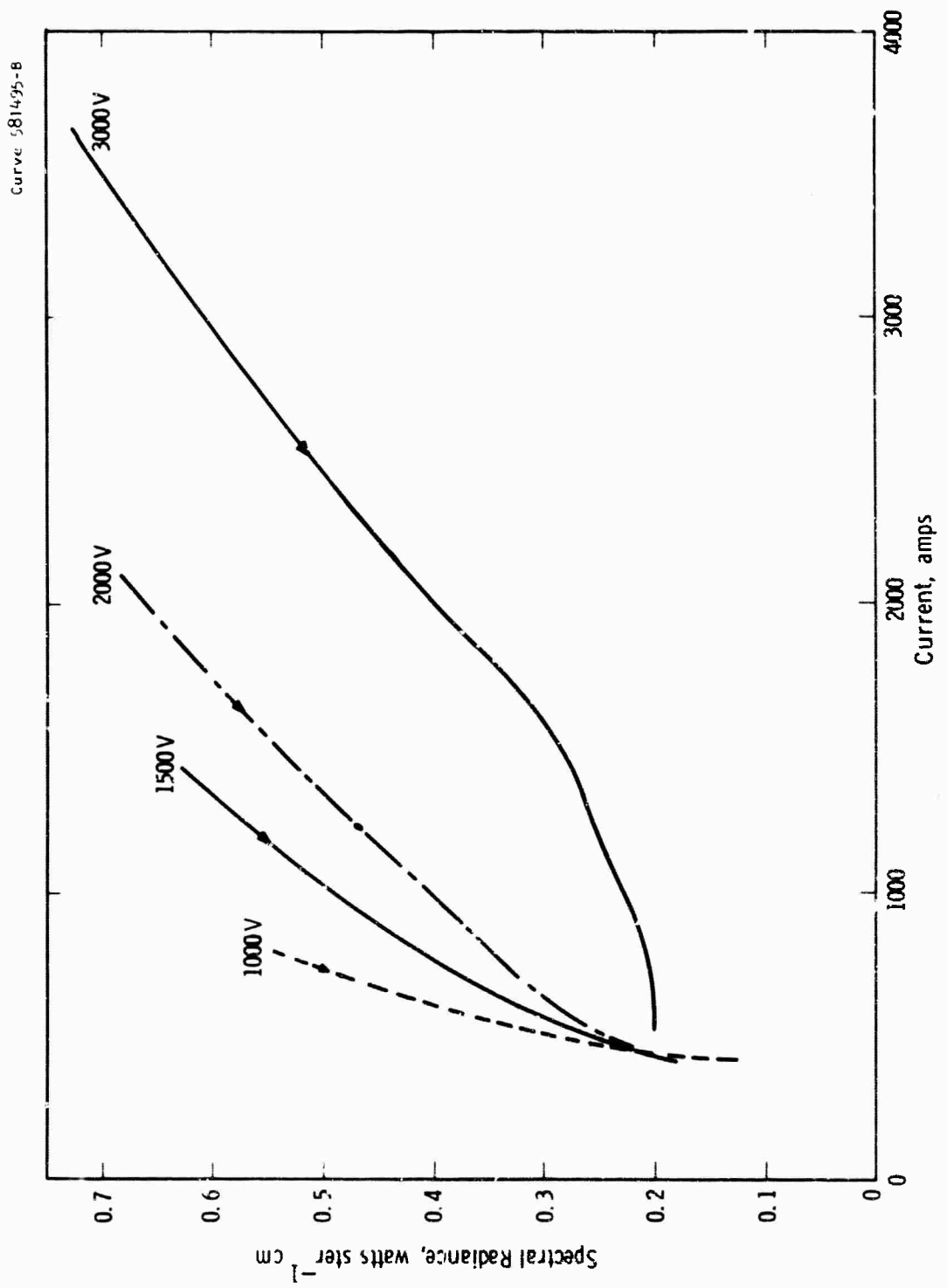


Fig. 9—Spectral radiance 8232Å

BLANK PAGE

UNCLASSIFIED

Security Classification

DOCUMENT CONTROL DATA - R&D

(Security classification of title, body of abstract and indexing annotation must be entered when the overall report is classified)

1 ORIGINATING ACTIVITY (Corporate author)		2a REPORT SECURITY CLASSIFICATION Unclassified
Westinghouse Electric Corporation		2b GROUP
3 REPORT TITLE Final Report, Arc Discharge Sources, Covering Period from 15 October 1964 to 28 February 1967		
4 DESCRIPTIVE NOTES (Type of report and inclusive dates) Also Semiannual Report covering period from 15 October 1966 to 28 February 1967		
5 AUTHOR(S) (Last name, first name, initial) Church, C.H. Liebermann, R. Geil, E. Sun, D. Swanson, B.W. Buchhave, P. Armstrong, L de Voto, R.S. Lowke, J Liberman, I. Basi, G.		
6 REPORT DATE 31 March 1967		7a TOTAL NO. OF PAGES 193
8a CONTRACT OR GRANT NO. Nonr 4647(00)		7b NO. OF REFS 52
b PROJECT NO.		9a ORIGINATOR'S REPORT NUMBER(S) 67-9C1-ARCSO-R1
c ARPA Order No. 306-62 d Code 4730		9b OTHER REPORT NO(S) (Any other numbers that may be assigned this report)
10 AVAILABILITY/LIMITATION NOTICES Qualified requestors may obtain copies from DDC		
11. SUPPLEMENTARY NOTES Models for Laser Pumps (F. -1 Lamps)		12 SPONSORING MILITARY ACTIVITY Office of Naval Research, Advanced Research Projects Agency, Department of Defense Under Project DEFENDER
13 ABSTRACT // This report summarizes the studies made on Contract Nonr 4647(00) towards the development of models for the highly radiative arcs used for the high energy pumping of lasers. The report also presents the experimental and theoretical studies since the last semiannual report. The experimental investigations were primarily concerned with more extensive measurements of the spectral radiance of the plasma to provide verification for the models. The theoretical work has resulted in computer methods, described in the appendices, to calculate the transport properties, the spectral absorptivities for the lines and the continuum of xenon, and the spectral radiance and temperature profiles in cylindrical arcs. Also included as an appendix is a theoretical analysis of the xenon arc using radiative transport techniques developed in other studies.		

UNCLASSIFIED

Security Classification

14 KEY WORDS	LINK A		LINK B		LINK C	
	ROLE	WT	ROLE	WT	ROLE	WT
Arc Discharges Laser Pumping Flash Lamps Xenon Models Calculation Computer Programs Plasmas Spectral Absorptivity						

INSTRUCTIONS

1. ORIGINATING ACTIVITY: Enter the name and address of the contractor, subcontractor, grantee, Department of Defense activity or other organization (corporate author) issuing the report.

2a. REPORT SECURITY CLASSIFICATION: Enter the overall security classification of the report. Indicate whether "Restricted Data" is included. Marking is to be in accordance with appropriate security regulations.

2b. GROUP: Automatic downgrading is specified in DoD Directive 5200.10 and Armed Forces Industrial Manual. Enter the group number. Also, when applicable, show that optional markings have been used for Group 3 and Group 4 as authorized.

3. REPORT TITLE: Enter the complete report title in all capital letters. Titles in all cases should be unclassified. If a meaningful title cannot be selected without classification, show title classification in all capitals in parenthesis immediately following the title.

4. DESCRIPTIVE NOTES: If appropriate, enter the type of report, e.g., interim, progress, summary, annual, or final. Give the inclusive dates when a specific reporting period is covered.

5. AUTHOR(S): Enter the name(s) of author(s) as shown on or in the report. Enter last name, first name, middle initial. If military, show rank and branch of service. The name of the principal author is an absolute minimum requirement.

6. REPORT DATE: Enter the date of the report as day, month, year, or month, year. If more than one date appears on the report, use date of publication.

7a. TOTAL NUMBER OF PAGES: The total page count should follow normal pagination procedures, i.e., enter the number of pages containing information.

7b. NUMBER OF REFERENCES: Enter the total number of references cited in the report.

8a. CONTRACT OR GRANT NUMBER: If appropriate, enter the applicable number of the contract or grant under which the report was written.

8b, 8c, & 8d. PROJECT NUMBER: Enter the appropriate military department identification, such as project number, subproject number, system numbers, task number, etc.

9a. ORIGINATOR'S REPORT NUMBER(S): Enter the official report number by which the document will be identified and controlled by the originating activity. This number must be unique to this report.

9b. OTHER REPORT NUMBER(S): If the report has been assigned any other report numbers (either by the originator or by the sponsor), also enter this number(s).

10. AVAILABILITY/LIMITATION NOTICES: Enter any limitations on further dissemination of the report, other than those

imposed by security classification, using standard statements such as:

- (1) "Qualified requesters may obtain copies of this report from DDC."
- (2) "Foreign announcement and dissemination of this report by DDC is not authorized."
- (3) "U. S. Government agencies may obtain copies of this report directly from DDC. Other qualified DDC users shall request through _____."
- (4) "U. S. military agencies may obtain copies of this report directly from DDC. Other qualified users shall request through _____."
- (5) "All distribution of this report is controlled. Qualified DDC users shall request through _____."

If the report has been furnished to the Office of Technical Services, Department of Commerce, for sale to the public, indicate this fact and enter the price, if known.

11. SUPPLEMENTARY NOTES: Use for additional explanatory notes.

12. SPONSORING MILITARY ACTIVITY: Enter the name of the departmental project office or laboratory sponsoring (paying for) the research and development. Include address.

13. ABSTRACT: Enter an abstract giving a brief and factual summary of the document indicative of the report, even though it may also appear elsewhere in the body of the technical report. If additional space is required, a continuation sheet shall be attached.

It is highly desirable that the abstract of classified reports be unclassified. Each paragraph of the abstract shall end with an indication of the military security classification of the information in the paragraph, represented as (TS), (S), (C), or (U).

There is no limitation on the length of the abstract. However, the suggested length is from 150 to 225 words.

14. KEY WORDS: Key words are technically meaningful terms or short phrases that characterize a report and may be used as index entries for cataloging the report. Key words must be selected so that no security classification is required. Identifiers, such as equipment model designation, trade name, military project code name, geographic location, may be used as key words but will be followed by an indication of technical context. The assignment of links, rules, and weights is optional.

UNCLASSIFIED

Security Classification

R11 35055